CONTENTS **PAGE**

LIST OF FIGURES

LIST OF TABLES

LIST OF SYMBOLS

A	Block area
CLR	Carbon Leader Reef
JRC	Joint Roughness Coefficient
JCS	Joint Wall Compressive Strength
τ	Peak shear strength
σ_n	Effective normal stress
ϕ_b	Basic friction angle
i	Average angle of deviation of asperities displacements from the direction of the applied shear stress
L	Actual sampling length
L_s	Standard sampling length
δj , ϑj	Dip and dip direction of the excavation
$N_{\delta j \vartheta j}$	Number of joints that fall into the class interval defined by mean dip and dip directions δj and ϑj respectively
$N'_{\delta j \vartheta j}$	Number of joints that would have been mapped from a perpendicular scan-line
$N''_{\delta j \vartheta j}$	Number of joints sampled had the tunnel been of the standard length L_s
SIMRAC	Safety in Mines Research Advisory Committee
V	Block volume
VCR	Ventersdorp Contact Reef
x	Block face length
z	Height of fall

CHAPTER 1

INTRODUCTION

The deep level gold mines of South Africa are known for their arduous and hazardous conditions. It is therefore not surprising that a large number of accidents occur in the industry. An analysis of accident trends from a Safety in Mines Advisory Committee, SIMRAC, (2004-2005) annual report (Figure 1.1a) taken from the period between 1984 and 2004 indicates a long-term decrease in accident rates for South African Gold Mines. However, a different scenario is observed when doing a short-term analysis. Figure 1.1b is a comparison of accidents records for different mining sectors and clearly the results for the gold mining sector are far from impressive. A closer look at Figure 1.1c shows that the major causes of accidents and fatalities in the gold mining industry are rockfalls and rockbursts. A study by Adams and Handley (2004) (Figures 1.1d and 1.1e) for the period between 1996 and 2004 illustrates the dominance of rockfalls and rockbursts in the fatality rates and the improved long-term mitigation of the two mining hazards. However, the long-term determent is not equally corresponded by short-term mitigation of the two hazards. Rockfalls and rockbursts are different forms of rock mass failure. A rock mass usually fails along planes of weakness and, joints being such planes, an analysis of their effect on stability will directly bring an understanding of failure mechanisms. Once rock mass failure is understood it will be possible to counter or contain failure by optimisation of excavation shape and positioning or through an effective and efficient support system. In short, rockfalls and rockbursts are hazardous as they result in unsafe working conditions. A decrease in injury and fatality rates has desirable effects on the economy in that the mining industry will be more sustainable. It should be noted that the estimated total cost of injuries and fatalities in the gold mining sector was approximately R330 million for 2003. Of interest is the fact that a conservative estimate of direct and indirect cost for a single fatality is R 1 million (Adams and Handley, 2004).

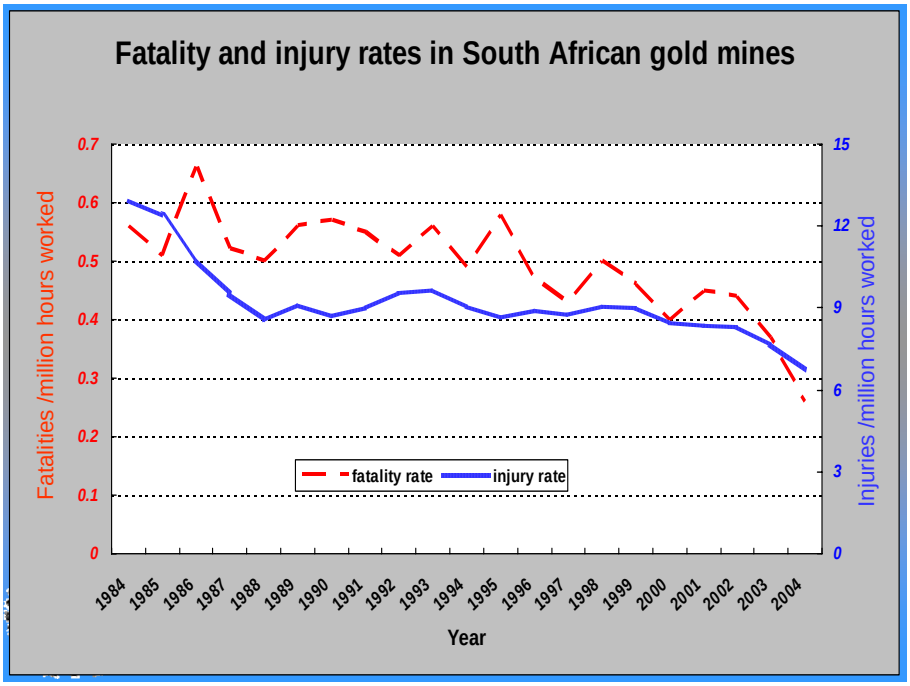

Figure1.1a Fatality and injury rates in South African gold mines from 1984 to 2004 (SIMRAC, 2005)

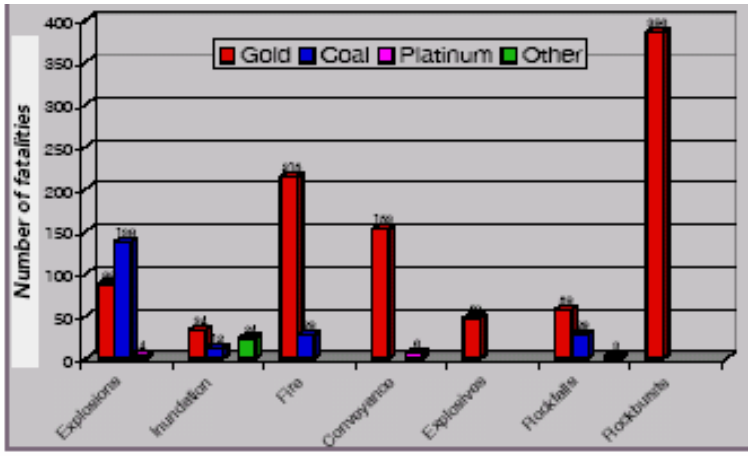

Figure 1.1b Fatality rates in the mining industry (SIMRAC, 2003)

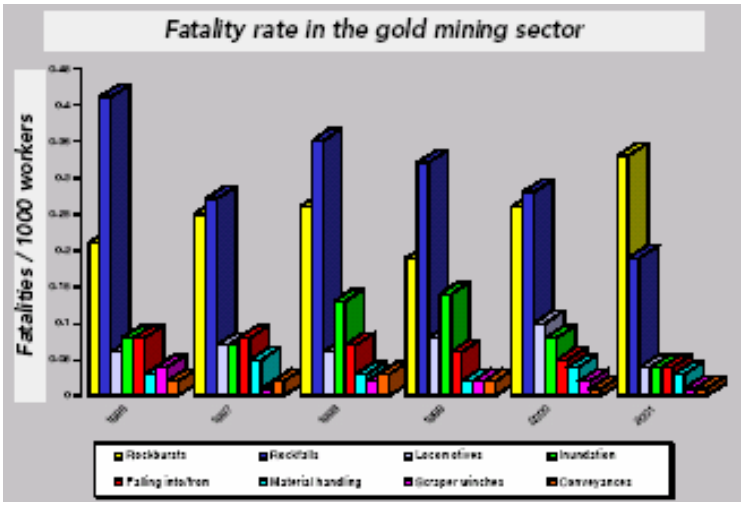

Figure 1.1c Fatality rate in gold mining industry from 1984 – 2001 (SIMRAC, 2003)

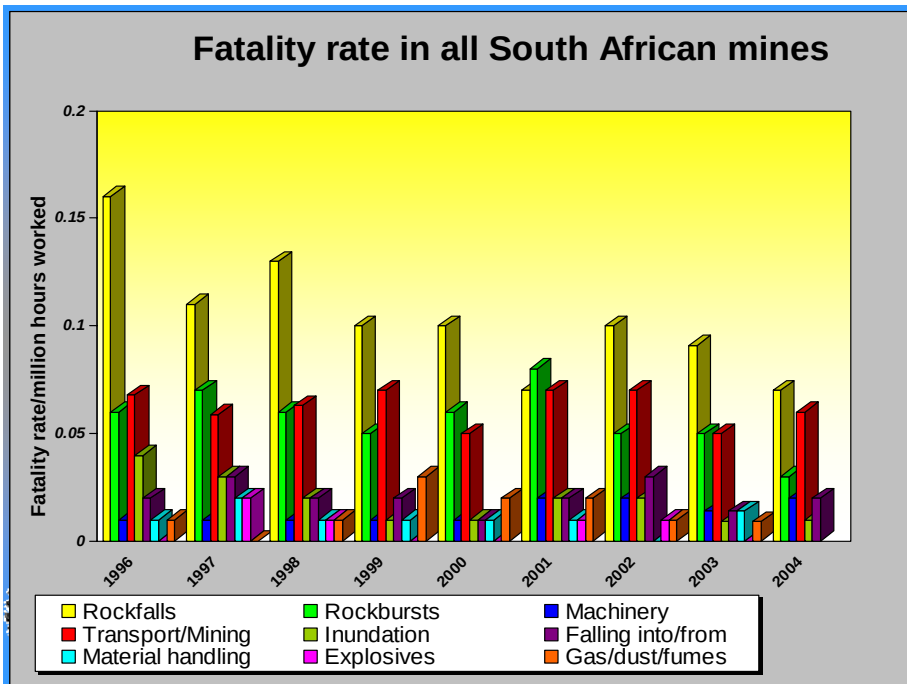

Figure 1.1d Fatality rates in all South African mines from 1996 to 2004 (Adams, 2005)

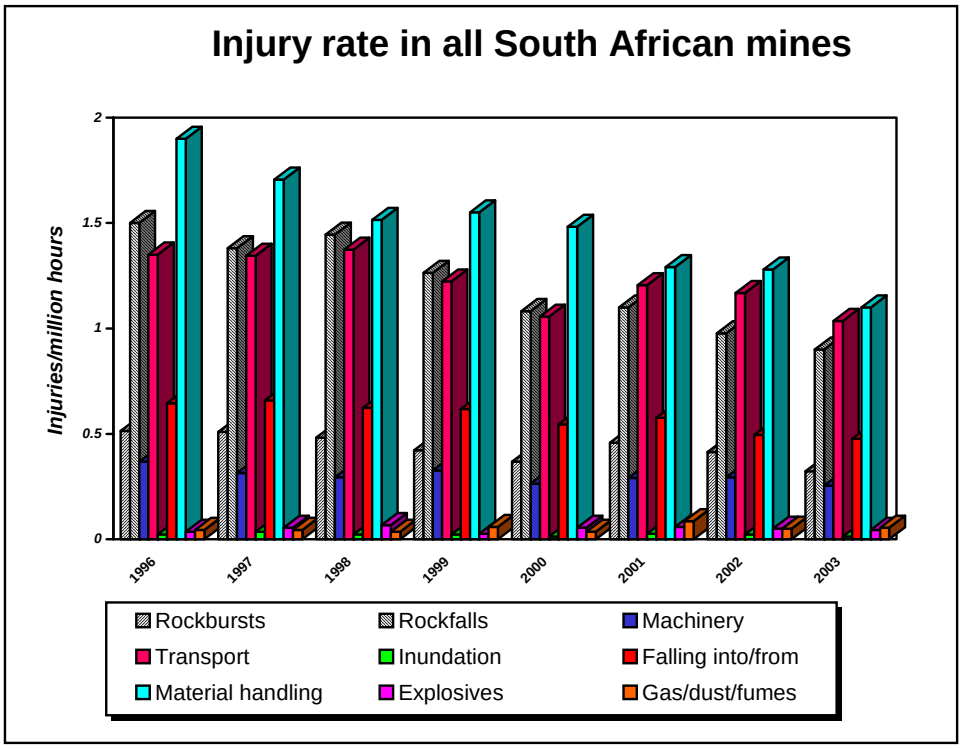

Figure 1.1e Injury rates in all South African mines from 1996 to 2003 (Adams and Handley, 2004)

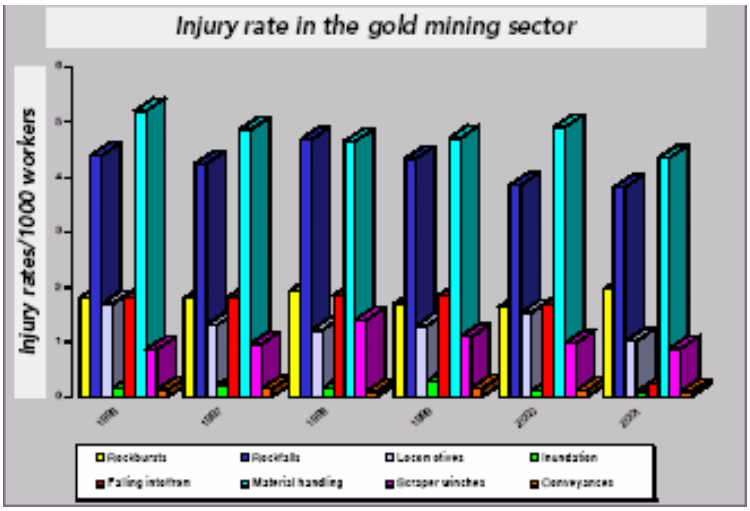

Figure 1.1f Injury rates in the gold mining industry from 1984 – 2001 (SIMRAC, 2003)

1.1 Problem definition

Although the gold mining industry acknowledges the existence of natural joints and bedding planes in rock mass, their effect on stability of excavations has "traditionally" been thought to be insignificant. The fact that currently there are no published papers on joint statistics and their effect on stability specifically for underground gold mines clearly underlines the fact that little attention has been paid to jointing by the industry. Whilst acknowledging that stress induced fractures contribute significantly towards rock mass behaviour for underground excavations (stopes and tunnels), rock falls will almost always be due to the combination of these fractures and one or more joint sets (Figure1.2). In these mines the stress levels are high and the associated contribution of stress induced fractures and joints results in the formation of planes of weakness and potentially unstable blocks in a rockmass. It is therefore important to characterise joints for typical rock types encountered in underground gold mines so as to improve rock fall management strategies. An improvement in rock fall management strategies will result in an increase in understanding of rock mass failure, and hence in a reduction of such failures and the mitigation of their effects. Furthermore, an investigation of potential unstable wedges and block sizes will not only lead to an improved and more efficient stope support design, but also to optimum positioning and shaping of tunnels and stopes.

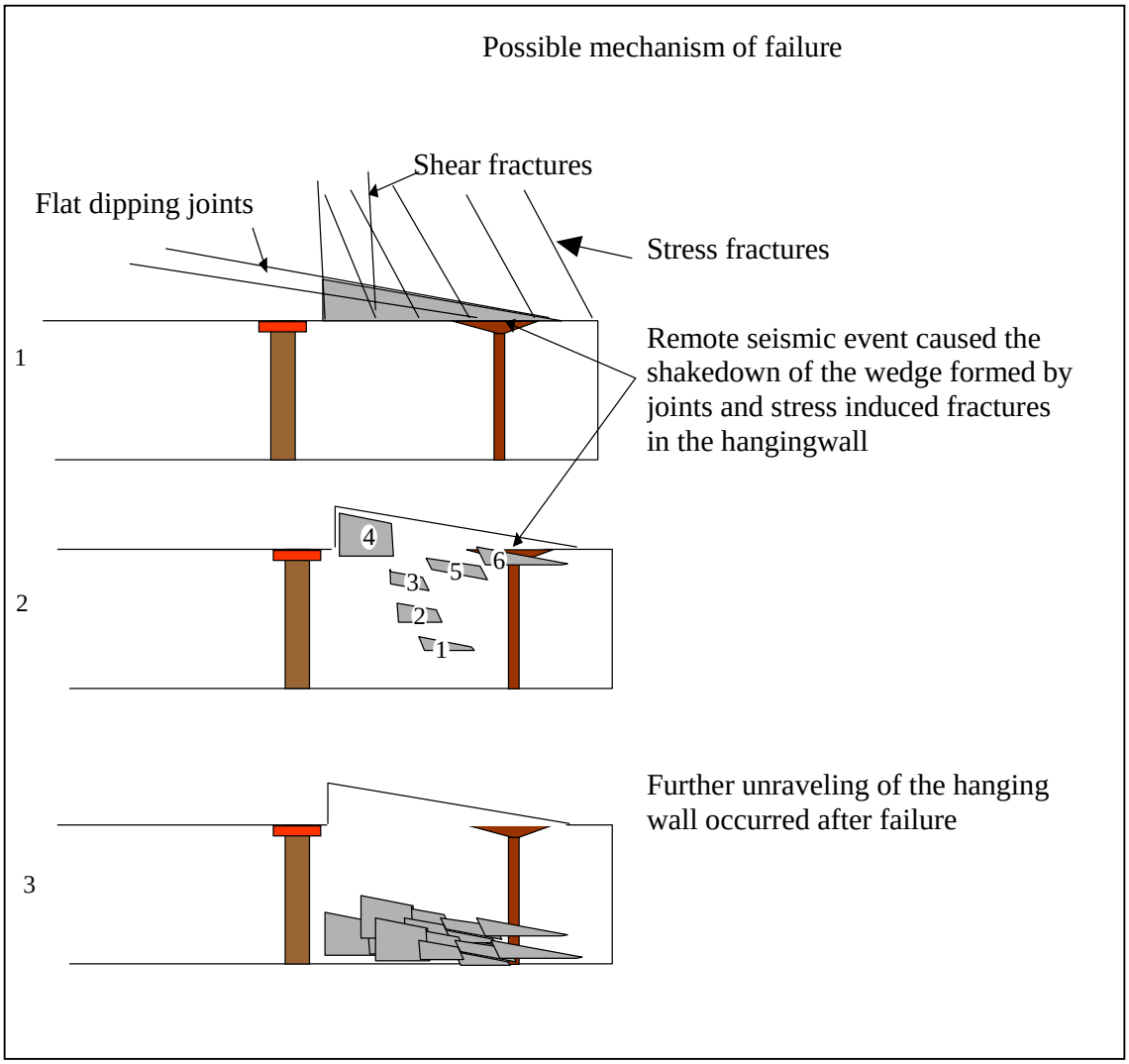

Figure 1.2 A two- dimensional representation of a combination of joints and stress fractures that resulted in a fatality in Tau Tona Mine 13/03/2003 (Statement submitted by the Rock Engineering Manager to the Inspectorate explaining the possible failure mechanism)

1.2 Objectives and Scope of the research

Discontinuities are planes of weakness in a rock mass and any rock mass failure, be it a rockfall or a rockburst, will preferentially tend to be facilitated by these weakness planes. For failure to take place in three dimensions there must be at least three release surfaces. Discontinuities tend to interact with each other to provide two of these release surfaces with the third one being the excavation surface. It is the objective of this dissertation to statistically characterise these planes of weakness (joints and bedding) for a typical rock mass in a gold mine. The contribution of joints to rock mass instability is assessed and analysed with the aim of preventing instabilities and improving the understanding of joints and their effect on rockmass failure for deep to ultra deep gold mines. Furthermore, characterising and understanding joint effects on rock mass stability is useful in stope support design.

For a thorough probabilistic stability analysis of underground excavations, a parametric study of significant contributing variables must be assessed and evaluated. This is effectively achieved by obtaining structural geological data from field mapping, using these statistical data to reconstruct representative rock mass trace models, and interpretation of these models to determine the probability of occurrence of geometrically unstable blocks.

1.3 Research Methodology

The research methodology adopted was structured as follows:

(i) Definition and description of parameters that characterise joints;
(ii) Joint data collection and analysis;
(iii) Identification of different joint sets, joint set properties and joint set statistical distributions;
(iv) Generation of a rock mass discontinuity trace model using data from (ii) and (iii);

(v) Analysis of the interaction between the generated rock mass trace model and different excavation geometries to obtain a distribution of the likely unstable block sizes and other block parameters;

(vi) Use of the results from (v) to determine the overall scale of instability and to identify the instability modes.

Joint mapping was carried out in two thin reef gold mining operations using the scan line mapping technique. A commercially available software program was then used for the identification of different joint sets. Identified sets were then statistically evaluated and analysed, with the resulting statistical parameters being used for joint modelling. An evaluation of excavation stability was carried out by simulating the joint occurrences using the statistical distributions and identifying potentially unstable blocks for different excavation orientations.

1.4 Content of the dissertation

A background description of joint properties and their characteristics is presented in the next chapter. Also described in the chapter are different types of joint mapping techniques. Chapter 3 is sub-divided into two major sections. The sub-sections illustrate, in detail, the joint mapping exercises that were carried out in each mine. The sub-sections describe the collection and statistical analysis of the mapped joint data. In Chapter 4, the resulting statistical joint data are used to predict and analyse the extent of instability for underground excavations in a jointed rock mass. Two different modelling techniques are used thus the chapter is also divided into two subsections. The chapter also demonstrates the use of joint data to obtain important support design parameters. Conclusions and recommendations are included in Chapter 5, as well as a description of the overall contribution of the research work to the South African gold mining industry.

CHAPTER 2

JOINTING IN A ROCK MASS

2.1 Introduction

Minerals are the building blocks of rocks just as ordinary bricks are in buildings or cells are in animal tissues. Technically, minerals are petrographical components of an intact rock. The intact rock is widely known as the rock material. On a microscopic scale, rock material is usually discontinuous in nature due to the presence of voids, grains and different crystal orientations. However, for most engineering applications and analysis, microscopic discontinuities are insignificant, such that individual crystals and grains do not affect the engineering property concerned. Hence rock material is considered as a continuum, i.e. where the engineering property concerned has a characteristic value. Natural and induced failure of the rock results in the rock material being a discontinuum, resulting in a marked variation of the engineering property concerned. A rock mass refers to an intact rock that has been rendered discontinuous as a result of natural and induced failure of the rock material. Thus a rockmass behaves as a discontinuum due to the presence of discontinuities. Discontinuities are planes of weakness in a rock mass, and are commonly joints, fractures, bedding planes and faults.

A rock mass consists of partially or totally separated blocks of rock material. In most cases, rock mass strength is significantly lower than rock material strength because of the discontinuities. Failure in a rock material is often along grain and void boundaries, while failure in a rock mass will often be partially through rock material and partially along discontinuities. However in most instances, failure planes in a rock mass tend to form along discontinuity planes. The spatial distributions of these discontinuities affect the strength and deformational properties of the rock mass.

To effectively analyse discontinuities, the following geological propositions suggested by Piteau (1970) are adopted: structural discontinuities are detectable features in a rock mass and can be described quantitatively; structural regions exist in a rock mass; failure surfaces will be on a plane or combination of planes. These propositions are enlarged below.

(i) Structural discontinuities are detectable features of a rock mass and can be described quantitatively.

In general, structural discontinuities in a rock mass can be described quantitatively. To quantitatively describe discontinuities, their geometric and shear strength properties must be known. Quantifying discontinuities involves physically mapping them to determine their position in rock mass, their position relative to excavations, their position relative to other discontinuities, their sizes and type.

(ii) Structural regions exist in a rock mass.

Though discontinuities in a rock mass are unique, they can have similar properties and characteristics. Depending on the property being investigated, discontinuities that have similar properties and characteristics are usually treated as unit. Grouping discontinuities that show similar statistical patterns indirectly defines structural regions within the rock mass.

(iii) Failure surfaces will be on a plane or combination of planes.

Rock mass strength is lower than rock material strength because of discontinuities, thus failure in a rock mass will tend to occur on a discontinuity plane or combination of planes. By identifying discontinuities as the most likely failure planes in rockmasses, one reduces infinite possible failure surfaces in a rock mass to a lesser, manageable and feasible number.

In conclusion, since many engineering constructions (tunnels, stopes, buildings etc) are in rock masses, it is important that rock mass features are known and characterised. Figure 2.1 is a schematic illustration of the relationship between rock material, rock mass and discontinuities from Hoek et al (1998).

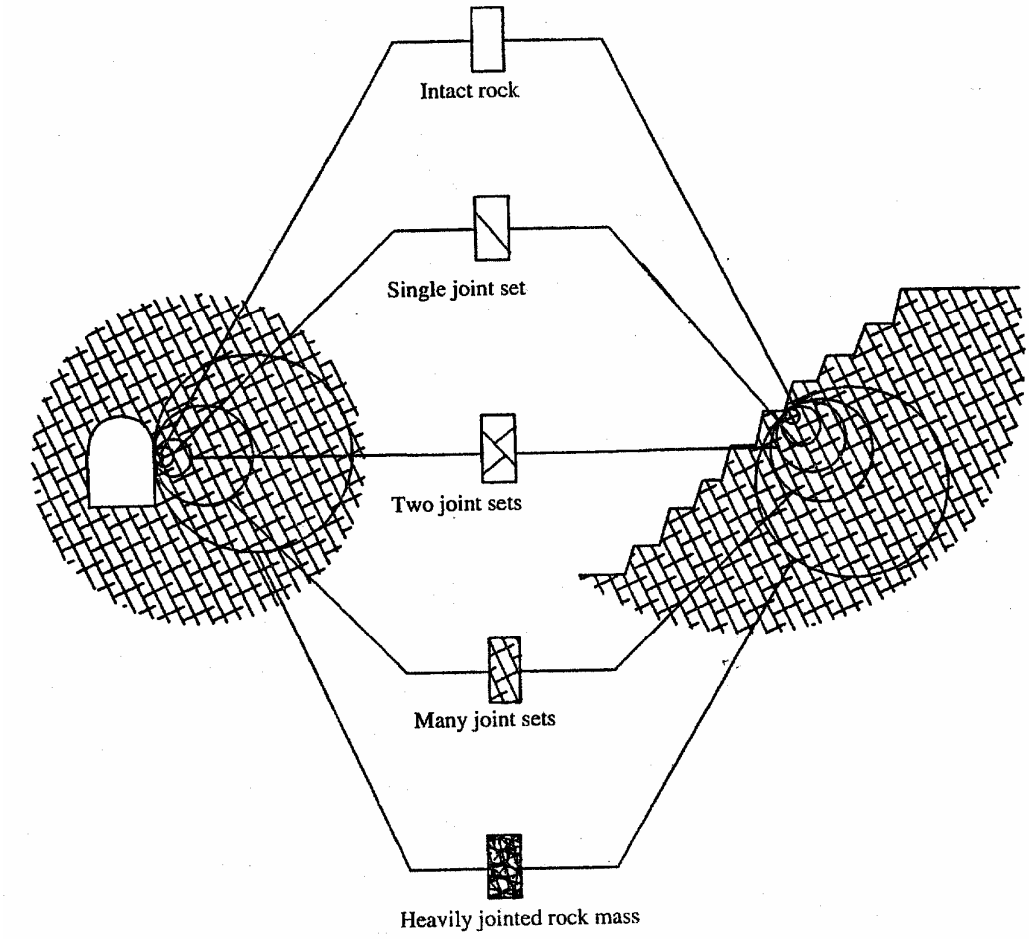

Figure 2.1 Relationship between rock material, rock mass and discontinuities (Hoek et al, 1998)

From the diagram above a rock mass can be summarised as a discontinuous medium consisting of individual blocks (rock material) that are heterogeneous in nature due to the variation of physical and lithological properties of the rock. Rock mass strength is mainly influenced by discontinuity features rather than intact rock strength.

2.2 Rock Joints

In the previous section on rock mass, it was shown that the difference between a rock mass and a rock material is the presence of discontinuities in the former. The types of discontinuities that are of interest in this dissertation are rock joints and bedding planes.

Joints are planar discontinuities of geological origin in a rock mass, along which there is no discernible or visible displacement. Being classified as discontinuities, joints are thus planes of weakness in a rock mass and hence they directly influence the stability of the rock mass. The definition is extended to bedding planes in this dissertation as they have the same effect on aspects being investigated. In fact, there are no sharp demarcations between joints and other fractures or geological structures. For instance, if there is a significant movement along a joint, the joint is usually known as a fault. If however, the movement is insignificant the joint is usually referred to as a slip, rift or a blind joint. Furthermore, if these blind joints are closely spaced resulting in the rock being able to part along parallel surfaces, the type of fracturing is referred as cleavage (Leith, 1923). When a joint or a fault is filled with or infiltrated by hydrothermal fluids or other mineral matter it is known as a vein. The same vein is also referred to as a lode if infilling minerals are of economic value.

In terms of their formation, joints tend to form at practically all ages in the history of rocks. Different hypotheses have been suggested to account for the development of joints (Leith, 1923; Price, 1966; Hobbs et al, 1976; and Suppe, 1985). These theories range from suggestions that joints form as a result of earthquakes to that they developed in response to tensile stresses, which resulted from contraction of sediments, folding or from regional compression. In general, joints are a result of rock reaction to:

i) Earth stresses responding to the mantle / crustal movements.

ii) Different expansion and contraction rates within a rock material or rockmass in response to temperature changes, mineral alterations and variations in moisture content.

iii) Rock material or rockmass response to stress changes due to loading and unloading of the overburden through denudation processes.

Although it is generally agreed that joints form mainly due to tensile stresses, they can, however, also form under compressive stresses (Price, 1966).

Joints usually exist in groups or families known as joint sets that are either sub-parallel or have similar geomechanical properties. These joint sets intersect to form joint systems. When failure in a rock mass takes place, one or more joint sets are generally involved, hence the importance of joint characterisation. Detailed joint characterisation usually gives insight into the state or manner of rock mass deformation or the structural region concerned. Also, there maybe certain types of joints which are restricted to particular structural areas or formations and it is therefore possible to correlate the jointing with a specific feature of the geological history (Leith, 1923). As already stated above, the filling in joints (lodes and veins) can be of economic value, thus characterising such joint types can be an indirect characterisation of the ore body. The importance of joint characterisation is not only relevant to underground excavations, but also to slope stability in open pit mining, block and size distribution in rock quarrying, topography and drainage, erosion, permeability and porosity. In conclusion, joints play a very important role in nearly all ground related engineering fields (e.g. mining, dam construction, quarrying, ground water hydrology, waste disposal etc).

2.2.1 Classification of joints

Classification of joints involves describing joints with respect to their characteristics such as shape, size and the combination of size and frequency of occurrence. Under shape classification, planar and parallel (sub parallel) joints that form sets are known as systematic joints. Irregular, curved joints are known as non-systematic joints.

Joints can also be classified by their size variations. For example joints which cut through a number of beds or rock units and can be traced over fairly large lengths are known as master joints, while their opposite in size characterisation are micro joints. On a medium scale, in between master and micro joints, there are major and minor joint ranges.

Under frequency classification, a set of joints that is often dominant i.e. by being larger or more frequent than other sets, is known as a primary joint set while a less dominant set is known as a secondary set.

Other different joint types are named in relation to the geological structures associated with them and their relative positions within the structure. Figure 2.2 shows typical joint forms in a folded stratum.

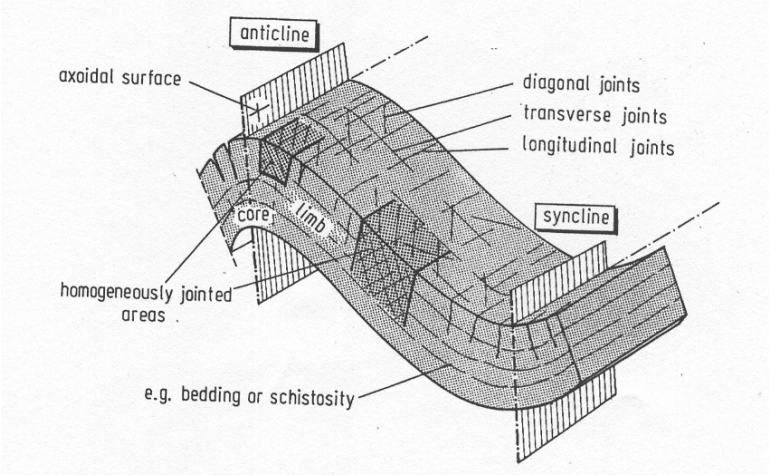

Figure 2.2 Joint classification with respect to geological structures (Wittke, 1990)

Joints can also be classified according to origin by dividing them into two major groups, i.e. contacts and fractures. Contacts originate from rock forming processes such as bedding planes in sedimentary rocks, flow banding in igneous rocks and foliation joints in metamorphic rocks (Robertson, 1977). Contacts have uniform

properties which are similar for all contacts of the same origin. Fractures are a product of local stress variations in rock material, resulting in rupture surfaces. Since they result from stress variations, a characteristic fracture pattern reflects the stress system under which it was formed.

As joint mapping described in this dissertation was done largely in sedimentary rocks, it is worth illustrating bedding planes (Figure 2.3), as they are the most dominant natural discontinuities in development tunnels in gold mines.

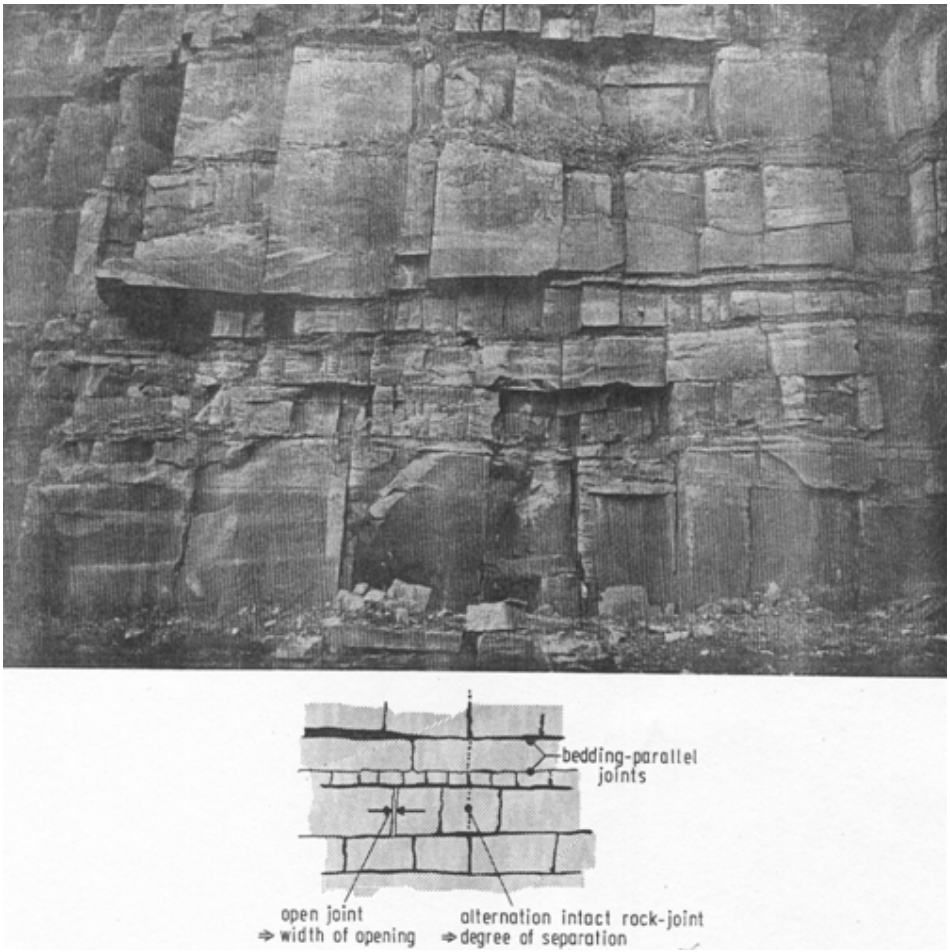

Figure 2.3 Bedding planes (Wittke, 1990)

2.3 Joint Properties

Joint properties of interest vary with the nature of the engineering problem. For instance, joint surface features (e.g. waviness, cohesion, etc) have a more significant effect on slope stability than on foundation stability whereas compressibility and permeability are more important in the latter than in the former. Joint properties considered important in this dissertation are joint orientation, length, spacing and shear strength. The joint properties (orientation, length and spacing), discussed below, collectively describe joint geometry.

2.3.1 Joint orientation

Joint orientation describes the attitude of a discontinuity in space. Orientation is the most important joint property since joints that are favourably orientated with regard to stability, relative to a free face, effectively neutralise the effects of other joint properties. As will be seen, joints dipping into a free face have a lesser effect on stability than those dipping out of a free face. In general, joint orientations are uniquely described by the dip and dip direction angles. Continuing with the declaration in Section 2.2 that joint orientations, in most cases, are found to be clustered in statistically preferred directions, an individual cluster of these joints defines a joint set. Given an ideal scenario where the stress propagation during joint development is constant and the rock material and rockmass are homogeneous, isotropic and elastic, joints will be found in single sets with insignificant dispersions. The relationship between a changing stress field acting on an inhomogeneous and inelastic rock material and rockmass is the reason for joint orientation dispersion (Saayman 1991). Joint set delineation usually involves demarcation of joint clusters that have a common statistical orientation. In joint analysis, all joints that are included in a defined set are given equal weighting for any characteristic property being investigated, thus the definition of the set has to be as comprehensive as possible. Joints that do not fall within the defined sets are known as random joints. In most cases random joints are excluded from further analysis. Nevertheless, if they contribute a significant proportion of the total number of joints, they are worth analysing as was the case in the development of

three dimensional joint models by Grenon et al. (2000). In this case random joints represented 31 % of the mapped joints. Furthermore, it was demonstrated in the same study that the formation of 22 % of unstable blocks involved at least one random joint set. The number of random joints and the joints within a given set depend on the choice of the limits (i.e. range of joint orientations) defined during the delineation of the joint sets.

2.3.2 Joint Length

The length of a joint describes the potential failure plane. It indicates the extent to which joints and rock material individually affect the engineering properties of a rock mass. In literature, the measurable part of a joint length is widely referred to as the trace length. Discontinuous joints result in a relatively stronger rock mass compared with a continuously jointed rock mass because, in the former, rupture must occur through intact rock prior to failure development. It is not easy to measure absolute length of a joint since the entire joint surface cannot easily be seen. Hence joint trace lengths are measured in “exposures” and the overall length is statistically predicted thereafter. Accurate measurement of joint lengths is more challenging than measurement of other joint properties mainly because of the following:

(i) Size bias due to the likelihood of measuring larger joints only, as they have a higher probability of being sampled than smaller joints. The sampling error introduced by the size bias can be as high as double the true joint length (Einstein et al, 1983).

(ii) Joint lengths are censored above or truncated below certain lengths that cannot be measured practically. In practice, it is impossible to differentiate small joints from fractures, and orientation measurements of these joints are error prone. Introducing an orientation error during the measuring stage effectively means that the joint(s) will be assigned to the incorrect joint set. Thus in field mapping, it is common to measure joints from a given minimum length (truncation). Joints below that given length are not measured, hence truncation errors result in the overestimation of joint lengths. The extent of this bias depends on the truncated length in relation

to true joint lengths. Some joints tend to extend into or out of the excavation face resulting in the impossibility of measuring the actual full lengths of the joints concerned. It is therefore common in joint length mapping not to measure joint lengths that are above a pre-defined length (censoring). Censoring bias consequently has the effect of underestimating the actual joint length.

Evaluation of extensive data has shown that the frequency distribution of joint lengths may be described either by a lognormal distribution or a negative exponential distribution (Robertson, 1977; Barton, 1976; Baecher et al, 1977 and Kulatilake et al, 1995). Sampling and measuring biases introduced in the sampling of orientations are discussed in Section 2.5.2.

2.3.3 Joint Spacing

Joint spacing is a measure of joint intensity in a rockmass, i.e. the number of joints per unit distance normal to the dip direction of the set. It is taken as the perpendicular distance between adjacent joints. In general, a highly jointed rock mass (closely spaced joints) is weaker than a sparsely jointed rockmass (widely spaced joints). Though orientation is considered a more important joint property than spacing, it should be noted that a widely spaced joint set, though critically oriented relative to the excavation, may have an insignificant effect on the stability of the excavation. Furthermore, the intensity of jointing determines whether a given rockmass should be treated using soil mechanics principles or rock mechanics principles. It should be noted that, when analysing rockmasses using soil mechanics principles, sampling and laboratory testing methods will differ from those used when the analysis is using rock mechanics principles.

Figure 2.4a demonstrates a uniform distribution where all the spacing values have an equal probability of occurring. A uniform distribution is a rare distribution for joint spacing as it implies that the stress-driven fracture propagation stage during the joint ‘life-span’ was constant. Figure 2.4b is an illustration of a normal distribution, where adjacent joints are correlated. In this case joint spacing values

will be normally distributed around a mean spacing value. A normal distribution usually occurs, for instance, when a fracture formed at a point where rock mass strength is exceeded resulting in stress being relieved for a distance equal to the mean spacing. After stress propagation for a distance equal to the mean spacing another fracture forms and the cycle is repeated thereafter.

A negative exponential distribution (Figure 2.4c) is when joint positions are mutually independent of each other and their occurrence is random within the set. Exponential distributions of joint spacings indicate that the intersection of joints with a sample line is a Poisson process and that joints are randomly and independently distributed in space (Saayman, 1991). Most researchers (Call et al, 1976; Priest et al, 1976; Wallis et al, 1981) conclude that a negative exponential distribution is applicable for joint spacings, while there is a possibility of a lognormal distribution (Steffen et al, 1975; Bridges, 1975; Barton, 1977 and Kulatilake et al, 1995).

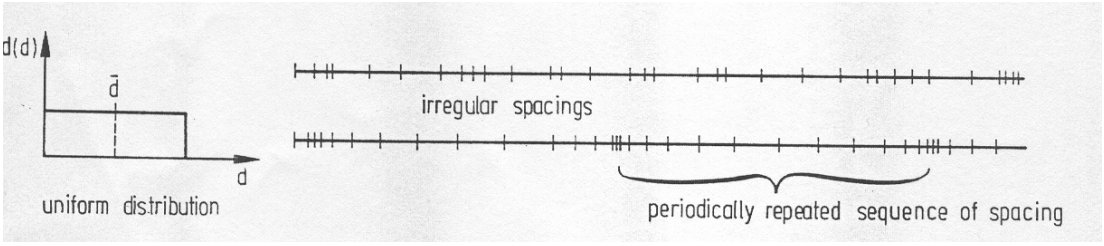

Figure 2.4a Example of a uniform statistical distribution of discontinuity spacings (Wittke, 1990)

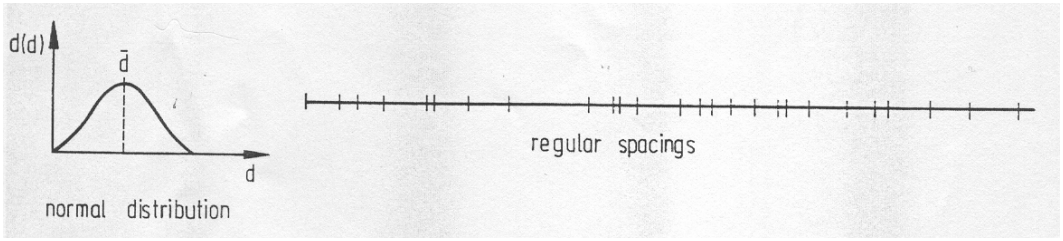

Figure 2.4b Example of a normal statistical distribution of discontinuity spacings (Wittke, 1990)

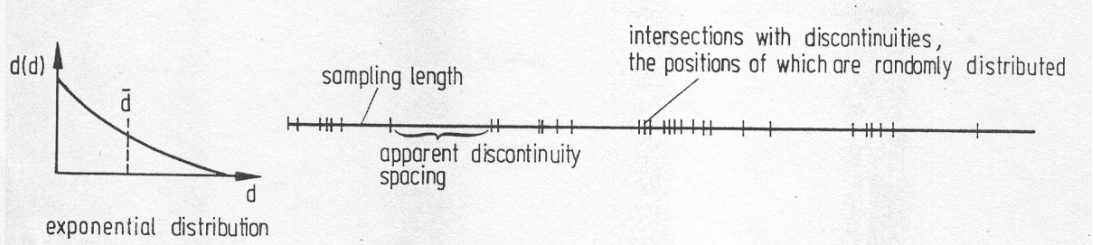

Figure 2.4c Example of an exponential statistical distribution of discontinuity spacings (Wittke, 1990)

In general, joint spacing values are positively skewed and can be approximated by exponential or lognormal functions. Since the intersection between joints and the sampling line is a Poisson process, the implication is that the orientation bias described in Section 2.5.2 will only affect joint frequency per unit length and not the form of distribution. In practice there is little difference between the assumption of a negative exponential or log normal distribution.

2.4 Joint shear strength

After joint geometry, the second most important input parameter in analysis of joint effects on rock mass behaviour is the shear strength of a potential failure surface. This surface may consist of a single continuous or discontinuous joint plane, or a complex surface along joints of the same set and joints from other sets. The shear strength of rock material can reliably be tested at a reasonable cost, but the same cannot be said for the shear strength of joints. Parameters that control joint shear strength vary significantly along single joint planes, within joints of the same set and within different joint sets. These variations render test results on joint strength to be representative of relatively small joint portions. However, these tests on joints are needed as they contribute to the understanding of failure mechanism and the scale of forces involved during joint shear failure. It is therefore imperative that during joint shear strength testing, most (if not all) of the contributing parameters are taken into consideration, including their variability.

The behaviour of a joint surface under stress is influenced by loading parameters such as normal and shear stress, joint geometric components and joint surface components. A number of empirical equations have been developed for the shear strength of joint surfaces, notably by Patton (1966), Landanyi and Archambault (1970), Barton (1973) and Barton and Choubey (1977). Most of these criteria are related to equation (1) that was developed by Newland and Alley (1957) for shear stress of joint surfaces at low normal stresses in a granular material.

$$\tau = \sigma_n \tan[\phi_b + i] \qquad (1)$$

where τ = Peak shear strength

σ_n = Effective normal stress

ϕ_b = Angle of frictional sliding resistance between particles

i = Average angle of deviation of particle displacements from the direction of the applied shear stress (dilation) (insert in Figure 2.5)

The Coulomb relationship in equation (2) is widely accepted as an estimation of shear stresses at high normal stresses.

$$\tau = c + \sigma_n \tan\phi \qquad (2)$$

where c = Cohesion

Although equations (1) and (2) imply a straight line relationship, Patton (1966) simulated different joint surfaces at low normal stresses and demonstrated the bilinear form of the joint shear strength envelope (Figure 2.5). He postulated that the two lines represented different modes of failure. At low normal stresses, i.e. line **OA** in the diagram, the peak shear strength is governed by sliding, while at high normal stresses (line **AB**) the shear strength is governed by shearing of rock surface asperities. He concluded that the change in the slope gradient represented changes in the failure mode. The change in the failure mode was related to the physical properties of the simulated joints. Equation (1) was shown to be true for shear strength along a rock surface when there was no shearing of surface asperities.

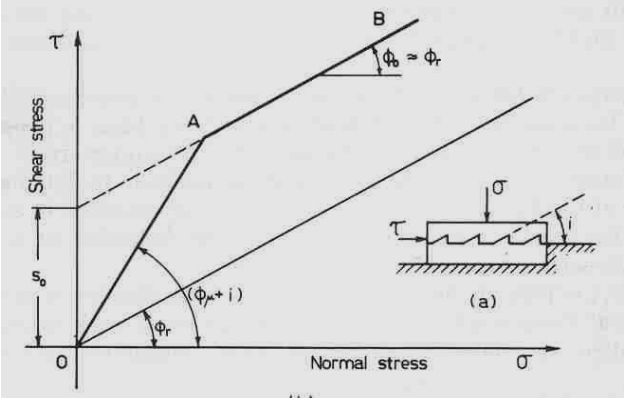

Figure 2.5 Bilinear failure criterion for joint surfaces (Patton, 1966)

Landanyi and Archambault (1970) further demonstrated that the above assumption/observation was valid for shearing of surfaces that have the same joint roughness coefficient values (discussed in detail below) prior to and at failure. Their proposed shear failure equation utilised the basic energy conservation equation. The widely used empirical equation for analysis and prediction of shear strength of rock joints is the one formulated by Barton and co-workers (1973; 1976 and 1977) in equation (3):

$$\tau = \sigma_n \tan\left[JRC \log_{10}\left(\frac{JCS}{\sigma_n} \right) + \phi_b \right] \qquad (3)$$

where $\tau =$ Peak shear strength

$\sigma_n =$ Effective normal stress

$JRC =$ Joint Roughness Coefficient

$JCS =$ Joint Wall Compressive Strength

$\phi_b =$ Basic friction angle

Equation (3) can be used for predicting shear strength, curve fitting and extrapolating experimental peak shear strength data. The equation is composed of three parameters, the joint roughness coefficient (JRC), the joint wall compressive strength (JCS) and the basic friction angle (ϕ_b). The three parameters are easily quantifiable both in the field and in the laboratory. The effective normal stress (σ_n) is the only external parameter in the equation and can also be reliably measured. Joint surfaces are made of asperities or surface irregularities that have

an interlocking effect during shearing. This interlocking effect tends to increase the shear resistance along the joint surface by increasing the effective friction angle of the joint above the base friction angle (ϕ_b). The joint roughness coefficient (JRC) is a measure of asperities/surface irregularities on a joint plane. A common method of measuring JRC values is by visual comparison of measured profiles against a set of standard JRC profiles suggested by Barton and Choubey (1977). An internet based survey by Beer et al (2002) proved the subjectiveness of the Barton and Choubey (1977) JRC estimation method; nevertheless it was also shown that the level of accuracy increases with increase in experience. For more accurate results, a back calculation of JRC from a simple index test can be done by making JRC the subject of the formula in equation (3).

Joint wall compressive strength (JCS) values represent the state of thin rock layers adjacent to joint walls and are affected by factors such as weathering, moisture content and permeability. For a fresh unweathered joint, the JCS value is equal to the unconfined compression strength (σ_c) of the rock. The value of JCS decreases with increase in state of weathering. Furthermore, for a joint surface that is at an advanced stage of weathering such that the rockmass is permeable throughout, σ_c values also drop to the values of the JCS (Barton, 1976 and Barton and Choubey, 1977). The Schmidt Hammer Index Test described in Barton and Choubey (1977) is used in measuring JCS values. Values for the base friction angle are determined from the Tilt Test also described by these two authors. Equation (3) has three limiting input values namely:

JRC = 20; which is the roughest possible scale in the Barton and Choubey JRC profiles.

JCS = (σ_c); for a fresh unweathered joint surface

(ϕ_b) = (ϕ_r) for a fresh unweathered joint surface with basic angle between 28.5º and 31.5º (Barton and Bandis, 1990). As a general conclusion, the shear behaviour of joints is characterised by sliding on the surfaces at low normal stresses. However, as normal stress increases, surface asperities are damaged during shearing leading to a decrease in dilatancy. Under these high stresses, the shear

behaviour of joints tends to resemble that of intact rock material. The three basic components of shear strength on joints are the basic friction component (ϕ_b), the geometric component controlled by surface roughness (JRC) and the asperity failure component JCS/σ_n. Figure 2.6 summarises the general failure envelopes for a joint (irregular rock surface), for intact rock material and for a smooth rock surface.

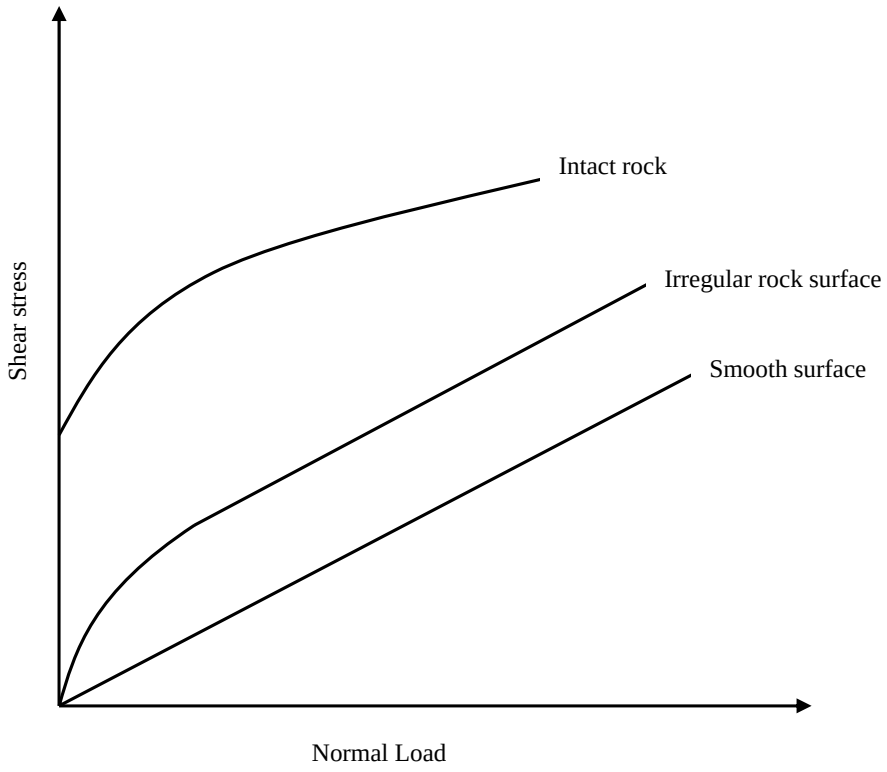

Figure 2.6 General failure envelopes for joint surfaces and intact rock (Patton, 1971)

2.5 Joint sampling and analysis

A population in a geological sense consists of objects or classes thereof, which are of direct interest in a geological study. A sample on the other hand is a sub-set of a population. Depending on the objectives of the study, a conceptual population is identified, whose parameters are of interest and this population is known as the target population. However, most of the target population is not available for sampling resulting in a smaller population being sampled. The portion of the target population that is available for sampling is known as the sampled population. Data from a sampled population can be used to compute sample statistics and the results are used to infer statistics of the target population (Walpole and Mayers 1993). To accurately infer a population from sampled statistics, samples have to thoroughly represent the population. Sampling bias is a result of a procedure which produces inferences that consistently overestimate/underestimate some characteristics of the population. Sampling bias is reduced by making independent observations at random i.e. random sampling. To utilise the inference of the sampled population to total population with regard to rock joints, it is imperative that sampled joints are as accurate as possible. However the accuracy is generally limited by the environment in which joint mapping is carried out, i.e.:

a. visible parts of joints are limited;
b. limits in accuracy of direct and indirect measurements;
c. joints at a distance cannot be directly measured;.
d. the difference between joints and other fractures is subjective.

With the above limits in mind, it is possible to have a reasonably accurate inference between the sampled joints and the whole joint population in the area of interest by carrying out a joint survey as described in the next sub section.

2.5.1 Joint Survey

Joint surveying techniques that can be used for underground mapping are cell or area mapping, scan-line mapping and interpretation of joint data from orientated drill core. *Cell mapping* involves systematically dividing the face to be mapped into zones of equal lengths called cells. Structural data are then mapped in areas

called cell windows (hence the name window mapping). Cell windows (Figure 2.7) usually have square dimensions (Nicholas and Sims, 2000). The actual mapping involves visually identifying joints within the cell window and recording their orientations, lengths, spacings and roughness etc. More effort should be dedicated to identifying as many individual joint sets as possible and as a rule of thumb, a joint that dips at a variance greater 20º from the average is recorded as a distinct joint or set. The *scan-line mapping* technique involves measuring all the joints that intersect a scan-line along its length (Figure 2.8). A measuring tape is usually used as a scan-line and only the properties of those joints that cross the tape are recorded. An *orientated drill core* is an indirect scan-line that can be used to measure orientations and joint spacings in unexposed rockmasses. It involves measuring and recording joint properties from a recovered drill core. Its main drawback relative to the other mapping methods is its inability to measure joint length data, the lack of continuous sample and the loss of orientation in regions of highly fractured ground and core loss.

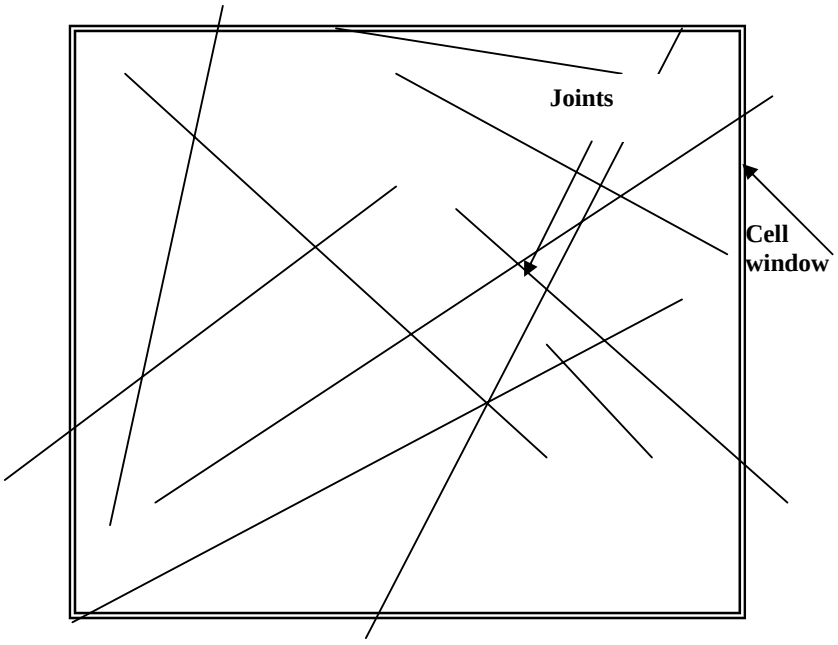

Figure 2.7 Cell window and joints in cell mapping

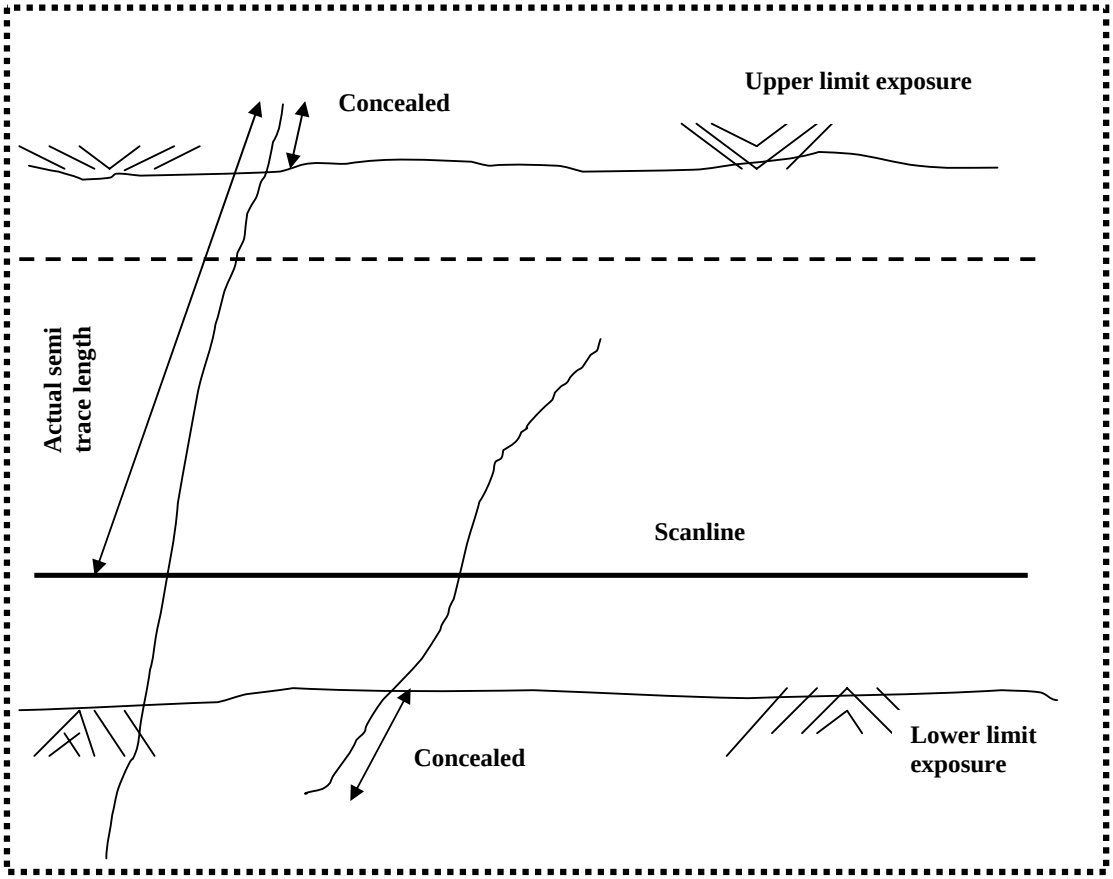

Figure 2.8 Trace lengths mapping in a scan-line survey (after Priest and Hudson, 1981)

Both cell and scan-line mapping techniques have the disadvantage of only mapping exposed surfaces, thus they cannot be used in determining joint properties behind the exposed surface. In scan-line mapping, less (to none) geological judgment is required during the actual data collection, hence not much geological mapping experience is required. In cell mapping, more data are collected over larger areas, but data from scan-line mapping represent more detailed information per specific location. The two methods can be combined (strip mapping) with some success, as was done in the joint mapping at Mount Isa Mines by Landmark and Villaescusa (1992). When the two methods were compared in the Mount Isa Mines project, line mapping was found to be slow, but accurate, while cell mapping was found to be less accurate, but more

measurements were taken. Listed below are the general advantages of scan-line mapping over cell mapping, as experienced by the corresponding users:

- Accurate (Landmark and Villaescusa, 1992).
- Systematic and easy to control (Piteau, 1970; 1973; Brady and Brown, 1993).
- Data from line sampling is easy to further process and analyse (Priest and Hudson, 1981 and Piteau, 1970).

Advantages of cell mapping over scan line mapping:

- Fast i.e. more measurements are taken (Mathis, 1987 and Landmark and Villaescusa, 1992) especially considering the limiting factors in underground mapping, which are time, access, lighting and exposure.
- Sparsely scattered joint sets are not readily detected with scan-line mapping, but are generally detected by cell mapping, hence local variations in properties are easily detected resulting in better knowledge of variability (Mathis, 1987).

Due to onerous conditions in gold mines and the need for an extensive joint database only the scan-line mapping technique was used in the dissertation. It is therefore imperative to provide a description of the biases that maybe encountered during scan-line mapping.

2.5.2 Sampling bias during scan-line mapping

They are four main biases introduced during scan-line sampling (Terzaghi 1965, Priest et al, 1981; 1985; Villaescusa et al, 1990; Kulatilake et al, 1984; 1993; 1995): orientation, size, truncation and censoring. These main biases will be dealt in turn.

Orientation bias

Joints that are perpendicular to the sampling line (scan-line) have a higher probability of being sampled than joints that are parallel to the line, hence the introduction of orientation bias. Terzaghi (1965) showed that the numbers of joints from joint sets that are sub-perpendicular to a scan-line are greater than the

numbers of joints from sets that are sub-parallel to the sampling line, as depicted below.

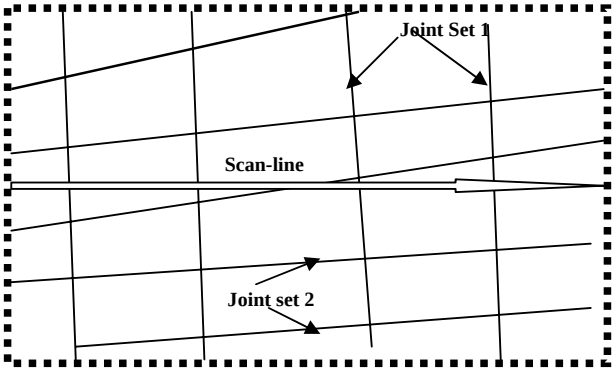

Figure 2.9 An illustration of joint orientation bias in a scan line survey

Given the scenario in Figure 2.9, for every four set 1 joints only one set 2 joint will be mapped. Thus the number of surveyed joints will vary with varying line orientation. Theoretically, three orthogonal sampling lines have to be mapped to minimize the bias, but establishing a vertical sampling line of sufficient length in an underground environment is usually not practical. The joint orientation bias is corrected for by using the formula below:

$$N'_{\delta j \vartheta j} = N_{\delta j \vartheta j} \frac{1}{\cos\left|\vartheta_I - \vartheta_j\right|.\cos\left|(\delta_I - \delta_j) - 90\right|}$$

Where, $N'_{\delta j \vartheta j}$ represents the number of joints that would have been collected had the sampling line been perpendicular to all the joints sampled. $N_{\delta j \vartheta j}$ is the number of joints that fall into the class interval defined by mean dip and dip directions δj and ϑj respectively. The derivation of the above equation is given in Terzaghi (1965). δj and ϑj are the dip and the dip direction of the excavation.

Standard length correction

Size bias is due to the fact that the probability of joints being sampled is proportional to the size of the joint. Both size and orientation biases affect all joint properties. Truncation bias is due to the tendency of systematically excluding small joints, which results in an increase in sample mean. As shown in Figure 2.8, the full trace length of some joints can be unobservable, thus the generation of censoring errors. The correction is made to reduce all data to that which would have been sampled had the sampling been done along a standard length L_s, instead of the actual sampling length, L (Robertson, 1977; Kulatilake et al, 1984; 1993).

$N''_{\delta j \vartheta j} = N'_{\delta j \vartheta j} L_s/L$

Where $N''_{\delta j \vartheta j}$ is the number of joints in a given class interval that would have been sampled had the tunnel been of the standard length L_s.

2.6 Joint Data Processing

Data from joint mapping are numerous and have to be processed first before making any engineering judgment. In this dissertation the following approach was used:

i. Determination of structural regions by analysing results with the Data Interpretation Package using Stereographic projection (DIPS) software from Rocscience to define zones with similar orientations.
ii. Determination of joint sets by defining the sets from DIPS.
iii. Determination of joint set properties such as lengths and spacings.

To adequately characterise joint properties, the following assumptions, as suggested by Kulatilake (1988), Piteau (1970), Robertson (1977), Steffen (1978) among other researchers, are adopted:

- all joints are planar;
- the size distribution of joints is independent of spatial location.

Stereographic projections are a convenient means of presenting geological data such as joints, faults, etc. A stereographic projection is a means of displaying three dimensional orientations of linear and planar features without regard to spatial relations. For more details on the construction and formulation of stereographic projections and stereonets, the reader is referred to Priest (1985), Hoek and Brown (1982). Data in stereographic projections can be represented by two types of nets namely the Wulff net (equal angle) and the Schimidt net (equal area). Data Interpretation Package using Stereographic projection (DIPS) is a computer program that uses the stereographic principles. It allows the user to analyse and visualise structural data following the same techniques used in manual stereonets. Furthermore, it has many computational features such as statistical contouring of orientation clustering, mean orientation and confidence calculation, cluster variability, qualitative and quantitative feature attribute analysis. Figure 2.10 is an example of joint orientations plotted using DIPS software.

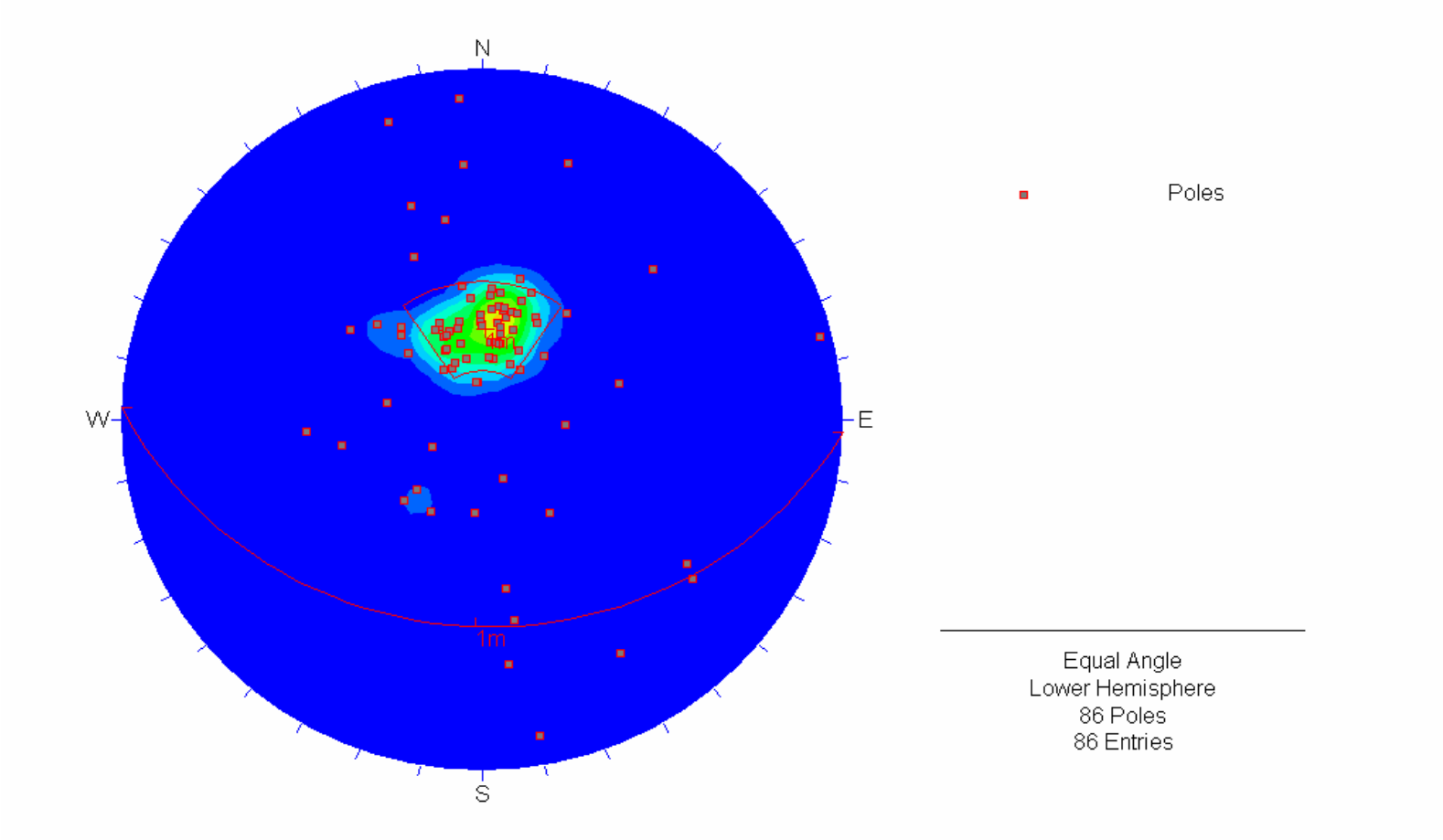

Figure 2.10 An illustration of joint orientation from DIPS software

2.7 Discontinuity survey and technology

Although the above conventional methods of measuring and analysing joint properties are easy to execute, limitations associated with their use are:

a) they are time consuming;
b) they are labour-intensive;
c) they require the physical contact with the rock surface, and
d) there is often limited access to areas of the rock surface, usually due to safety restrictions, but also due to the tendency of many mines to utilise backfill, shotcrete or wire mesh as support, obscuring the surface soon after excavation.

Consequently, data obtained are often incomplete. This might affect the reliability and accuracy of mapping data, hence the recent development of sophisticated mapping and analysing techniques. The latest developments in joint mapping include the use of the photogrammetry principle in which a 3-D joint map is produced from digital images of the rock face. It involves 3-D mapping by measuring images of the object concerned using the principle of triangulation. Reid and Harrison (2000), Beer et al (1999), Harrison (1993) and Franklin et al (1988) have applied this principle in characterising fracture geometry. Windsor and Robertson (1992) utilised an electronic compass, an electronic notebook and computer software to map fractures in a granite quarry.

Other recent techniques can be developed for specific rockmass exposures in conjunction with the mentioned method. For example, in a case study on rockmass exposures in Sweden by Feng et al (2001), close range digital photogrammetry and a geodetic total station were used. The total station was used to establish a local coordinate system and for capturing control points from the image coordinate system into an object coordinate system. Du et al (2001) showed how information on rock discontinuities could be obtained by using Geographic Information Systems. Hadjigeorgiou et al (2003) used common photographs in an approach to limit time spent in discontinuity mapping. Their study involved comparing performances of different algorithms in sensing geological features from photographs. Hammah and Curran (1998) demonstrated the use of a fuzzy based

algorithm to solve the issue of joint set delineation in discontinuities. The most notable advantage of the clustering technique introduced in Hammah and Curran (1998) is the incorporation of other measured joint properties such as spacing and roughness during joint set delineation. Feng et al (2003) again used the geodetic total station, but this time as a point-sensor laser-scanner to automatically scan a defined area of the fracture surface. This is a non-contact method for measuring surface roughness and the roughness results are almost equivalent to those of the 3 D strip sensor laser scanner that is usually used for laboratory roughness studies. Adams and Jager (1980) used a petroscope for mapping fractures ahead of a stope face. The procedure involved inserting a petroscope into a borehole using extension bars and then observing the position and direction of fracturing. Rorke and Brummer (1985) described the use of a two camera system to map fractures in underground excavations. The photographs are processed by stereo-photographic principles to obtain three-dimensional discontinuity images.

Recently CSIRO Exploration and Mining, a division of CSIRO Australia, has developed Sirovision. It is a structural mapping technique used for complete rock structure analysis using imaging, laser-scanning and photogrammetric techniques. The original version was developed in the early 1990s and the current system, which is comprised of two components and has been under development over the last five years, was released for use about three years ago. Its components are Siro3D and Sirojoint. Siro3D is the imaging system while Sirojoint is the structural mapping and analysis system. Siro3D provides the facilities for the creation of 3D images and plan mapping tasks using 3D images. It also uses 3D images to obtain spatial data and the information can be exported to other mining software. On the other hand, Sirojoint provides facilities to analyse discontinuity sets and structures, to visualise structure, and can even display a detail of the 3D video image from which joints are mapped (www.em.csiro.au/mine_environment_imaging/capabilitie/ 22/10/2004). For orientation measurements an orientation plane is identified and defined. After that the ‘underlying’ 3D spatial data can be used to estimate the position and size of the plane by using the spatial location of each point within the boundaries of the

selected plane. Identifying and defining a plane involves selecting any set of points in space (polygon). Sirojoint then uses the spatial location of every point in the selected polygon to estimate a plane orientation that is the best fit of all points within the polygon (refer to the Figure 2.11 below).

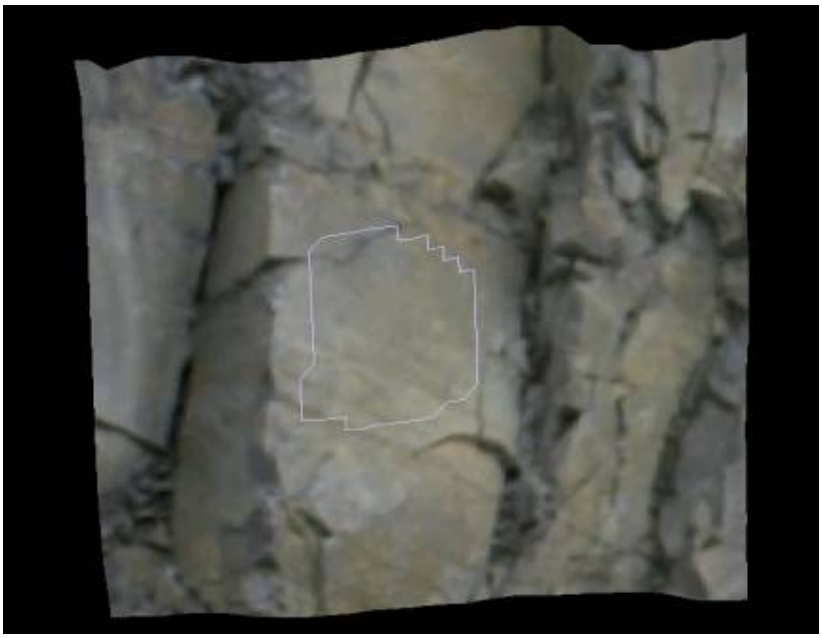

Figure 2.11 Estimation of a joint plane on the left by a polygon (www.em.csiro.au/mine_environment_imaging/capabilities/imaginganddata)

In conclusion, the current trend in rock joint characterisation is towards developing specific techniques for a particular mapping exercise and building on developments from other fields including imaging techniques, simulation, surveying techniques, fuzzy mathematics, stereoscopic methods, laser and radar scanning etc. Most of these latest joint characterisation techniques would have been appropriate for this dissertation but were not available.

2.8 Summary and conclusions

The relationship between rock material, rock mass and discontinuities has been demonstrated. Rock material is considered as a continuum in most engineering applications while a rock mass is a discontinuum. Discontinuities are planes of

weakness in a rock mass, i.e. planes along which failure in the rock mass is likely to take place. Joints are by far the most common and abundant type of discontinuity. They can be mapped and analysed statistically into sets having common properties. Joint mapping methods have been discussed with emphasis on the scan-line mapping technique since this method is the one employed in this dissertation. The latest joint mapping techniques were reviewed by demonstrating the trend from physical to mechanical and, finally, to the latest semi-automated mapping techniques.

This is the background to the description of detailed joint mapping exercises in two gold mines, which is dealt with in the next chapter. A review of the joint mapping that has been done in the past for underground South African gold mines will be followed by a detailed description specific to each mine.

CHAPTER 3

JOINT MAPPING IN TWO MINES

3.1 Introduction

In the previous chapter important joint parameters and methods of collecting them were described in some detail. In this chapter, the application of these techniques to mapping is demonstrated. The work described in this chapter assumes the validity of the following geological propositions (Piteau, 1970):

(i) structural discontinuities are detectable features of a rock mass and can be described quantitatively;
(ii) structural regions exist in a rock mass.

Joint mapping was carried out in two gold mines i.e. South Deep Gold Mine which is jointly owned by Placer Dome and Western Areas mining companies and Tau Tona Gold Mine a subsidiary of Anglogold Ashanti. In the first sub-section (3.2), a brief description of South Deep Gold mine, mining operations and other relevant information is given. The description in sub-section 3.2.4 includes a detailed procedure on the line survey carried out at the mine. The statistical manipulation of the collected joint data is explained in sub-sections 3.2.7 and 3.2.8. Joint mapping carried out in Tau Tona mine followed the same procedure and the description is given sub-section 3.3. Sub-section 3.4 is a conclusion on the statistical results on the joint mapping and the characteristics of the joint sets of the two mines.

3.1.1 Review of joint mapping in underground gold mines

Most of the work relevant to joint mapping data for underground gold mines was documented and published in the late 1970s and early 1980s. In most cases joint mapping was done as a secondary procedure, the primary aim and emphasis being to map fractures ahead of the mining face. As such, most mapping was done from drill cores, and joint properties such as lengths and spacings were not recorded. In fact, all published papers indicate that the mapping was limited to joint orientations (Kersten, 1969; Van Proctor, 1978; Adams and Jager, 1980; Hagan, 1980; and Brummer, 1987). Hagan (1980) gave a relatively detailed description of joint properties, referring to the vertical orientation of quartz filled joints and estimating their spacing to be between 0.2 m to 2 m. Again, however, there was no mention of other properties, but he did acknowledge that the interaction of joints (including bedding planes and minor faults) and stress induced fractures were responsible for the hangingwall instability at the then Western Deep Levels gold mine. Van Proctor (1978) also mentioned the tendency for stress induced fractures in the quartzite hangingwall to follow quartzite filled joints. Besides this information, no other documented information on joint properties in South African gold mines was available in spite their important effect on stability of excavations.

3.2 Location and Geology of Mine One

South Deep Mine, similar to most gold mines in the Witwatersrand gold basin, is tabular and is mined at deep to ultra deep levels (more than 2400m deep). Mining at these depths is characterised by high stresses, seismicity, heat and the prevalence of stress induced fractures. The mine is situated approximately 50 km west of Johannesburg and 20 km south of Randfontein (refer to Figure 3.1). It is bounded by Kloof and Libanon gold mines at its western side and Randfontein Estates Gold mines at its northern side.

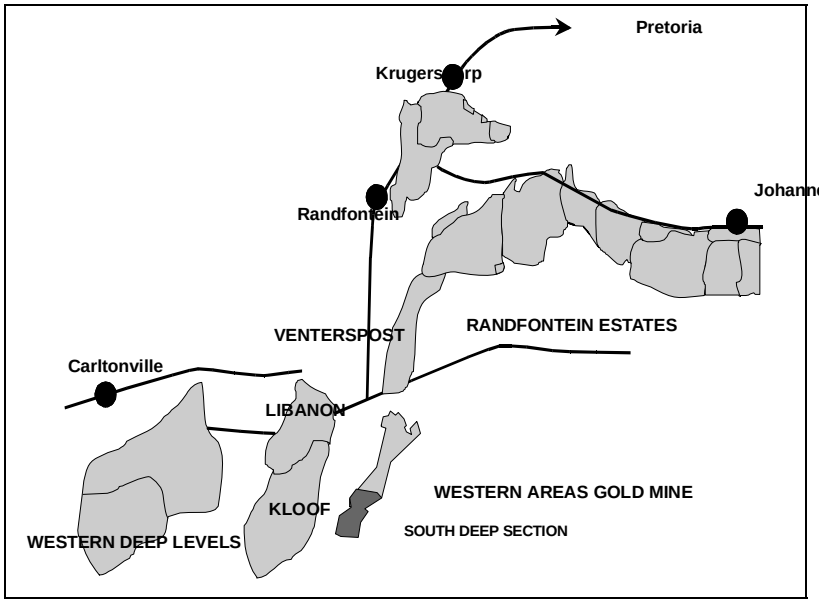

Figure 3.1 The location of the mine relative to neighbouring mines (Nagel et al, 2004)

Gold-paying reefs are the Ventersdorp Contact Reef (VCR) and the Upper Elsburg reef. The Ventersdorp Lava overlies both reefs while the footwall package is made up of the Elsburg formation. The Upper Elsburg thickens towards the east forming a wedge with a maximum thickness of 120m (Figure 3.2) (South Deep Mine Code of Practice, 2003). Unlike the massive Upper Elsburg reef, the VCR has an average thickness of twenty centimetres.

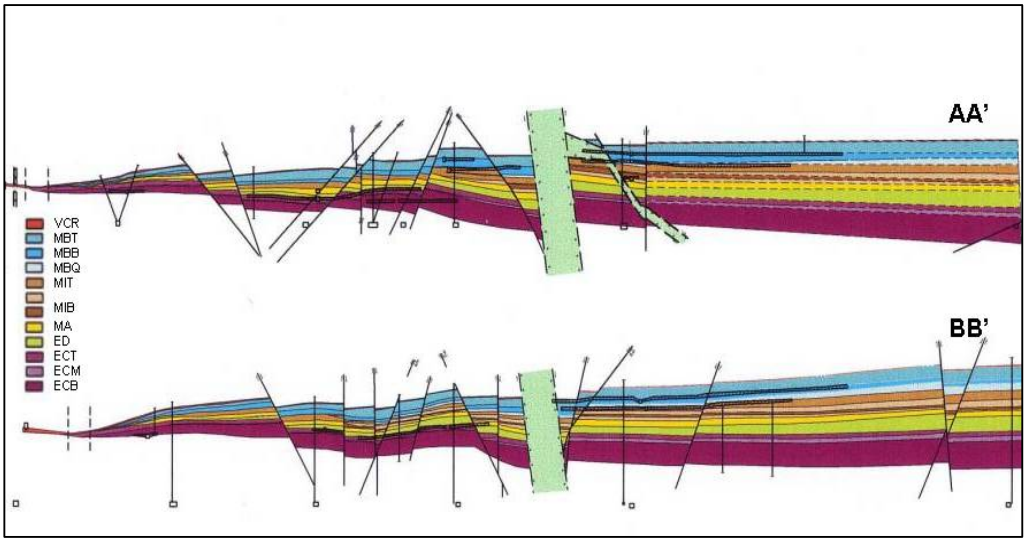

Figure 3.2 Elsburg reef stratigraphy (Joughin et al, 2004)

Due to variation in the size and thickness of both reefs, different mining methods are applied for each reef. In the western boundary of the mine, only the VCR is mined by the conventional tabular narrow reef mining method. As depicted in Figure 3.2, the thickness of the ore body gradually increases towards the east resulting in a different mining method being applied. For thicknesses that are more than 5m, the trend is to first mine an intermediate tabular mining cut (1.5m to 2.0m) and then mine the remaining ore body using massive mining techniques (Joughin et al, 2004).

3.2.1 Discontinuity characteristics

As in most underground gold mines in South Africa, geotechnical mapping at South Deep Mine is restricted to areas of specific concern i.e. where greater characterisation of the rockmass is required. These areas include dykes, major faults and any other geotechnical areas where there are high levels of instabilities. With regard to joint mapping, there has been no systematic mapping done and the only available documented joint data are in Table 3.1 (South Deep Code of Practice, 2003). This further highlights the already mentioned fact that there is no

systematic joint mapping in gold mines. For instance, recording joint geometry (orientation, spacing and length) as being variable in Table 3.1 says little, as variability is one of the typical joint characteristics and such quantification or description has limited engineering application.

Table 3.1 General discontinuity characteristics at South Deep Mine

	Faults	**Dykes**	**Joints**	**Bedding planes**
Strike	ENE and SSW	N and E	Variable	Parallel to reef
Dip	70° to 90°	70° to 90°	Variable	Parallel to reef
Spacing	1m to 30m	5m to 500m	Variable	0.2 to 2m
Infill	Fault gouge	Dolerite etc	Calcite, quartz etc	None or argillaceous
Persistence	Up to several km	Up to several km	Up to several m	Up to several 100m
Displacement	Up to 15m	Up to 10m	None	None
Thickness	mm to cm	Up to 30m	mm to cm	mm to cm

3.2.2 Discontinuities and stability

Figure 3.3 shows the rockfall accident statistics for the period 2002 to 2004 at South Deep Mine (Nagel et al, 2004). From the graph, there is a lack of consistency in combating falls of ground.

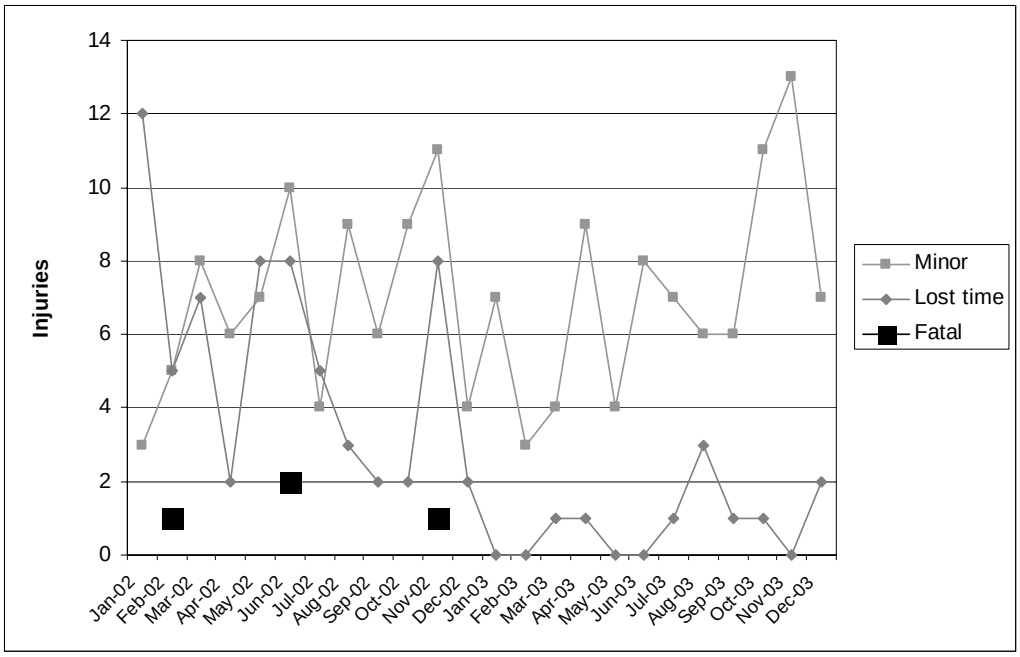

Figure 3.3 Rockfall accident record for the period between 2002 and 2004 (Nagel et al, 2004)

Another internal report on rockfall and rockburst incident analysis (1995 to 2002) indicates that 77% of accidents occurred in stopes (South Deep Mine Code of Practice 2003). To be more specific, 80% of accidents in stopes were on the stope face, 45% being in the middle of the face, 15% in the tight end and 20% at the gully face intersection. Most accidents (57%) occurred between the face the and last line of support. Fall of wedges is the most common failure mechanism (38%), followed by unravelling (15%) and beam failure (15%). 84% of the rockfalls and rockbursts occurred in the hangingwall, while the remainder was evenly split between the face and sidewalls. The Code of Practice (2003) further states that rockfalls in the face and sidewall were mainly due to the combination of least one steeply dipping fracture set (70°-90°) and joints, faults or other extension fractures (Figure 3.4) (South Deep Mine Code of Practice 2003). The above description of common causes of rockfalls further emphasises the statement of the problem for this dissertation. Figures 3.4a, 3.4b and 3.4c show the types of joints and bedding planes found in stopes and development tunnels.

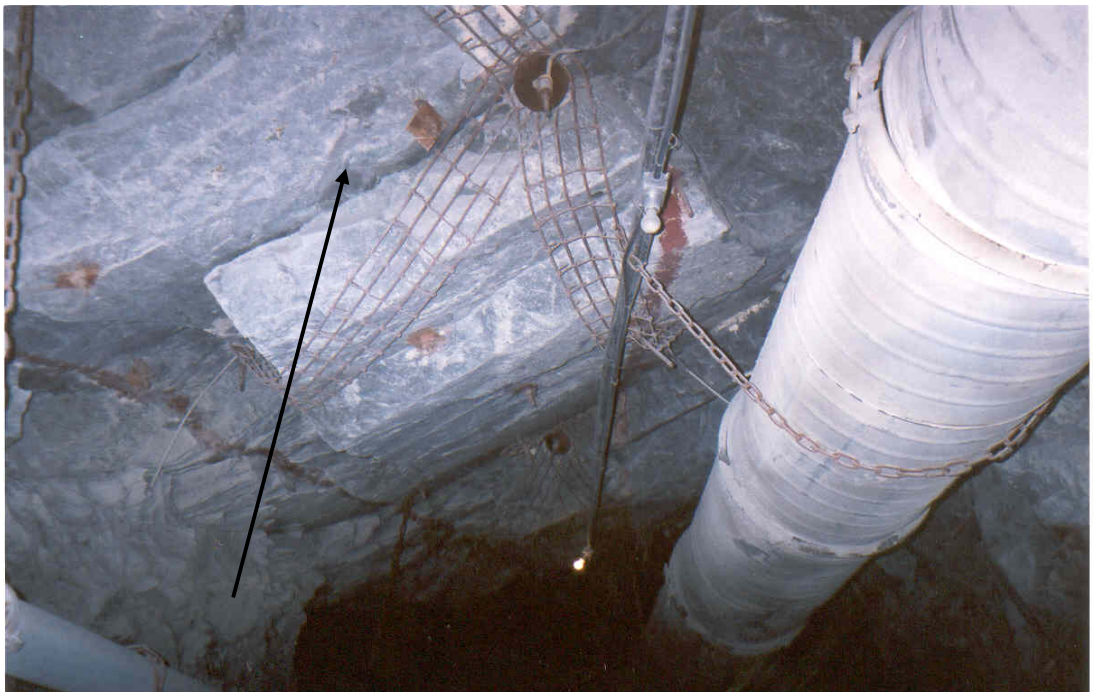

Figure 3.4a Bedding planes in the hangingwall of a development tunnel (Note the benching)

Figure 3.4b Joint planes in stope hangingwall

Figure 3.4c Low angle fractures

3.2.3 Joint Mapping

Joint mapping was carried-out in VCR stopes and in development ends using the scan-line survey technique. A total length of 420m, and approximately 200 discontinuities, were mapped in development ends. More than 150 discontinuities were mapped in stopes over a total length of 450m. Stress induced fractures parallel to the face were not mapped in detail as they were numerous and ubiquitous (parallel and closely spaced), a single measurement was taken and was considered representative enough for the set (Figure 3.5).

Figure 3.5a Stress induced fractures in a development end

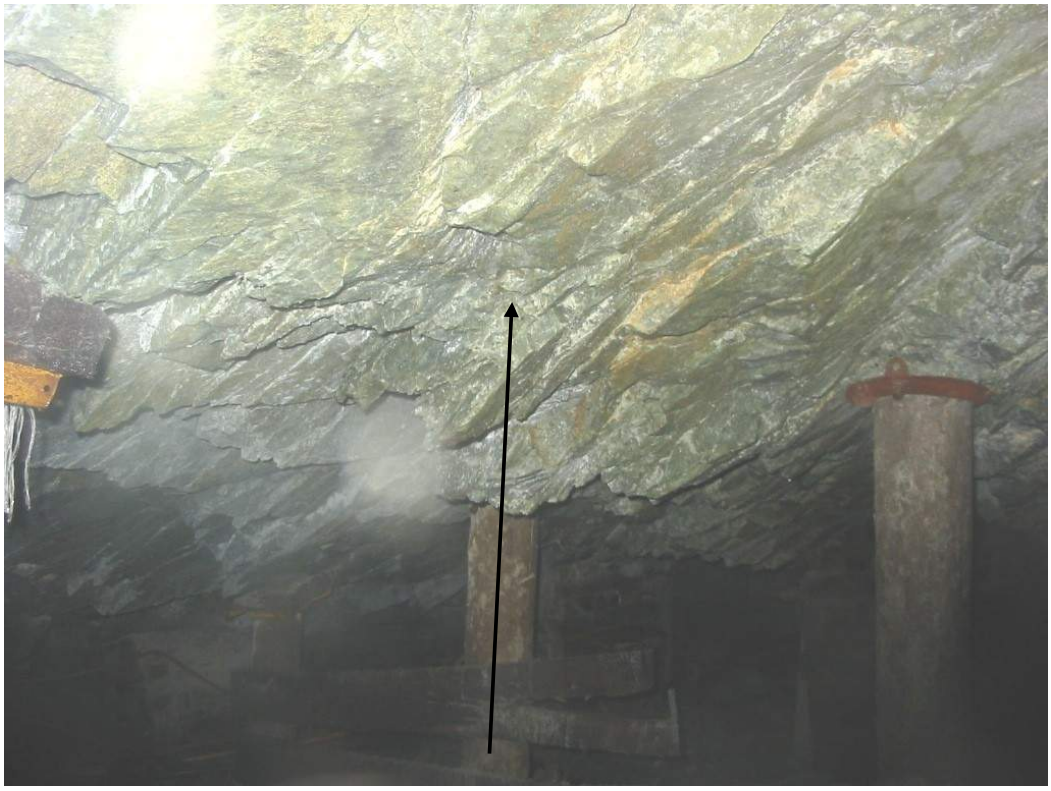

Figure 3.5b Stress- induced fractures in stopes

3.2.4 Detailed Line Survey Procedure

A 30m measuring tape was held straight and tight between two strike gulleys for stope mapping. To avoid tape sag, the tape was looped over rock bolts during development mapping and attached by wire to timber packs or props during stope mapping (Figure 3.6). In development mapping, the tape was aligned with the grade line so that the scan-line had the same orientation as the tunnel. In stope mapping, the tape was run from one gulley to another. Once the tape was fixed, every discontinuity intersecting the tape was measured and recorded. The discontinuity survey sheet used is shown in Figure 3.7. The mapping procedure involved the following:

a) The distance (l_0) along the scan-line (measuring tape); the point where the discontinuity intersects the line. No joint censoring was done.
b) Discontinuity type column; whether the discontinuity was a joint, fault etc.
c) Dip and dip directions were then measured using a compass.
d) Termination of joint planes was noted as to whether they were terminating into or out of the rock mass. Also noted was the distance (l_1) from discontinuity-scanline intersection to joint termination.
e) Any interesting feature of the discontinuity was recorded such as filling, roughness, and, most importantly, the average orientation of neighbouring stress induced fractures.
f) Calculation of the dip and dip directions for the tunnel or stope was done on surface using geosurvey maps.

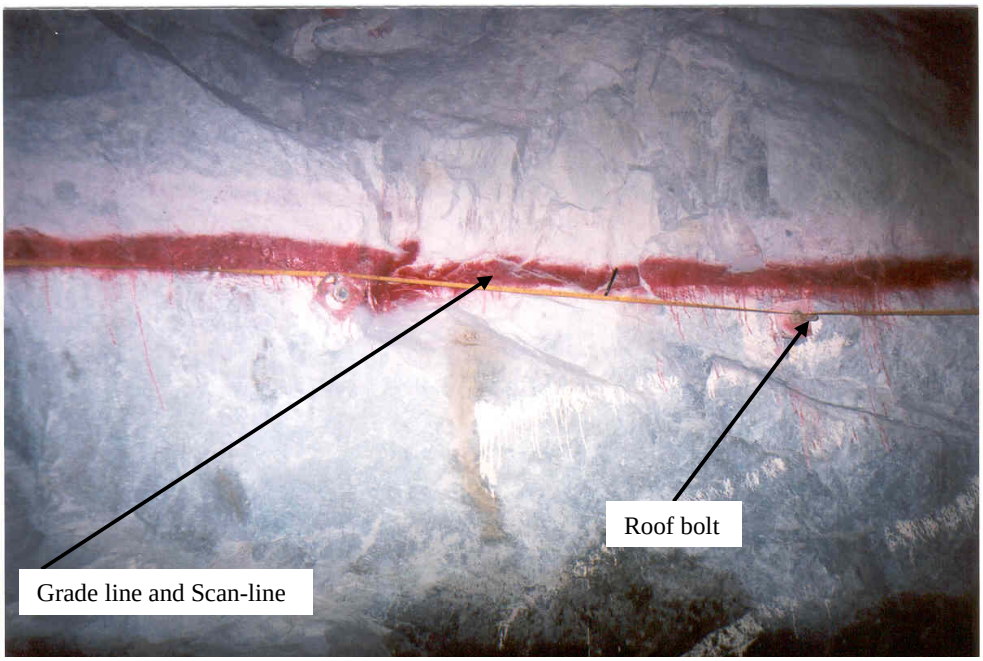

Figure 3.6 Alignment of the tape along the grade line in tunnel mapping. (Note the looping over rock bolts as a means of avoiding tape sag)

Discontinuity Survey Data Sheet														
PROJECT:		Development Mapping		FACE:					LEVEL					
TUNNEL ORIENTATION				SCANLINE ORIENTATION:					FILENAME:					
FROM POS.:		A		TO POS.:		A2			DATE:	2004/05/28				
Msc 2 Mapping				LOGGED BY:		H.G								

Discontinuity Type	Location		Rock			Orientation		Continuity				Remarks
	Distance (m)		Type	Hardness	Surface	Dip	Dip Direction	Dip		Strike		
									Ends	Length (m)	Ends	
B/P (Bedding Plane)	0.7	2.2	Elsburg			33	193				Into RM	No Filling
B/P	1.1	3.3	Elsburg			33	179				Into RM	No Filling
B/P	1.35	3.8	Elsburg			25	189				Into RM	No Filling
B/P	5.7	8.3	Elsburg			25	153				Into RM	No Filling
B/P	6.3	7.2	Elsburg			29	158				Into RM	No Filling
B/P	8.7	11.1	Elsburg			30	180				Into RM	No Filling

Figure 3.7 Discontinuity survey data sheet

3.2.5 Line Survey Results

The diagram below (Figure 3.8) shows areas where joint mapping was carried-out. Measured orientation data (dip and dip direction) from the discontinuity survey sheet was transferred to the DIPS software. The software plots joint positions in space making it possible to visually delineate different joint sets. Once joint sets are identified, joint spacings are then calculated and, together with other properties (e.g. lengths, filling etc), are allocated to their corresponding sets. For analysis of statistical distributions, commercially available statistical software (JMP 4) was employed. In the analysis of results, data from excavations with common orientations were combined (e.g. 90-8 W stopes and 95-6W in Figure 3.8). In instances where the mapped data are considered to be too few for acceptable statistical decisions in individual stopes or combination thereof, the data are added and analysed with the overall data (Figure 3.9b).

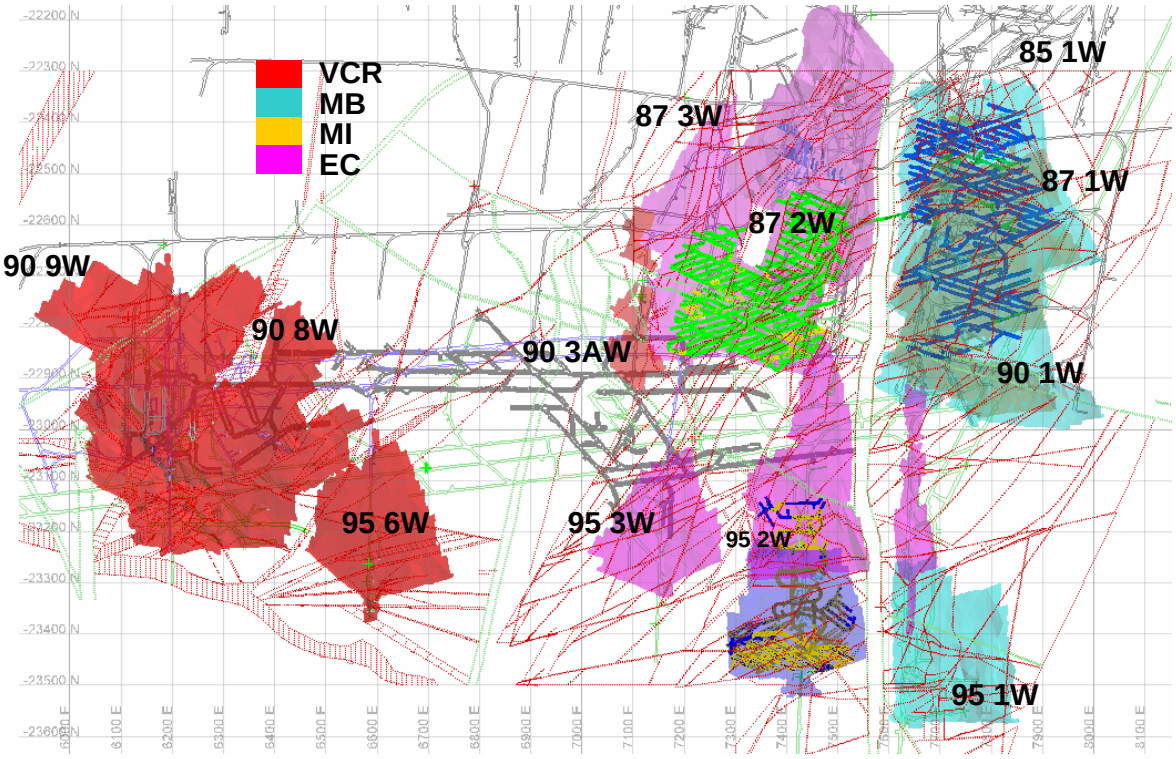

Figure 3.8 Mapped areas

3.2.6 Joint Orientation

An illustration of joint orientation results for one of the Alberton hangingwall lava stopes is shown in Figure 3.9a, and Figure 3.9b illustrates overall joint orientation for all mapped stopes.

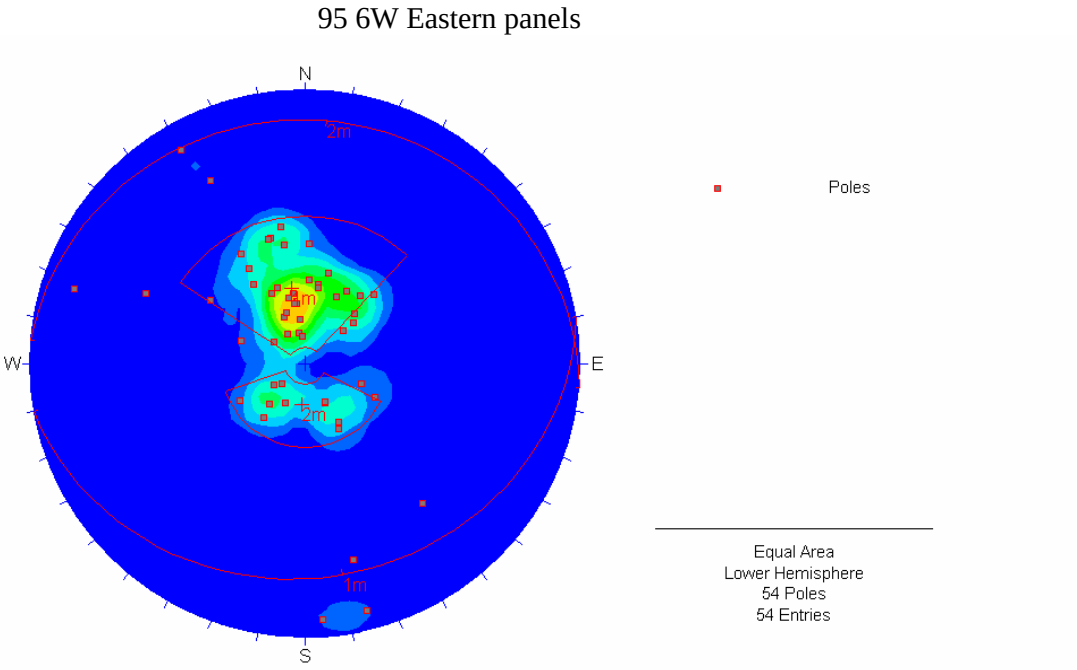

Figure 3.9a Joint orientation in 95 level 6 West Cross cut

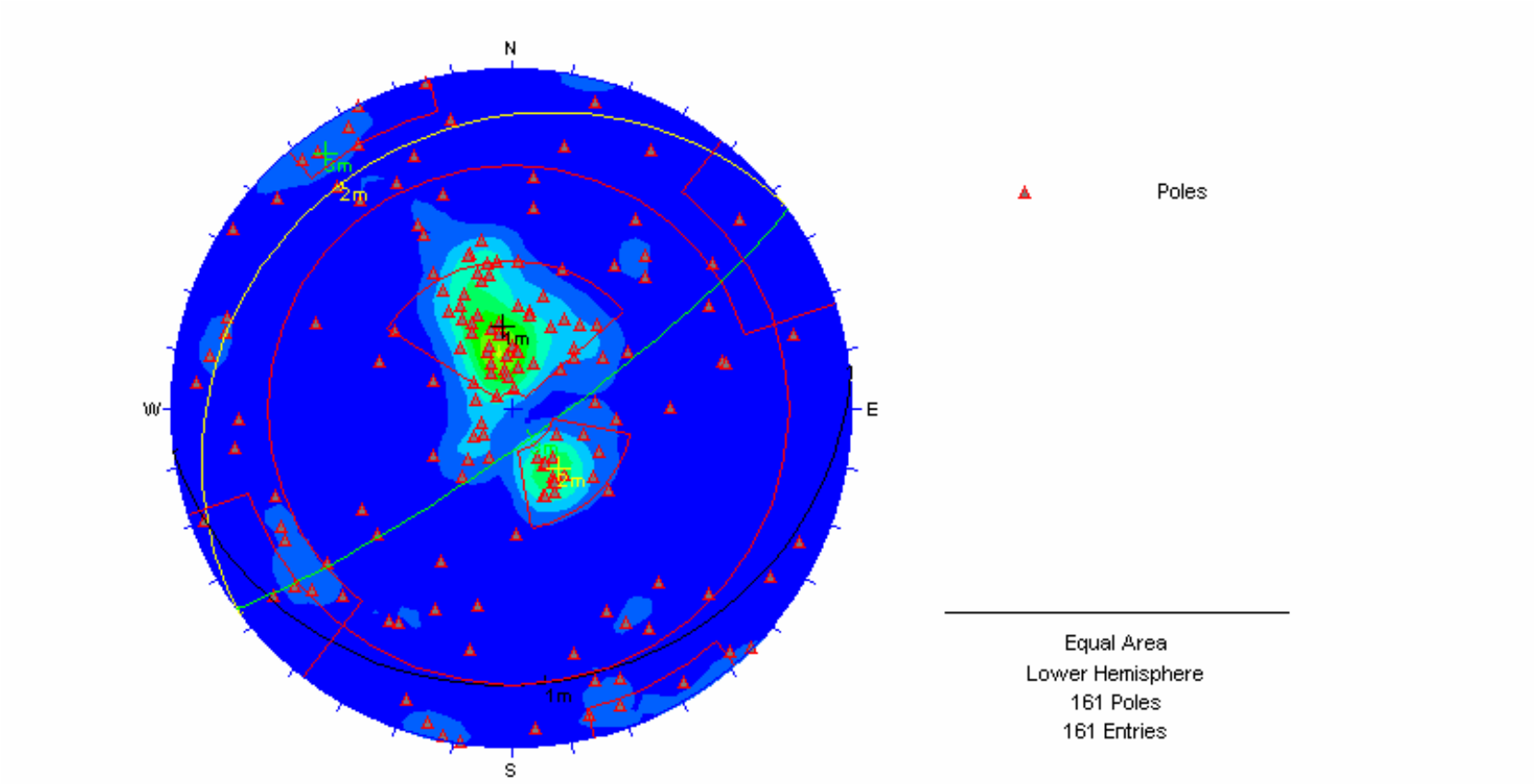

Fig 3.9b Overall joint orientation in hangingwall stopes

Two joints sets were delineated; the dominant set is termed ***set 1*** and the lesser set is termed ***set 2***. The remaining joints mapped are random joints. Average orientations of sets 1 and 2 are 20°/167° and 19°/322° (from DIPS) implying that they are shallow dipping. Most of the joints in stopes were unfilled. However, the few filled joints were steeply dipping and had rough quartzite as the filling material, with a thickness ranging between 2cm and 5cm. Stress fractures were observed to follow the direction of quartz filled joints. This alignment of stress induced fractures parallel to quartzite filled joints was also observed by Van Proctor (1978) during fracture mapping of Doornfontein Gold Mine, although he used the term quartz vein to describe these joints. Statistical distributions of joint orientations were observed to be normal (Figure 3.10a). Their cumulative probability frequency curves demonstrate the typical ***S*** shaped orgive, and analysis of corresponding Box and Whisker plots additionally illustrates the normal distribution of the orientations. A comparison between means and medians indicates a small difference between the two, which is another characteristic feature of a normal distribution. The results correspond well with what most researchers have concluded when analysing joint orientation distributions.

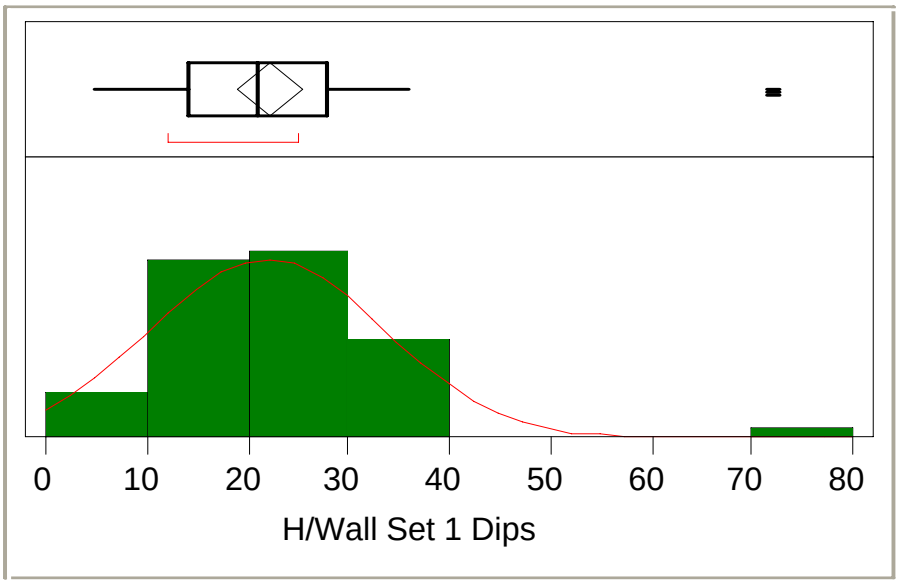

Figure 3.10a Set 1 hangingwall dips

Quantiles

100.0%	maximum	72.000
99.5%		72.000
97.5%		64.800
90.0%		36.000
75.0%	quartile	28.000
50.0%	median	21.000
25.0%	quartile	14.000
10.0%		9.800
2.5%		5.000
0.5%		5.000
0.0%	minimum	5.000

Moments

Mean	22.191489
Std Dev	11.558242
Std Err Mean	1.6859429
upper 95% Mean	25.585116
lower 95% Mean	18.797862

Mean and median comparison

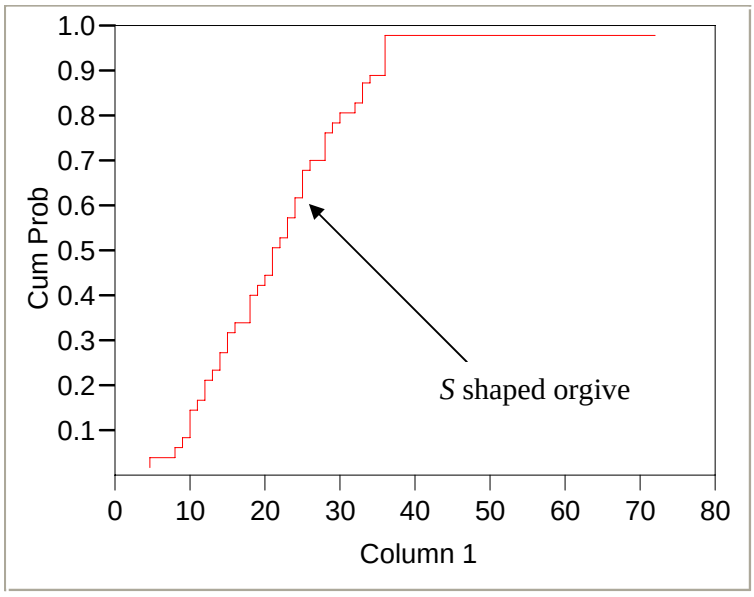

Figure 3.10b Cumulative distribution plots of the hangingwall dips

There is a single shallow dipping dominant joint set mapped in development tunnels, ***set 1*** in Figure 3.11. This dominant set represents a cluster of bedding planes. Quite a few of these bedding planes are filled and whenever they are filled, the filling is usually a phyllonite or quartzite infill, approximately 2 to 3cm in thickness. The phyllonite infill is soapy and very smooth. Failure observations in tunnels, indicate that the most common failure is a result of a combination of these bedding planes and stress induced fractures.

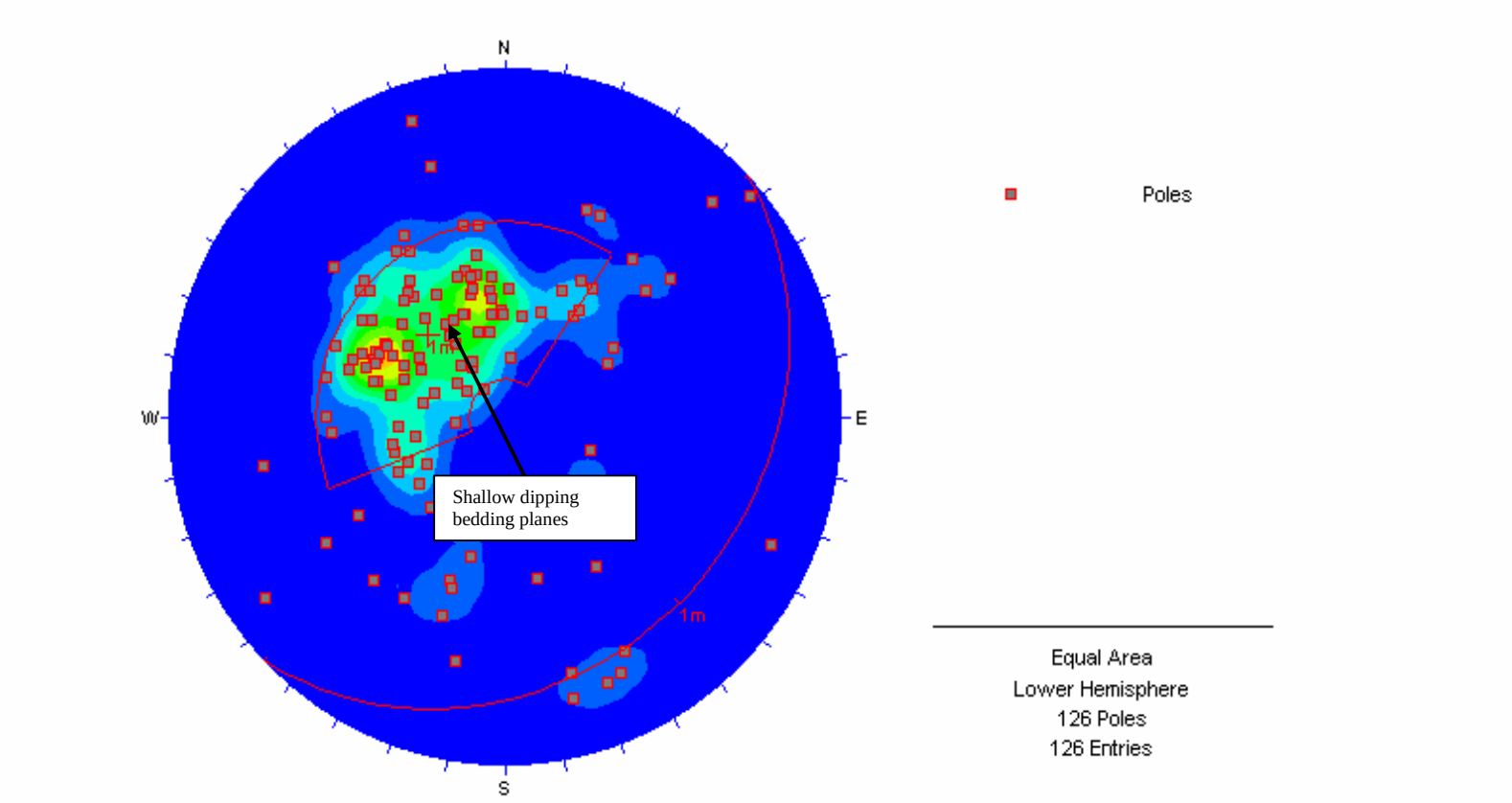

Figure 3.11 Overall joint orientations in the footwall tunnels

3.2.7 Joint Spacing and Lengths

Joint data from a discontinuity survey sheet are entered to an Excel spreadsheet and allocated set numbers identified from the DIPS software. Joint spacings are then calculated as the perpendicular difference between distances x_o and x_1, normal to joint set (Figure 3.12).

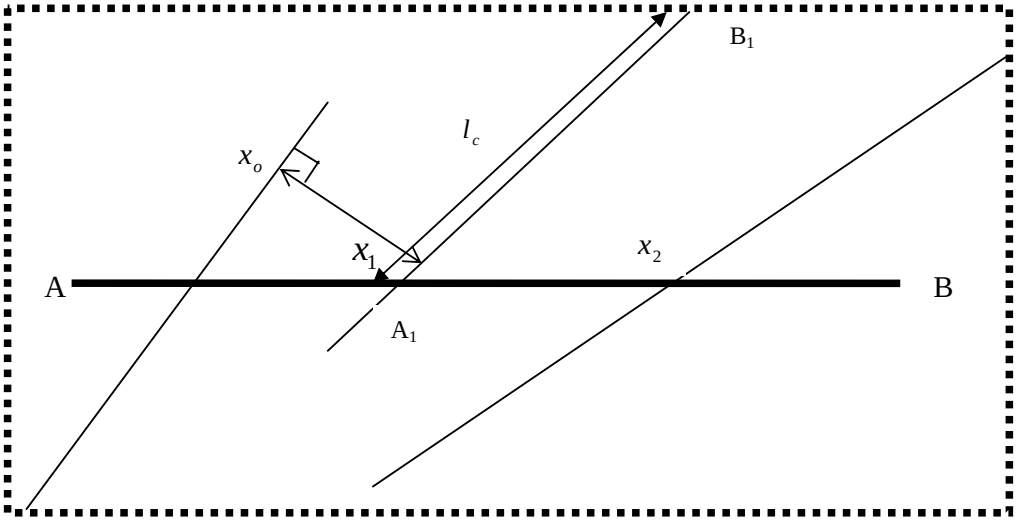

Figure 3.12 Illustration of joint spacing and length measurement along scan-line AB in exposed face

The half trace-length (l_c in the above diagram) was recorded as the distance between A_1 and B_1. The spacing and length calculations described above are performed easily on an Excel spreadsheet for numerous joint data. Analysis of the statistical distributions of joint spacings was done using both the Excel spreadsheet and JMP 4 statistical software. A sample of the conventional methodology used for statistical calculations using an Excel spreadsheet is given in Table 3.2 and Figure 3.13. An illustration of spacing and length parameters using JMP 4 is given in Figure 3.14a and Figure 3.14b.

Table 3.2 Set 1 Cumulative frequency in the Alberton lava

Set 1 Spacing				
Spacing (m)	Frequency (m)	Spacing greater than: (m)	Cumulative frequency	% Cumulative frequency
0 - 1	4	0	4	100
1 - 2.	10	1	14	88.2
2 - 3.	5	2	19	58.8
3 - 4.	0	3	19	44
>4	15	4	34	44

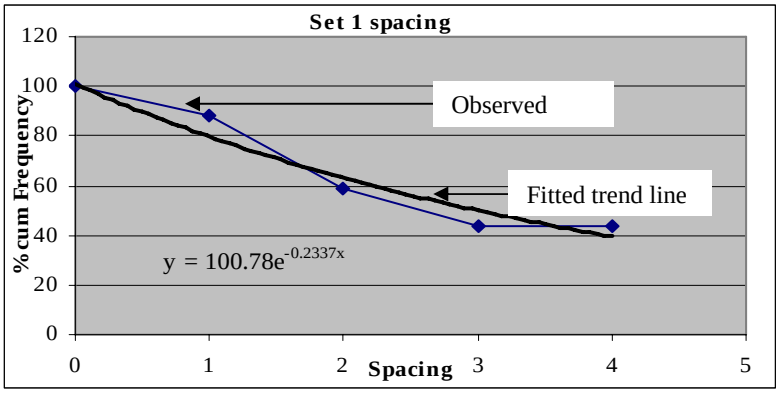

Figure 3.13 A negative exponential distribution in the hangingwall from an Excel spreadsheet

Probability distributions of joint spacing using the JMP 4 software are given in Figures 3.14a and 3.14b below:

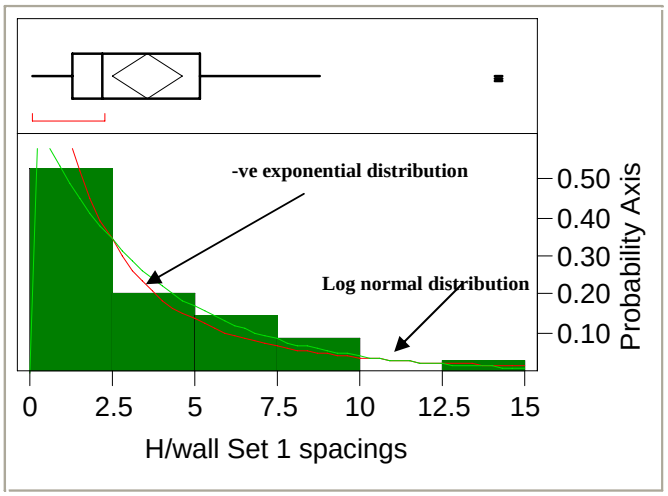

Figure 3.14a Set 1 spacing in the hangingwall lava showing both the negative exponential and lognormal probability distributions

Mean	3.5617647
Std Dev	3.048722
Std Err Mean	0.5228515
upper 95% Mean	4.6255141
lower 95% Mean	2.4980153

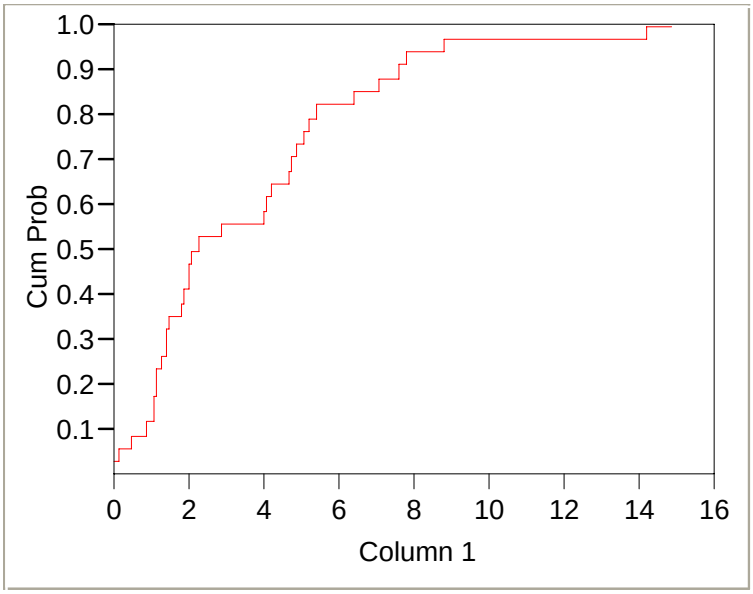

Figure 3.14b Set 1 joints spacing in the hangingwall lava showing a cumulative distribution frequency plot

3.2.8 Discussion of results

A statistical analysis of hangingwall and footwall joint properties confirms a normal distribution for orientation, and a negative exponential distribution for trace lengths. Both negative exponential and lognormal distributions can be fitted for spacings. Only a single joint set is delineated in development tunnels and these joints are the bedding planes. Most of them are not filled and the few that are, have a soapy phyllonite as filling material. The bedding planes showed consistent statistical characteristics with their orientation distributions being nearly ideal. Two joint sets are found in stope hangingwalls. Both sets are shallow dipping, but they have opposing dip directions. Stress induced fractures in the hangingwall were more closely spaced (5-15cm) than footwall fractures (30-40cm). Combinations of steeply dipping stress induced fractures and the shallow dipping hangingwall joints are the main cause of rockfalls in stopes. The hangingwall joints have quartzite as their filling material. Hangingwall joints do not show the same level of statistical uniformity demonstrated by joints in development tunnels (footwall). This can be partly attributed to the fact that bedding planes generally show more conformity and persistence than other joints. Also, in development mapping there is a longer mapping span (continuous) available while in hangingwall stope mapping, the mapping length is limited to a stope face length of 30m.The table below gives an overall summary of results.

Table 3.3 Overall joint data sets for South Deep mine

Hangingwall lava				
Location	**Set**	**Orientation**	**Spacing**	**Semi Trace Length**
		(Dip/Dip Direction)		
95 level 6 west	**1**	23/170	2.5	2
	2	12/05	3.4	2
90 level 9 west	**1**	20/325	6.2	3.5
90 level 8 west	**1**	27/156	6.2	5.3
	2	50/154	2.5	0.6
	3	77/336	2.4	1.3
87 level 3 west	**1**	51/218	5.2	3.9
	2	10/253		
	3	69/56		
	4	88/136		
Overall	***1***	***20/170***	***3.6***	***2***
	2	***19/322***	***5***	***2.5***
	random*	***65-85/160-200***	***1.9***	***1.6***
Elsburg Footwall				
mih	**1**	25/131	5	2
87 level 8 west	**1**	28/151		
	2	28/315		
3b raise	**1**	3/123		
Overall	***1***	***28/130***	***4.3***	***3.3***
	random*	***60-80/140-200***	***5***	***2.6***

Random*; presentation of random joints

3.3 Location and Geology of Mine Two

Tau Tona Mine is about 70 km south west of Johannesburg near the boundary between Gauteng and Northwest Province. The mine is part of the West Wits Operations (refer to Figure 3.15) that has been operating for the past 43 years and, with current mining operations at about 3600m, it is arguably the deepest mine in the world.

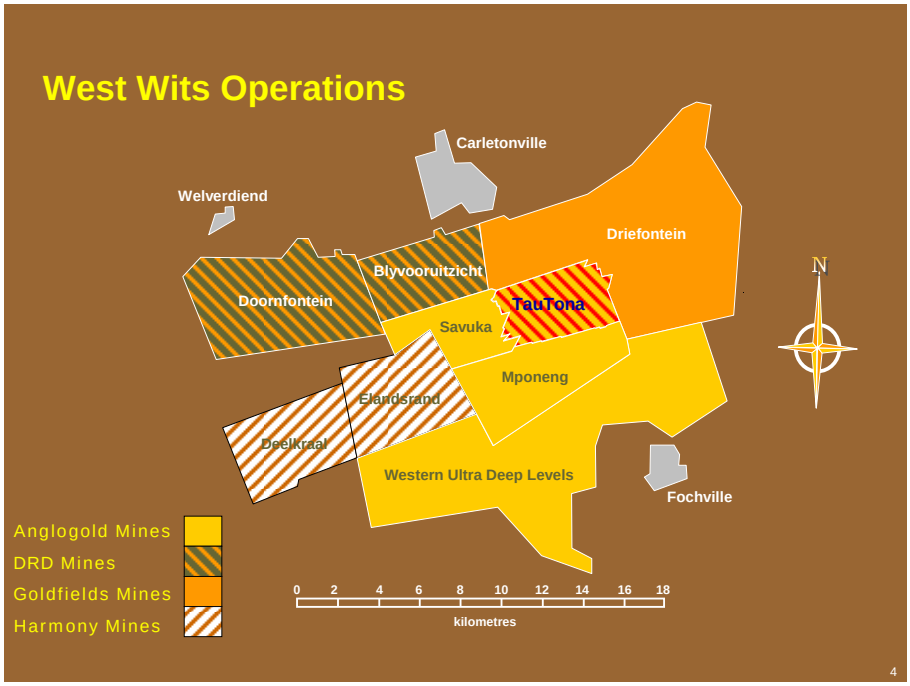

Figure 3.15 An illustration of West Wits Operations showing the position of Tau Tona mine relative to its neighbouring mines (Tau Tona Incident reports 2003-04) (unpublished internal report))

The mine exploits two economically viable reefs, namely the Ventersdorp Contact Reef (VCR) and the Carbon Leader Reef (CLR). Figure 3.16 shows the relative position of the two reefs.

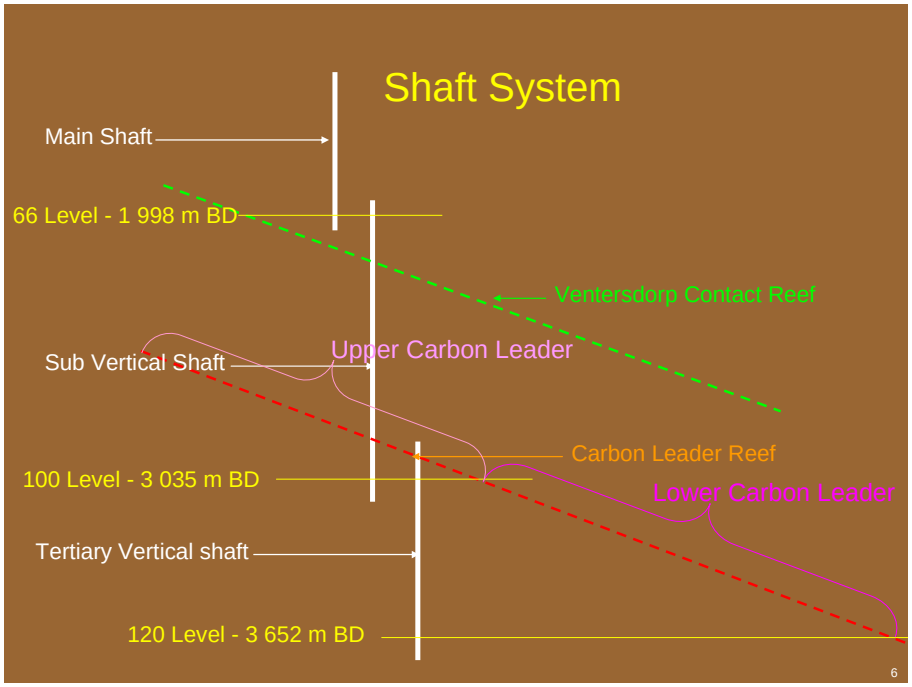

Figure 3.16 Relative positioning of the VCR and CLR (Tau Tona Incident report 2003-04-01 (unpublished internal report))

Ventersdorp Contact Reef (VCR)

Within the mining lease area, the VCR strikes at 62˚ east of north with an average dip of 21˚ southwards. Reef thickness varies from 0 to 5 metres and the reef unconformably overlies the Elsburg Quartzite Formation in the west and Luipaardsvlei Quartzite Formation in the east. It is conformably overlain by lavas of the Alberton formation. Mining of the VCR has ranged between depths of 1500 and 3000m below surface.

Carbon Leader Reef (CLR)

The CLR is a thin tabular, quartz conglomerate formed near the base of a package of quartzite and conglomerate making up the Main Conglomerate Formation. The CLR strikes at 76˚ east of north with an average dip of 22˚ southwards. The Maraisburg Quartzite Formation (MQF) is the immediate footwall rock within the mining lease area. The immediate hangingwall conformably overlies the CLR and is usually clean, highly siliceous quartzite of 2-meter thickness. To date, the CLR

has been exploited to depths ranging from 2300 meters to 3500 meters below surface (Tau Tona Mine Code of Practice, Reference number DME 16/3/2/1-A3).

3.3.1 Discontinuities and stability

There are no documented internal or external reports on rock joint characterisation in the mine. The siliceous quartzite hangingwall is heavily fractured and the fractures combine with joints, faults and dykes to break hangingwall beams into distinct blocks.

An analysis of the general causes of accidents in the mine shows that most accidents are caused by falls of ground (about 30 % in Figure 3.17)

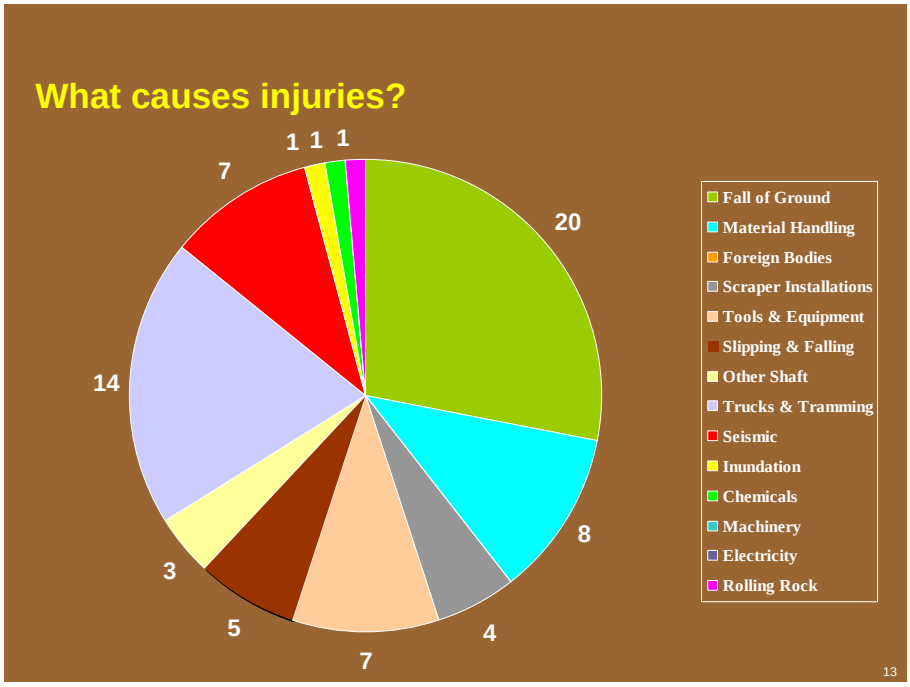

Figure 3.17 Causes of injuries in Tau Tona Mine (Tau Tona Incidents Report 2003-unpublished internal report)

3.3.2 Results on joint geometry

The same procedure as described in sub-section 3.2 was followed for the joint mapping and results analysis. Figures 3.18a and 3.18b are sample plots from DIPS software illustrating joint orientations in the quartzite hangingwall for three stopes and for the overall hangingwall orientation.

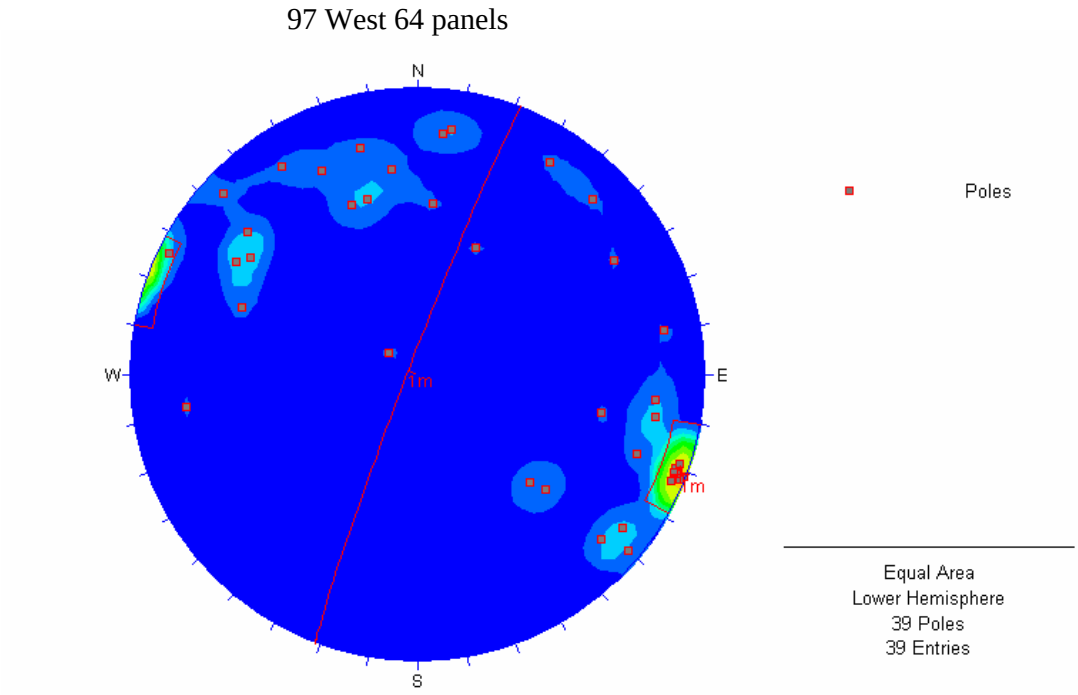

Figure 3.18a Stope hangingwall joint orientations in West 97-64 panels 1, 2 and 3

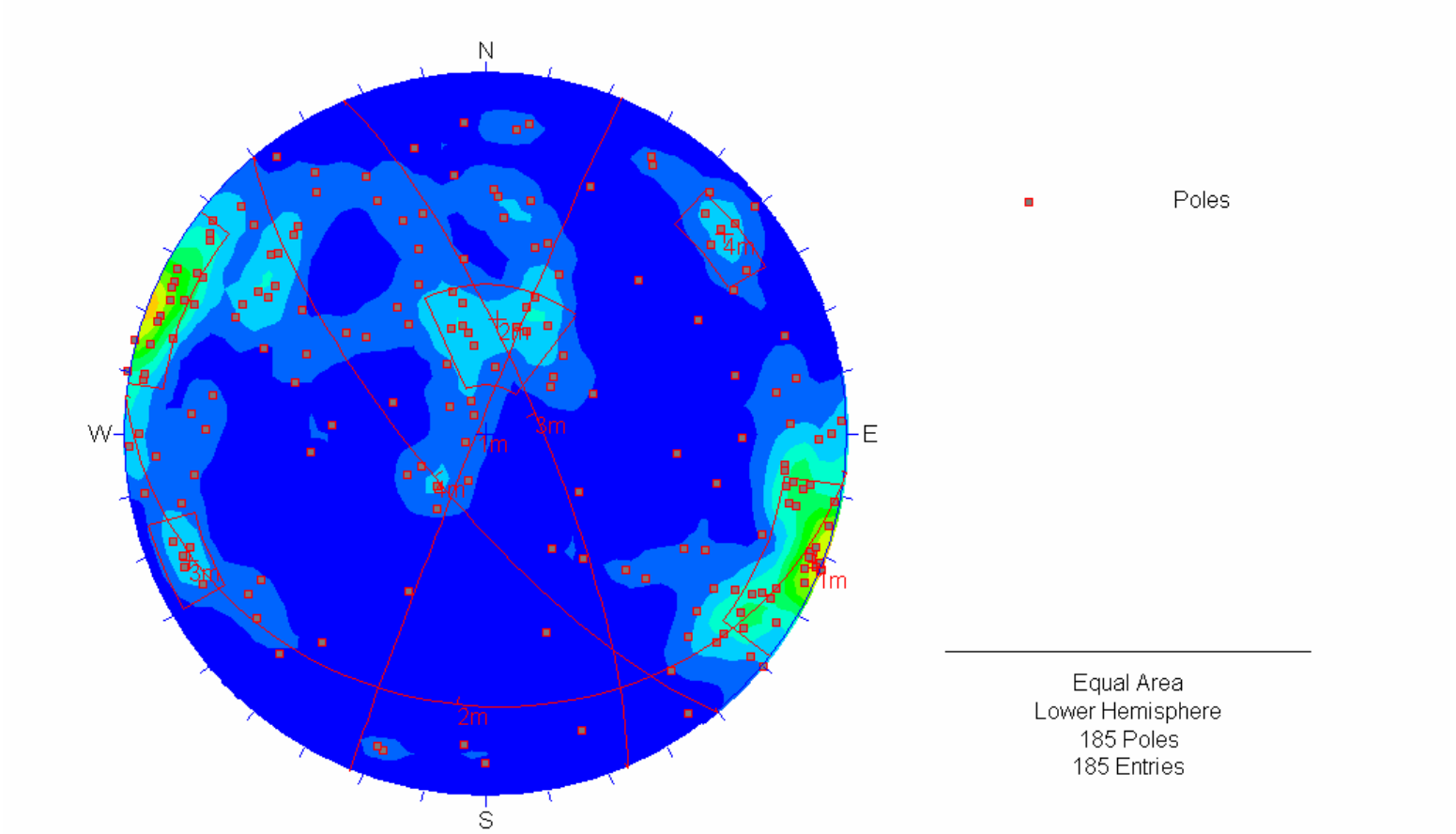

Figure 3.18b Overall hangingwall joint orientations in stopes

The dominant joint set (***Set 1***) is a steeply dipping (88°/292°) quartzite filled joint set. The quartzite infill thickness ranges between 1cm and 5cm. ***Set 2*** joints are shallow dipping (26°/186°) and it is possible that they are represented as the dominant set in South Deep Mine recorded as ***Set 1*** in sub-section 3.2.6. Minor sets (joint ***Set 3*** and ***Set 4)*** are probably an extension of ***Set 1***, but, for easy joint set delineation, they are contoured separately. However, in the analysis of other joint properties such as spacing and length, set 1 and the minor sets (3 and 4) are combined. From the hangingwall orientation results of the two mines it can be concluded that random joints are the most abundant "set" as they contributed 60% of all mapped joints in both instances (62% for South Deep and 63% for Tau Tona). Jointing in the Maraisburg Quartzite Formation (MQF) footwall is similar in many aspects to that of Elsburg quartzite in South Deep. It is characterised by a single dominant set of bedding planes and about 45% of mapped joints are random (compare with 37% for South Deep).

Joint lengths and spacings are statistically analysed using the JMP 4 statistical software. Fitted statistical distribution for spacings and lengths demonstrate similar trends to those of South Deep.

3.3.3 Discussion of results

Two joint sets are delineated in the quartzite hangingwall. Of the two, a steeply dipping and quartzite filled joint set is the more dominant, while the less dominant one is shallow dipping. The interaction of these two sets with random joints and stress induced fractures results in the formation of unstable blocks in stope hangingwalls. An exponential distribution was fitted for joint lengths and both exponential and lognormal distributions were fitted for joint spacing. 63% of hangingwall joints were random compared with 45 % in the footwall. Footwall joints (bedding planes) are usually unfilled and their properties demonstrate a close statistical uniformity. The table below (Table 3.4) is a summary of joint properties in Tau Tona mine.

Table 3.4 Overall joint data sets for Tau Tona mine

Hangingwall Quartzite				
Location	**Set**	**Orientation**	**Spacing**	**Semi Trace Length**
		(Dip/Dip Direction)		
97-64 Westside panels	**1**	87/291		
97-86 panels	**2**	22/175		
99-91 panels	**2**	19/216		
109-112-78 panels	**1**	86/287		
Overall	***1***	***88/292***	***5***	***2.3***
	2	***26/186***	***3.9***	***3.6***
	random*	***40-80/150-180***	***2.1***	***2.4***
Maraisburg Quartzite Footwall				
66-64 Leg 1 and 2	**1**	28/130		
104-105 East Haulage	**1**	30/174		
105 West and Cross cut North	**1**	28/151		
	2	28/315		
Overall	***1***	***23/139***	***3.9***	***4***
	random*	***30-50/170-190***	***3.9***	***2.6***

Random*; presentation of random joints

3.4 Conclusions

In this chapter, mapping of joints in two mines has been described. Mapping was carried out in hangingwall stopes and in development tunnels. A comparison of the joint mapping results from South Deep and Tau Tona mines reveals the following:

a) From the numbers of random joints mapped in the two hangingwalls it can be concluded that in thin reef gold operations, nearly 60 % of the joints are random.
b) The shallow dipping joint set in Tau Tona mine (*set 2*) corresponds with the dominant set (*set 1*) in South Deep.
c) Footwall joints in both mines were consistent in their characteristics and gave nearly ideal statistical distributions. These footwall joints/bedding planes are usually unfilled, although in South Deep some bedding planes were observed to contain a soapy phyllonite filling material. Those in Tau Tona are not filled.
d) Random joints in the footwall make up about 40% of the joints. In both the hangingwall and footwall, random joints constitute about half of mapped joints and are usually steeply dipping. With this orientation, random joints increase the likelihood of unstable block formation, hence enhancing the probability of occurrence of rock falls.

It is believed that these results represent the first measured and documented joint data in the gold mines of South Africa. It would have been ideal to have obtained jointing data for more geotechnical areas in more gold mines. Nevertheless, the mapped and interpreted joint data in this dissertation are more enlightening than the 'traditional' descriptions such as "variable joint geometry", since these 'traditional' descriptions have little engineering meaning. Observations have shown that joints, in combination with stress-induced fractures, form blocks which are potentially unstable. This emphasises the important contribution of jointing to instability and therefore the importance of obtaining jointing

information. Table 3.5 below compares the jointing in the two mines. Now that these joint data are available, it is possible to make use of them to evaluate stability in mining excavations. This is dealt with in the next chapter.

Table 3.5 Overall joint data sets for the two mines

Hangingwall				
Mine	**Set**	**Orientation**	**Spacing**	**Semi-Trace Length**
		(Dip/Dip Direction)		
	1	***20/169***	***3.6***	***2.***
South Deep	***2***	***19/322***	***5***	***2.5***
	Random*	***76/180***	***2***	***1.6***
Tau Tona	***1***	***88/292***	***5***	***2.3***
	2	***26/186***	***3.9***	***3.6***
	Random*	***58 /178***	***2.1***	***2.4***
Footwall				
South Deep	***1***	***28/130***	***4.3***	***3.3***
	Random*	***77/160***	***5***	***2.6***
Tau Tona	***1***	***23/139***	***3.9***	***4***
	Random*	***48/192***	***4***	***2.6***

Random*; presentation of random joints

CHAPTER 4

EXCAVATION STABILTY IN A JOINTED ROCK MASS

Rockfalls in South African gold mines usually result when unstable rock blocks are formed from the interaction of stress-induced fractures with natural jointing in rocks. Bedding planes will usually provide release planes, allowing these blocks to fall. To evaluate realistically the probable dimensions of potentially unstable blocks and the probability of occurrence of rock falls, and to be able to carry out a defensible design of support to cater for the identified potentially unstable blocks, data on joint characteristics are essential. In the previous chapter, the collection and statistical analysis of joint data in two gold mines was described. The work described in Chapter 4 involves the use of these joint set data to predict the occurrence of instability and therefore the extent of support required.

4.1 Introduction

Discontinuities in a rockmass are ubiquitous and as such they intersect to form blocks or wedges. The blocks formed are usually of varying shapes and sizes. Relative block movement is limited by surrounding blocks. However, when an excavation is created in rockmass, the interlocking effect of surrounding blocks is disturbed by the new free surface and usually additional blocks are formed. This results in relative movement of blocks with some falling or sliding into the excavation free face. Movement of a block is controlled by its shape, size, and orientation and, most importantly by other blocks i.e. key blocks (Goodman et al, 1985). As an illustration, creating an excavation in a jointed rock mass shown in Figure 4.1 will result in block “a” falling under gravity and this will trigger a progressive action where blocks “b”, “c”, “d” and “e” also fall under gravity.

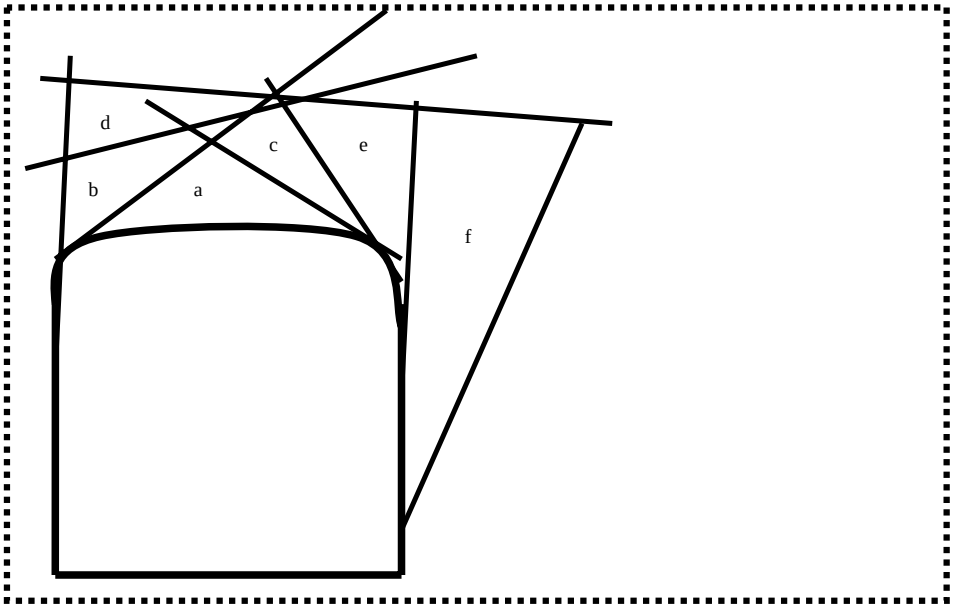

Figure 4.1 Falling and sliding of blocks/wedges in a jointed rock mass

If no action is taken to stabilise the wedges, blocks will continue to fall into the excavation and will probably stabilise by the sliding of block ‘f’, creating natural arching in the rockmass. Wedge ‘a’ is commonly referred to as a keyblock. A keyblock by definition is any finite block that is free to move into free space (excavation) without displacing adjacent blocks. An unsupported keyblock results in hazardous mining conditions in the form of rockfalls. It is the objective of any support system to prevent the falling of keyblocks.

Traditionally, the analysis of excavation stability in jointed rock masses is usually carried out by using rock mass classification systems and simple limit equilibrium analyses. These traditional analysis systems do not provide detailed predictions and descriptions of rock mass instability parameters, thus their usage is only limited to validation and “check” exercises. Detailed excavation stability parameters are obtained by using rock mass models described in the next sub-section. There are no sharp demarcations on the described types of rock mass models, as some tend have overlapping characteristics.

4.1.1 Review of stability analysis in jointed rock masses

Three types of jointed rock mass stability analyses have been identified and these are: numerical, analytical and probabilistic models (Figure 4.2).

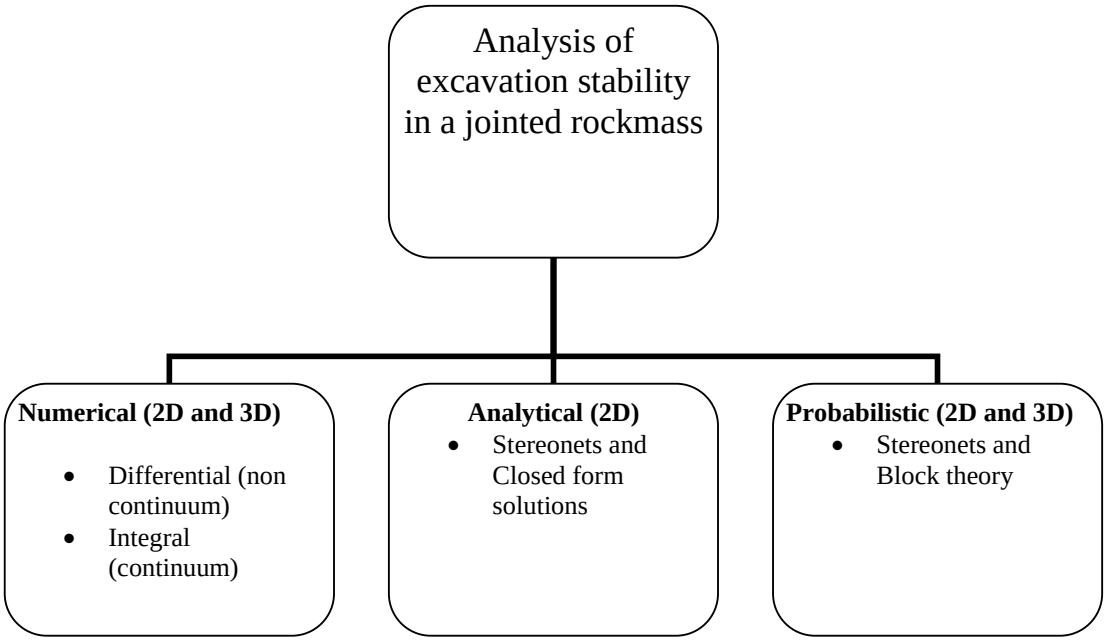

Figure 4.2 Analysis of excavation stability in jointed rock masses

Numerical models are mainly divided into two types namely, the differential and integral methods. Differential methods are usually used to model continuum material hence their limited use in jointed rockmass modelling. The common types of differential methods include the finite element and finite difference models. In fact, among the early proponents of modelling discontinuity effects on rock mass behaviour are Zienkiewicz and Cheung (1966) and Malina (1970). During that era there was widespread use of two dimensional finite element methods for stability analyses. However, the use of differential methods in jointed rock masses is restricted by the limited number of discontinuities that can be modelled and the availability of other efficient modelling tools.

Common types of integral methods are the direct boundary integral method, fictitious stress method and the discrete element method. As already mentioned, there are no sharp demarcations on model types for instance, the discrete element

method can also be classified under differential methods. Due to the limitations of finite element methods, Cundall and Strack (1979) introduced distinct element methods for the analysis of excavations in blocky rock masses. The Universal Distinct Element Code (UDEC) is a two-dimensional distinct element modelling tool that was introduced by Cundall et al (1980) to try and model jointed rock masses more efficiently. Examples where UDEC has been used include Sun and Lin (2002) in the analysis of underground excavations that were envisaged to be used for dumping radioactive waste. A three dimensional version of UDEC, 3 DEC, was utilised by Jakubowski and Stypulkowski (2002) together with the Block Simulation Method (MSB) for stability analysis of a large cavern in Sweden.

Analytical modelling of jointed rockmass instability involves the use of stereonets and closed form solutions. The method is not widely used for underground excavation stability because it gives crude results due to assumptions in the calculations such as infinite joint lengths and the disregarding of important joint properties such as spacing.

Whilst results obtained from analytical models, and to some extent numerical models, tend to be unique, **Probabilistic modelling** utilises probability principles to model excavation instabilities and obtain results in a probabilistic sense. In previous chapters, it was demonstrated that joint properties follow certain statistical distributions, hence the fitting use of probabilistic models in this dissertation. Also, results from jointed rock mass probabilistic models are usually more detailed and practical. In the early 80s, Goodman et al (1982) introduced block theory and wrote programs for analysing keyblock formations. Block theory is not a true probabilistic model as it can also be classified under both analytical and numerical (integral) models. However, the subsequent usage of the principle has found extensive application in probabilistic analysis and for the purposes of this dissertation it is classified under probabilistic models. Most relevant modelling tools were developed from the keyblock theory notably, Discontinuous Deformation Analysis (DDA). DDA was introduced in the mid 1980s by

Goodman and Shi (1984; 1988) and since then it has been used extensively in the analysis of keyblock stability. In demonstrating the effects of joint attributes on excavation stability, Yeung and Leong (1997) used the two dimensional DDA numerical modelling tool. Different hypothetical combinations of joint properties were used to study the effects of orientations and spacings on the stability of tunnels at shallow and deep levels. Wang and Garga (1993) developed an extension of the DDA, by using the Block Spring Model (BSM) for the analysis of deformation in a jointed rock mass. In the model, the rock mass is simulated using different shaped blocks. The BSM can be also used for both surface and underground excavations and its application has been demonstrated by Wang et al (1995; 1997) and Zhu et al (1997). Among other users of DDA or its variations are Yeung and Blair (2000), Morris and Blair (2000), Kuszmaul and Goodman (1992), Mauldon (1992;1995), Ohnishi et al (1995), Te-chih (1995), and Hsiung and Shi (2001). Trueman and Tyler (1992) developed the B3LHS program by modifying then existing keyblock programs to include the natural variation of joint geometric properties. Also the program was one of the first keyblock generation programs that assumed blocks bounded by joints of finite persistence.

Haines (1984) described a two dimensional technique (JPLOT) of extrapolating joint patterns using field measured joint properties. The interaction between the generated discontinuity pattern(s) and different excavation orientations was analysed and characterised by identifying keyblocks formed within the periphery of the excavation. In describing a procedure for the design of large underground excavations Stacey and Haines (1984) demonstrated the use of the above method for larger underground openings. Stacey et al (2004) used the principle described by Haines (1984) to investigate the stability of rock passes. The passes were superimposed on the simulated rock mass and probability of occurrence of potential rock falls was identified. Another widely used probabilistic modelling tool is the Underground Wedge Analysis (UNWEDGE) from Rocscience software. It is used extensively for the analysis of single wedges defined by three intersecting discontinuities (Hoek et al, 1998). Probabilistic analysis of excavation stability in jointed rock masses has also been extended to three-dimensional cases

as demonstrated by Grenon and Hadjigeorgiou (2000) for a mine in north-western Quebec, Canada. Generation of joint patterns was achieved by converting mean trace lengths from a scan-line survey to diameters of circular joints (i.e. Stereoblock program). The results from Stereoblock simulated joint patterns were then used to evaluate support effectiveness by comparing the numbers of blocks with their corresponding volumes, areas and safety factors. In another related study, Grenon and Hadjigeorgiou (2003) used three-dimensional joint networks on three case studies in Quebec Mines (including the one described in Grenon and Hadjigeorgiou (2000)). Joint pattern generation was again simulated using the Stereoblock computer program. Kinematically unstable blocks in the open stope's periphery were then identified including the statistical distributions of their sizes and volumes. Kuszmaul (2000) and Song et al (2000) have utilised the DDA principle for three-dimensional modelling to analyse excavation behaviour in a jointed rock mass. In Kuszmaul (2000), the unit cell method was used together with DDA to model the effect of both joint orientations and spacings in a rockmass. Other examples of probabilistic three-dimensional modelling tools in jointed rocks include the JBLOCK developed by Esterhuizen (2003). JBLOCK was used simulate the occurrence of keyblocks in excavation hangingwalls. Simulated blocks were then used to determine the likelihood of failure for different support layouts in hangingwall excavations.

Overall, the general steps in probabilistic modelling involve executing the following:

1. Identification of statistical joint properties in the rock mass;
2. Generation of joint networks in the rock mass;
3. Stability analysis.

The first step has already been executed in the preceding chapters. Joint geometric distributions defined from joint surveys are then used to construct likely two or three dimensional discontinuity patterns in the rock mass. Evaluation of excavation instability is carried out in the next section by analysing the interaction

of the excavation and the simulated rock mass using two different modelling tools.

4.2 Excavation stability analysis using the JPLOT program

JPLOT makes use of statistical results from the field mapping of joint geometric properties to simulate a two dimensional joint trace model of the rockmass. A detailed procedure on joint pattern generation using the JPLOT program is given in Haines (1984). In brief, the process involves the use of Monte Carlo sampling techniques to sample joint geometric properties from statistical distributions of joint geometries that have been mapped from surface exposures. Figure 4.3 illustrates a simulated joint trace model of the rock mass using joint data from Tau Tona hangingwall. The different colours in the trace model represent different joint sets.

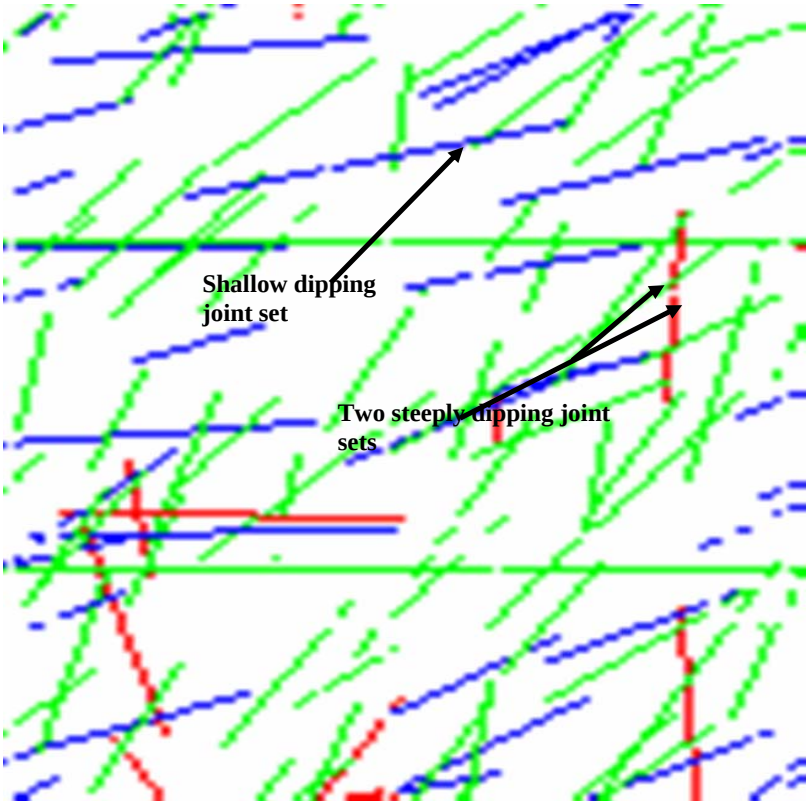

Figure 4.3 Simulated rock mass using joint data from Tau Tona Mine

Excavation geometries (sections) are then superimposed on simulated trace-models and potentially unstable wedges and blocks identified. As an example, for a hypothetical excavation with key block **'a'** in Figure 4.4, the longitudinal (shaded), cross-sectional (hatched) and plan (un-shaded) views of the excavation are superimposed on the simulated trace-model.

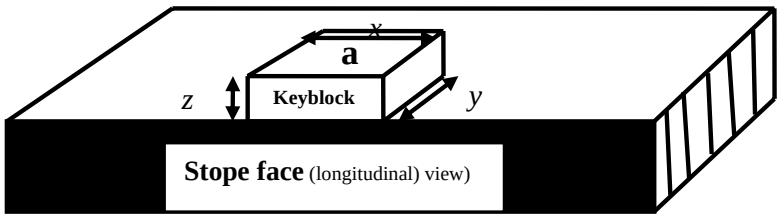

Figure 4.4 A potential keyblock in an excavation

The identification keyblocks involves visual analysis of the interaction between the excavation geometry and the trace-model and then identification of joints that intersect, in a critical manner, to form potential keyblocks as demonstrated below (Figure 4.5a and 4.5b). Since the joint traces are generated randomly, the blocks identified from different sectional views are completely unrelated to each other.

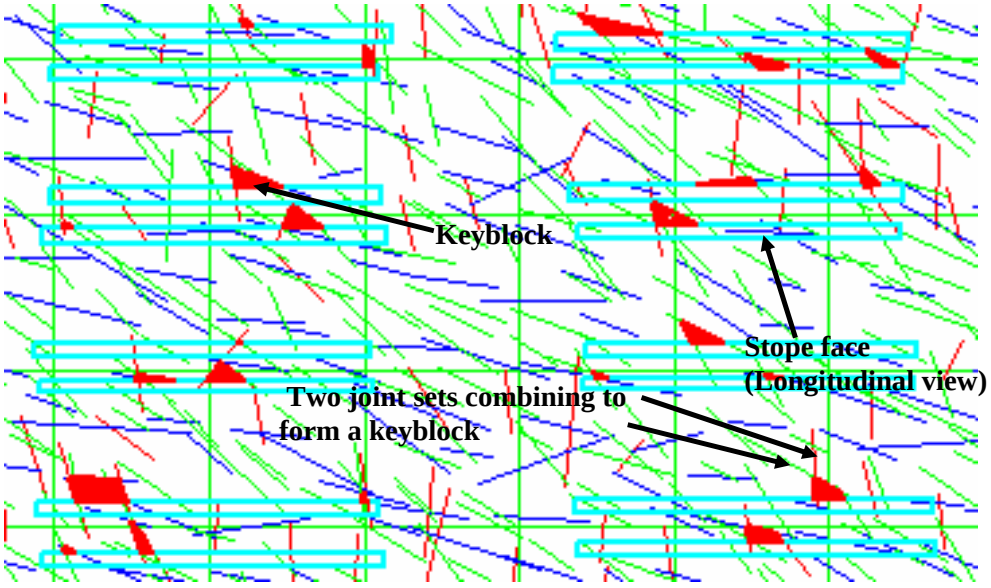

Figure 4.5a Potential keyblock in longitudinal view of a stope in Tau Tona (section 15°/170°)

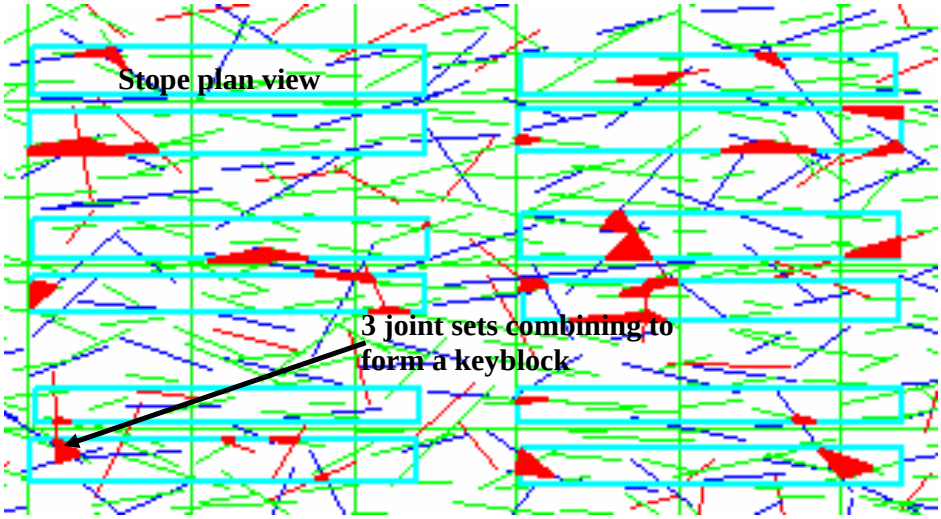

Figure 4.5b Potential keyblocks in plan view of a stope in Tau Tona (section 15°/170°)

The above interpretation is systematically repeated for a large number of excavation superimpositions to obtain distributions of the following unstable keyblock parameters:

- number of blocks along the excavation length;
- typical volumes of unstable blocks;
- total failure volume per stope;
- spacings between unstable blocks;
- identification of the range of block sizes for which support must be designed.

As an example, in the above hypothetical stope (Figure 4.4), knowing dimensions x from the longitudinal section of the stope and y from the cross sectional view, it is possible to calculate the surface area of the keyblock. If depth, z, behind block surface is also known, the volume of the keyblock can also be found. The parameters x, y and z are widely used during the stope support design process (Daehnke et al, 2001). For instance, depth (z) is the potential rock fall thickness in stopes, and x and y define the required areal support coverage for tributary area calculations. The parameters can also be used in the calculation of expected block

volumes and spacings which also determine the required excavation support intensity.

4.2.1 Discussion of JPLOT results

Figures 4.6a and 4.6b illustrate the distribution of block areas (A), from a plan section, and depth (z) of blocks, from a longitudinal section, respectively. The product of the fitted exponential distribution of A and the fitted exponential distribution of z gives the expected block volume. To take into consideration the effect of different block shapes, a factor (f_1) is introduced from random sampling of numbers between a third for a three-sided prism to a value of one for a hypothetical block with (theoretical) an infinite number of sides. An example of the statistical distribution of wedge volumes is shown in Figure 4.6c.

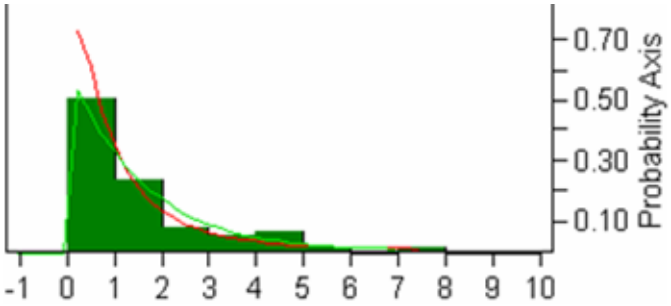

Figure 4.6a Distribution of block area in a 30m stope from plan section (Tau Tona- 15°/170°)

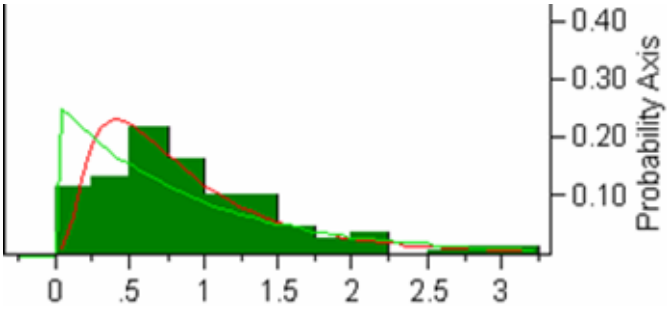

Figure 4.6b Distribution of block heights (depth z) in a 30m stope from a section (21/70)

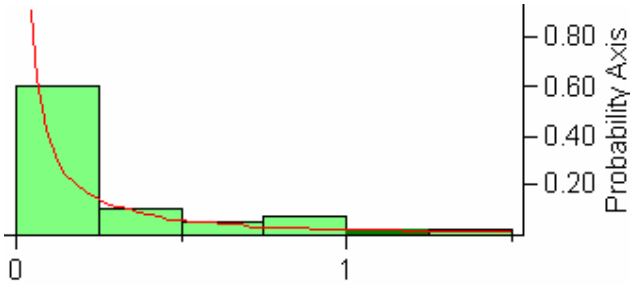

Figure 4.6c Distribution of block volumes per stope (section 21/48)

Running the above simulation for different excavation orientations for the two mines indicates that there is at least a single unstable block per stope in South Deep mine compared to two for Tau Tona mine (Table 4.1). In determining block spacing, a stope must have at least two blocks. This resulted in limited sample data in South Deep since the average number of wedges per stope is one. Nevertheless, a conservative block spacing of eight meters per stope will suffice for both mines (average of 8m and 10m for Tau Tona and South Deep respectively, Table 4.1). For different excavation sections in South Deep, the 95% rock fall thickness of blocks (z) was found to be 1.6m and this compares well with the 1.5m that the mine is currently using. The 1.5m thickness was deduced from analysing twenty-six rock fall incidents and accidents over a ten-year period (Petho, 2005). The average fall thickness for the mine is close to the 1.4m suggested by Daehnke et al (2001), for use in the stope support design criterion for VCR stopes (Figure 4.7a). However, average rock fall thicknesses determined from JPLOT for Tau Tona are higher (2.2m) than those of South Deep. This is mainly due to the steeply dipping joint set in the Tau Tona stopes. Currently, the mine is using a rock fall thickness of 1.1m that was recommended by Daehnke et al (2001) for *general* CLR stopes. However, it should be noted that the input data used in arriving at this thickness (Daehnke et al, 2001) is based on a very limited number of cases. It therefore cannot be concluded that it is any more correct than the 2.2m calculated from the JPLOT simulation. Expected rock fall thickness in both footwall tunnels is 1.7m. In both mines, the average block volume is about a cubic metre. Uncharacteristically small volumes in Table 4.1 for two South Deep stopes are primarily due to small sample numbers in the sections concerned.

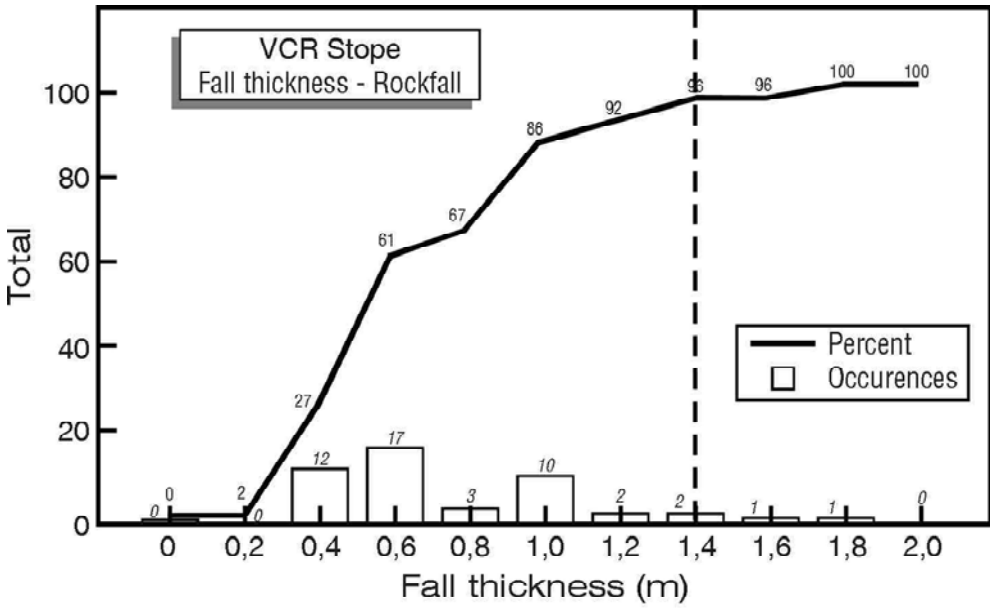

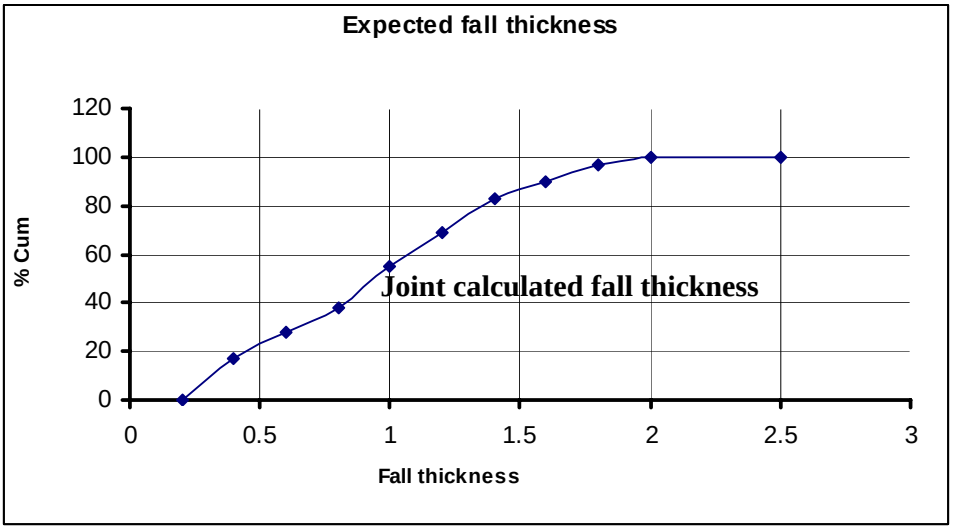

Figure 4.7a Comparison of 'joint-calculated' rock fall thicknesses with Roberts (1999) and Daehnke et al (2001) empirically determined fall thickness for VCR stopes

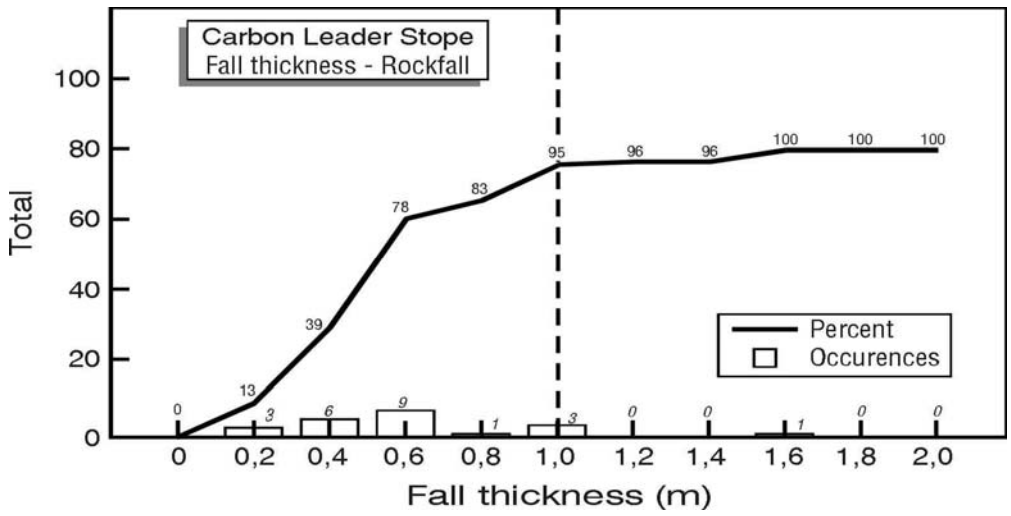

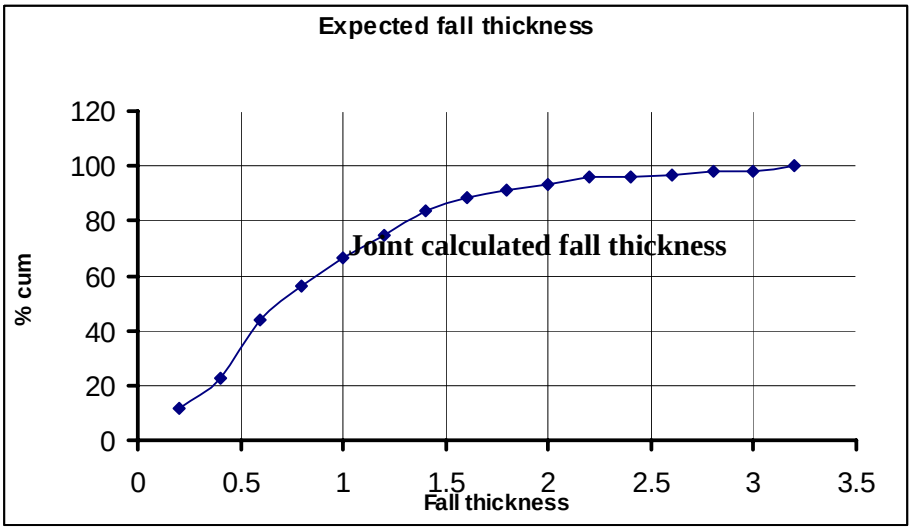

Figure 4.7b Comparison of 'joint-calculated' rock fall thicknesses with Roberts (1999) and Daehnke et al (2001) empirically determined thickness for CLR stopes

Table 4.1 Block parameters

Tau Tona Hangingwall					South Deep Hangingwall				
Section	**Number of wedges /30m stope**	**Wedge spacing(m)**	**Block Volume**	**95 % expected fall thickness**	**Section**	**Number of wedges /30m stope**	**Wedge spacing (m)**	**95 % expected fall thickness**	**Block Volume**
21/70	2.12	8.35	2.55	**1.8**	**10/177**	0.32		**1.8**	0.1*
25/23	1.6	8.31	1.32	**2.2**	**13/160**	1.43	11.82	**1**	0.82
15/170	0.41	11.36	1.03	**2.5**	**15/170**	0.35		**1.5**	0.47*
21/48	2.03	7.06	1.09	**2.2**					
20/288	2.36	8.41	1.38	**2.5**	**8/200**	1.03	10.98	**2.1**	1.076
Tau Tona Footwall					**South Deep Footwall**				
Section	**Number of wedges /30m tunnel**	**Wedge spacing(m)**	**Block Volume/stope**	**95 % expected fall thickness**	**Section**	**Number of wedges /30m tunnel**	**Wedge spacing (m)**	**95 % expected fall thickness)**	**Block Volume/stope**
04//15	0.44		0.3	**1.7*** **	**05/300**	0.23		**1.7****	1.06
0/70	0.4		1.15	**1.7****	**0/180**	0.28		**1.7****	0.9

* due to small sample parameter numbers i.e. since the number of blocks per stope is one, it leads to sample parameters which in-turn influences volume parameters

** Combined sample data due to small sample parameter numbers
*** Combined sample data due to small sample parameter numbers

Although the method described above may appear to be 'cumbersome', it provides a "feeling" for the rock mass that would not be obtained were the method more automated. The design parameters obtained can be used for support design in situations in which there are inadequate records of actual rock falls, particularly considering the comparable results obtained. In conclusion, the method can be used together with existing support design criteria to improve the support of underground excavations.

The next section demonstrates the use of the joint statistical data to obtain some of the above parameters and other additional parameters that could not be obtained from the JPLOT modelling tool.

4.3 Excavation stability analysis using the JBLOCK program

As mentioned before, JBLOCK is used both in the probabilistic assessment of gravity driven rockfalls and the evaluation of support effectiveness. All the stability calculations are done in three dimensions, but the excavation surface is in two dimensions. The modelling tool generates keyblocks in the hangingwall by using joint set statistical data. The identified keyblocks are randomly placed in an excavation with known support elements. The program then determines whether the identified keyblock will fail the predefined support elements or fall between support elements and the corresponding failure mode (Esterhuizen, 2003). Figure 4.8 illustrates a plan view of a stope with a keyblock that is supported by four support elements.

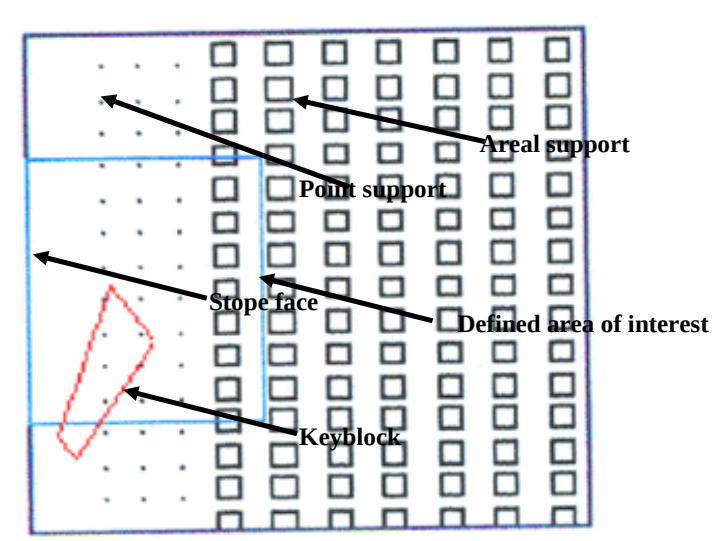

Figure 4.8 An identified keyblock supported by four support elements

The calculations are repeated a large number of times and the results are presented in the form of histograms showing failure probabilities, distributions of sizes of failure and the failure modes. The probability of failure is calculated as the ratio of unstable blocks to the total number of blocks tested. Joint data from Chapter 3 is used as input data and Figure 4.9 is an example of the data input window. Simulations were done for different support elements commonly used in gold mines ranging from point supports (elongates) to line support (point supports with headboards). The simulation runs were carried out for a predefined area of interest

that was fifteen metres from the stope face, and five thousand blocks were generated in each simulation. The generated blocks were saved and used to re-analyse excavation stability under a different support system or support layout. The variation of support elements and layouts was carried out for the first three rows of support elements.

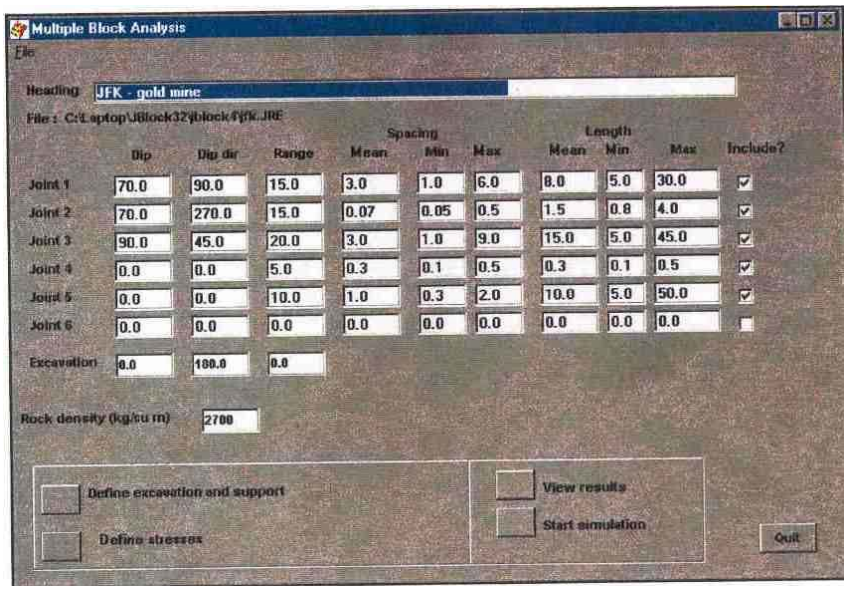

Figure 3.9 Data input window in the JBLOCK program

4.3.1 Discussion of JBLOCK results

Simulation of a large number of keyblocks for different excavation orientations in South Deep stopes indicates that 60-80% of generated keyblocks in stope hangingwalls are less than a cubic-meter in size (Figure 4.10a). The probability of these blocks falling between support elements is between 10% and 15%. Large blocks (two or more cubic metres) have less than a 3% failure probability, but, unlike the small blocks (1m^3), they are more likely to fail support elements than to fall between supports.

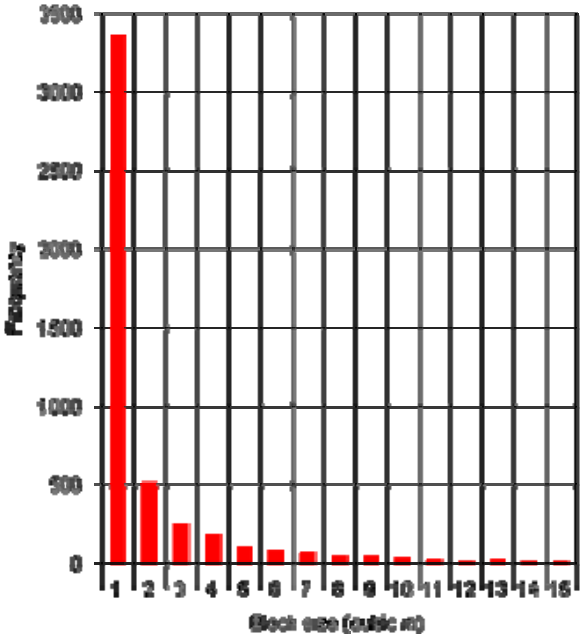

Figure 4.10a Keyblock size distribution in South Deep Mine (15°-170°)

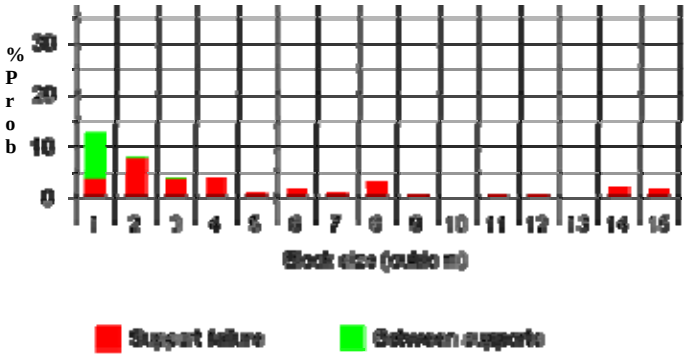

Figure 4.10b Distribution of failure probabilities in South Deep Mine (13°/160°)

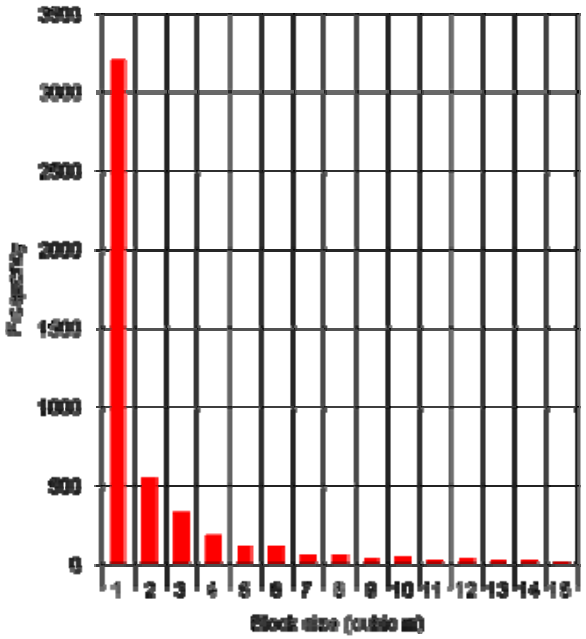

Figure 4.10c Keyblock size distribution in Tau Tona Mine (21°-048°)

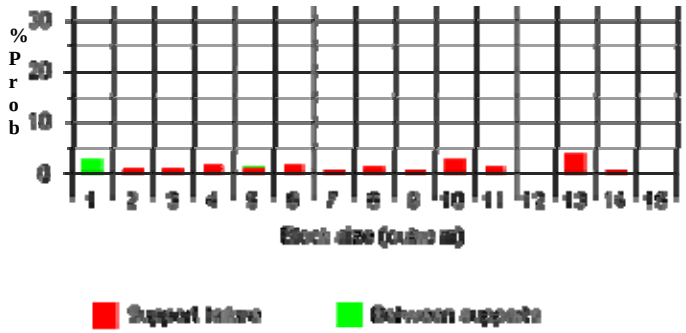

Figure 4.10d Distribution of and failure probabilities in Tau Tona Mine (20°-288°)

As shown in Figure 4.10c, the distributions of size of failed blocks in Tau Tona and in South Deep are very similar. However, failure probabilities in Tau Tona stopes are significantly less than those of South Deep (less than 5%). This is because, in South Deep, there are two shallow dipping joint sets with opposite dip directions and this increases the likelihood of block formation in the hangingwall. In Tau Tona, one joint set is shallow dipping and the other is steeply dipping. Furthermore, the two sets have almost similar dip directions. The probability of keyblock formation in the hangingwall with this joint geometry is less than in South Deep, hence the difference in failure probabilities (Figures 4.11).

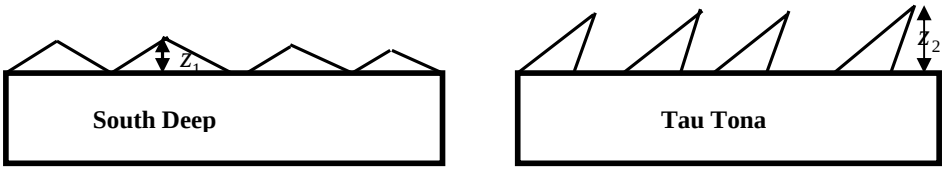

Figure 4.11 A two-dimensional illustration of reasons for the difference in failure probabilities

Failure probabilities in Tau Tona are greater than those in South Deep if one is more concerned with sidewall stability in a tunnel or large cavern. The two shallow dipping sets in South Deep are responsible for the lower fall of thickness in stopes (z_1) while the opposite is true for Tau Tona stopes (z_2) hence the latter had a higher fall thickness (compare1.5m and 2.2m in Table 4.1).

4.3.2 Failure and Stability Modes

The JBLOCK results show that 60% of the small blocks in South Deep are likely to fail by single plane sliding along shallow dipping planes (20°-30°). This shallow sliding plane is probably one of the joint sets identified in Chapter 3 (Figures 4.12a to 4.12e). It should be noted that South Deep had two such planes and this additionally explains the higher failure probabilities described in the preceding sub-section. About 40 % of small blocks fail as 'drop-outs' between support elements compared to 80 % in Tau Tona. As expected, 'drop-out' of larger blocks (i.e. greater than 2 m^3) is unlikely. The most common failure modes for larger blocks are single plane sliding and rotation (Figures 4.12a and 4.12d). Rotational failure occurs when block weight is less than support capacity, but the block is still able to fail support by the turning moment (leverage) provided during block rotation (Esterhuizen, 2003). Stability of small blocks is mainly mobilised by friction (75 %), while stability of the remaining 25% is provided by the support elements. Larger blocks are generally stabilised by support elements. The variation of stress-induced fractures only has the effect of increasing the percentage of 'drop-outs', but does not affect the overall failure probabilities.

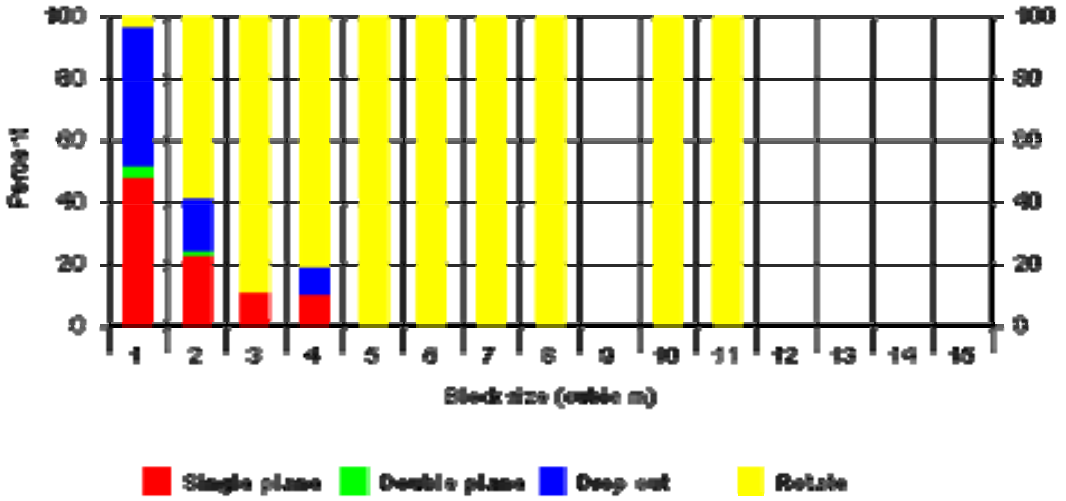

Figure 4.12a Block failure modes in South Deep Mine (13°-160°)

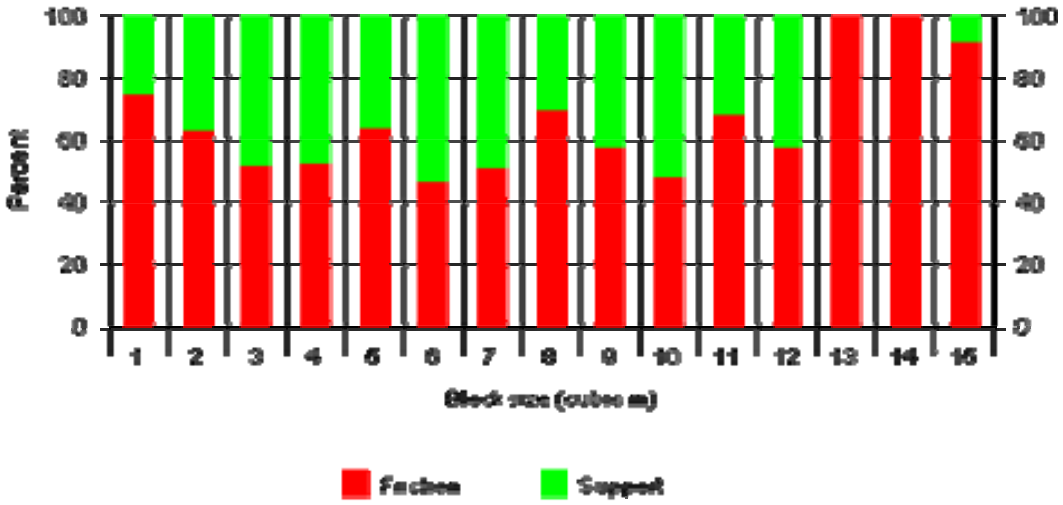

Figure 4.12b Stability modes in South Deep Mine (13°-160°)

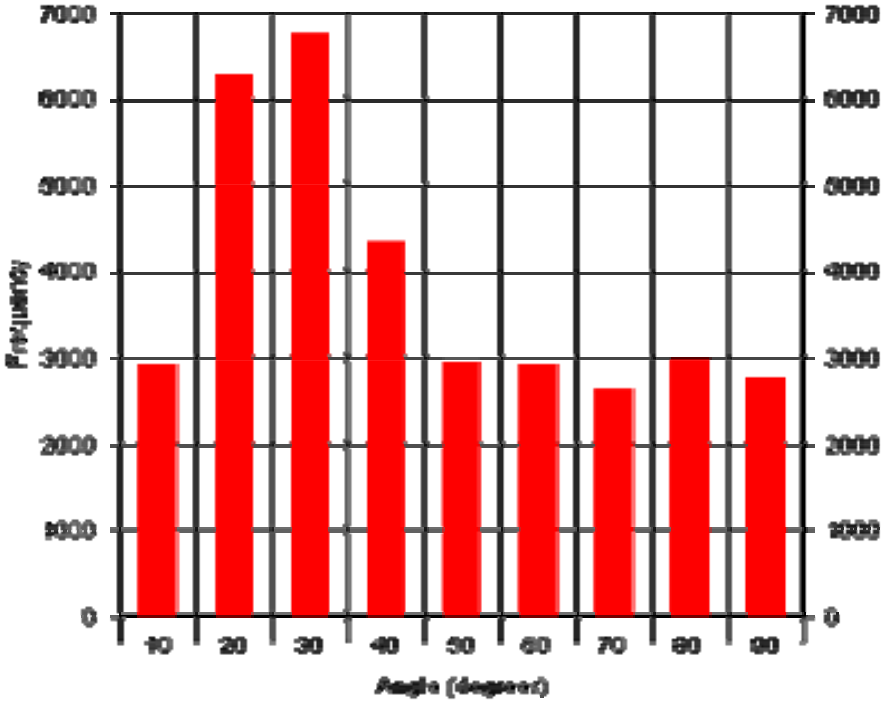

Figure 4.12c Distribution of sliding angles of keyblocks in South Deep Mine (13°-160°)

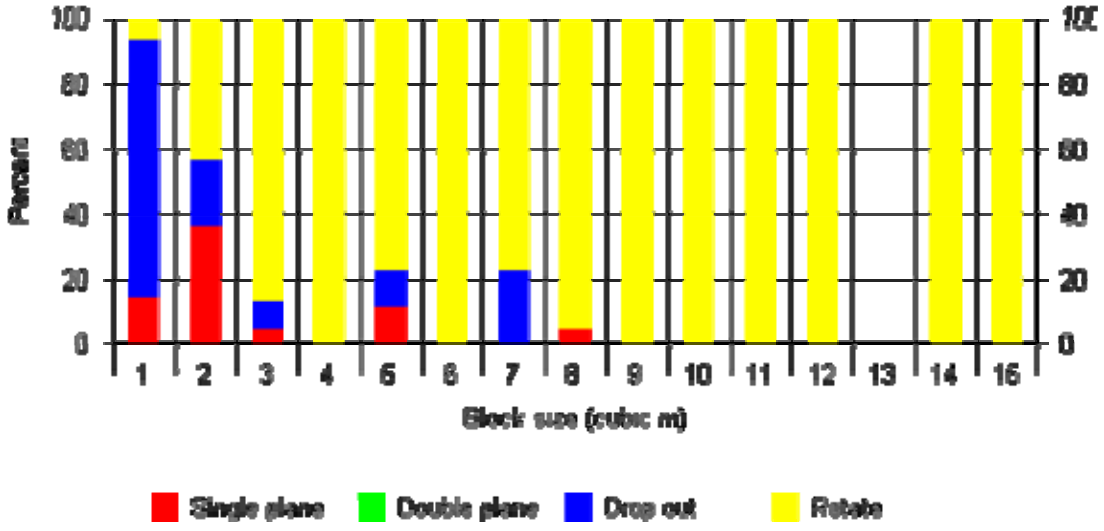

Figure 4.12d Block failure modes in Tau Tona Mine (20°/288°)

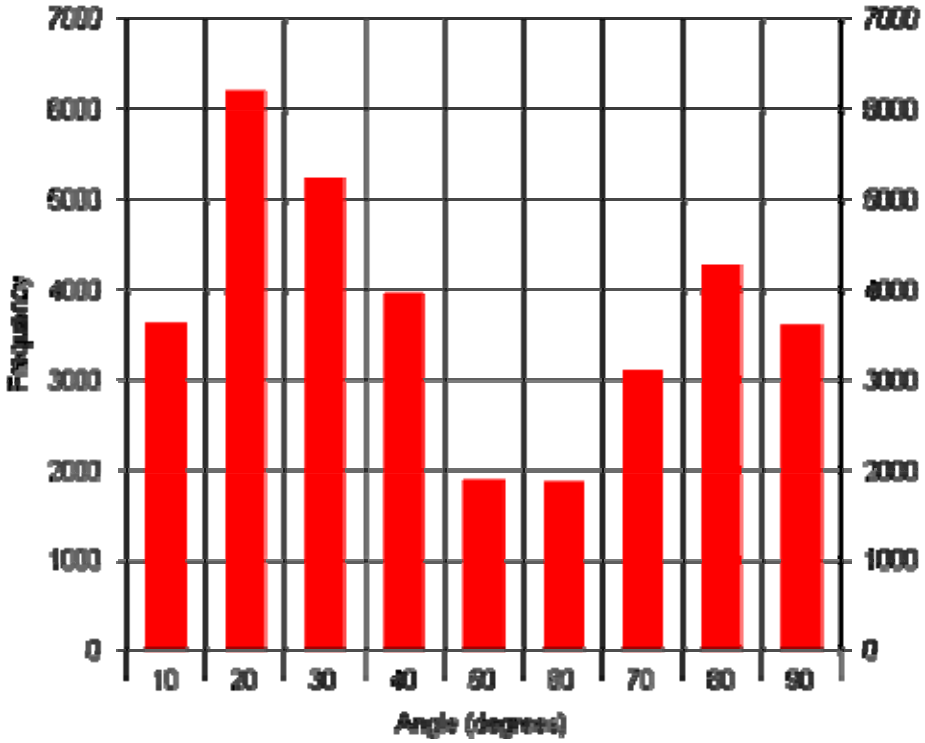

Figure 4.12d Distribution of sliding angles of keyblocks in Tau Tona Mine (20°/288°)

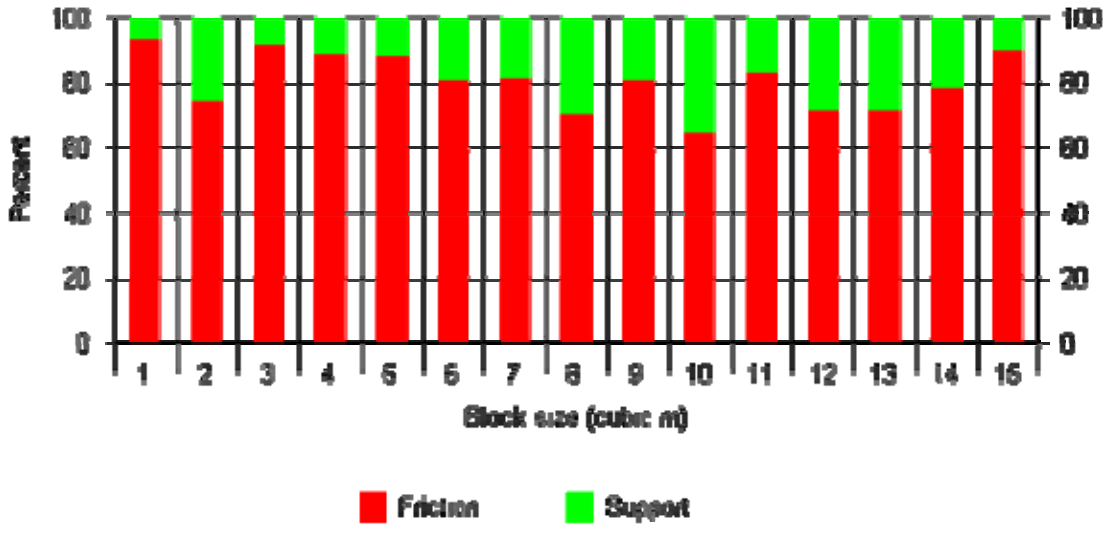

Figure 4.12e Stability modes in Tau Tona Mine (20°/288°)

4.3.3 Support layout and stability

The main purpose of support is to ensure safety and to stabilise the excavation. Ideally, a support system must stabilise all possible keyblocks, but a pragmatic support system is one that reduces the probability of keyblock failure to acceptable safety levels. Support spacing has a significant influence on stability. Figures 4.13a and 4.13b below are an extrapolation from simulation runs carried out for different support spacings in South Deep stopes. Changing from a 2m x 2m point support spacing to a 1m x 1m spacing halves the failure probabilities, i.e. from 14% to 7%, while a similar reduction in line support spacing (point with headboards) decreases the failure likelihood from 11% to 7%.

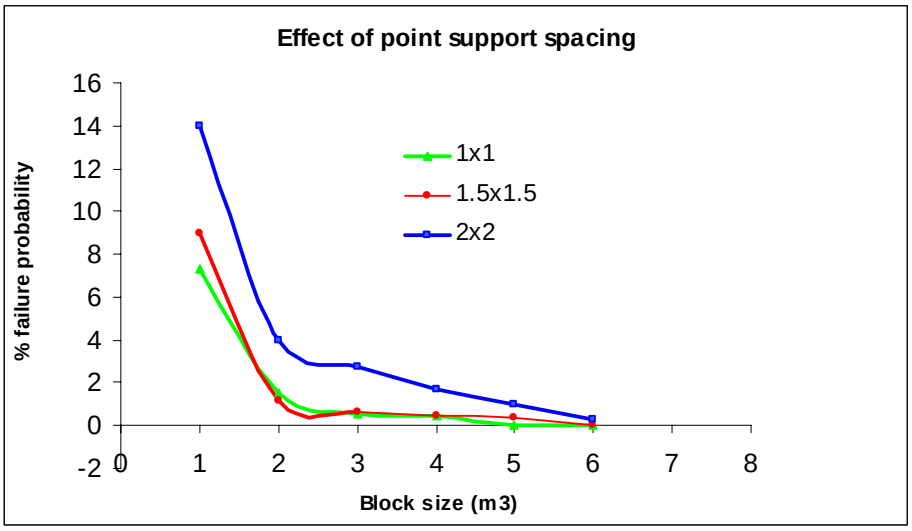

Figure 4.13a Effect of point support spacing on stability parameters

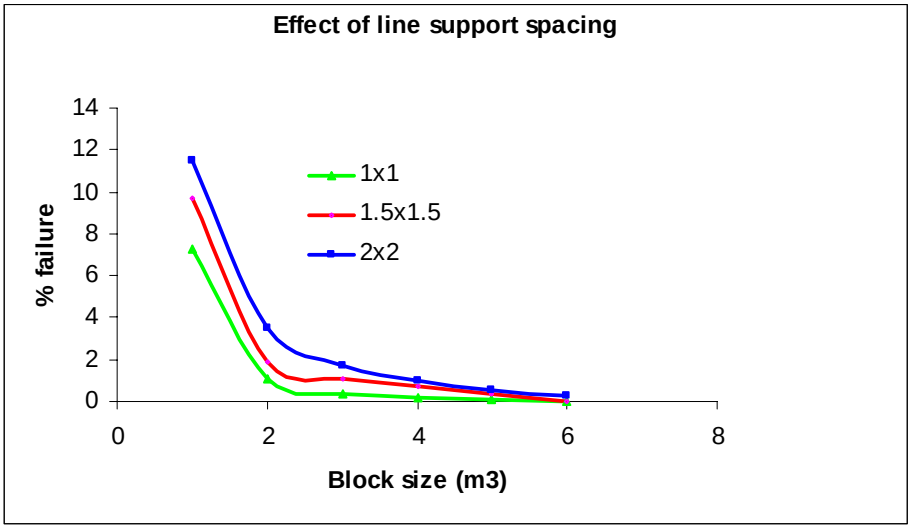

Figure 4.13b Effect of line support spacing on stability parameters

Line support increases the areal coverage of the support, thereby significantly decreasing the likelihood of 'drop-outs' of small blocks. Comparing failure probabilities between the two support systems (Figure 4.14) reveals that, for 2m x 2m support spacing, headboards reduce failure probabilities by 3% (14% to 11%).

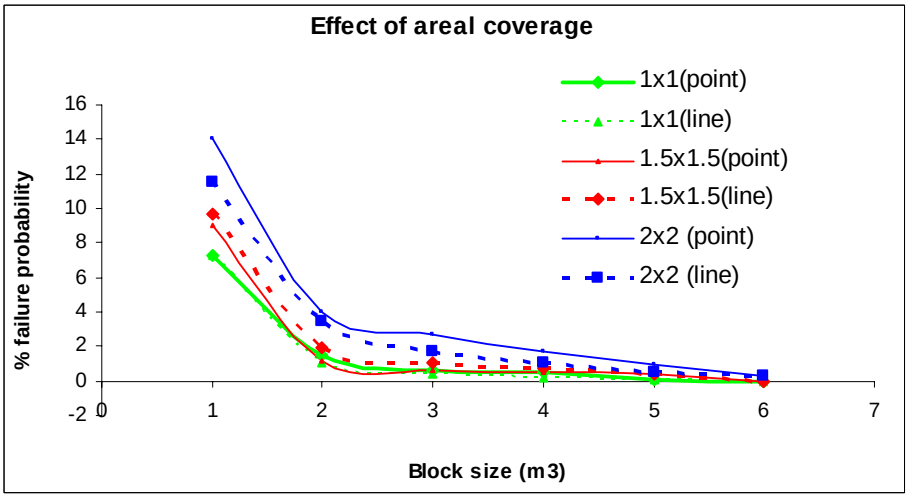

Figure 4.14 Effect of areal coverage on stability parameters

Aligning support elements in an offset or alternating manner can also increase support areal coverage. As demonstrated in Figure 4.15, offsetting a 2m x 2m point support reduces failure probabilities of a 1 cubic metre block by 4 % and 2%

for point and line support respectively. Any improvement in areal coverage decreases percentage 'drop-outs' by reducing unsupported spans in the hangingwall.

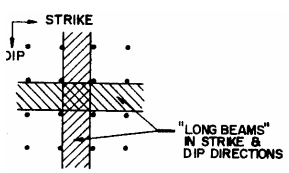

Regular layout

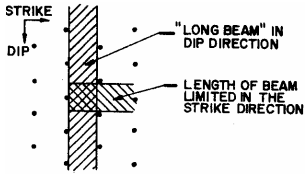

Offset layout

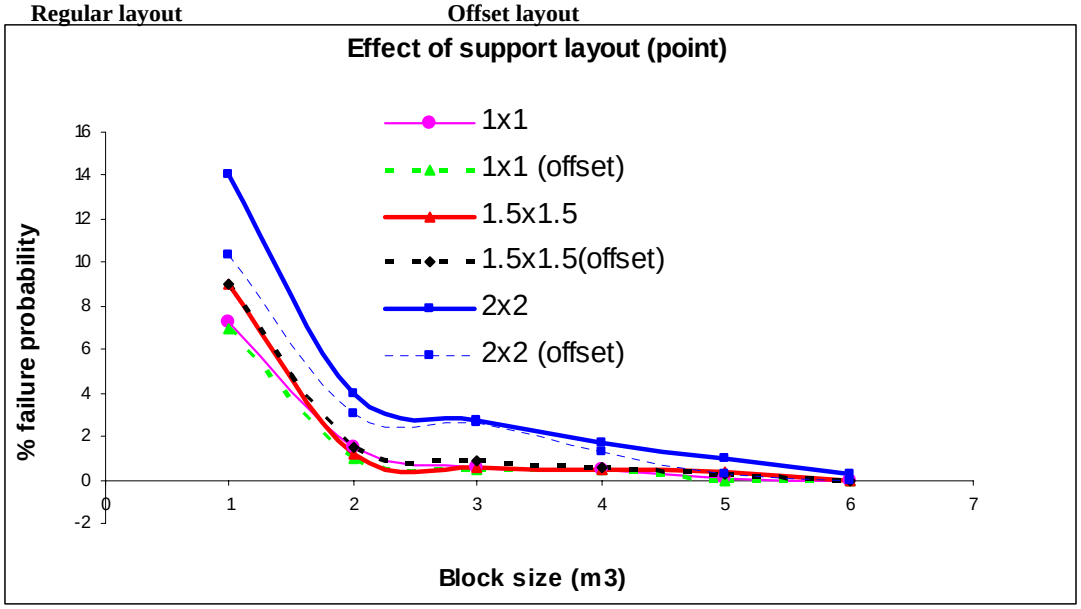

Figure 3.15a Effect of support layout on stability (point supports)

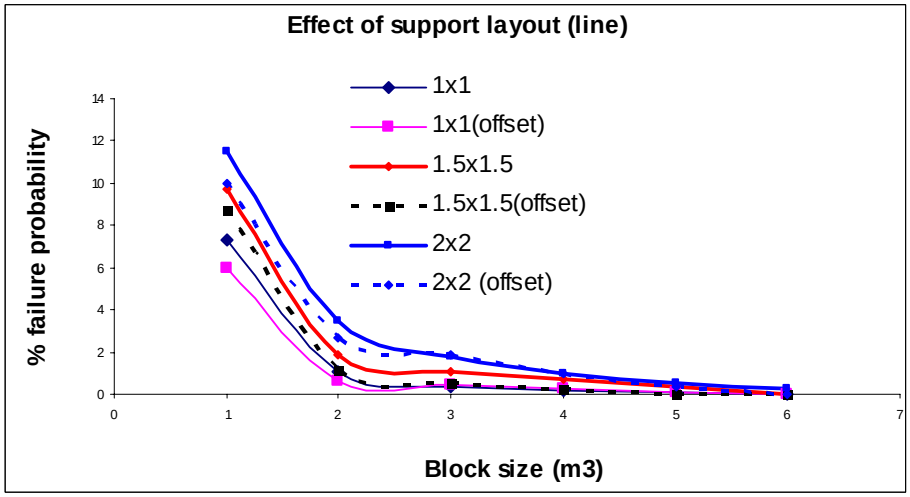

Figure 3.15b Effect of support layout on stability(line supports)

A summary of South Deep support stability analysis is given in the tables below. A similar support analysis for Tau Tona was not done due to lower failure probabilities for the worst case scenario i.e. 3 % failure probability at 2m x 2m point support.

Table 4.2 Failure probabilities for different block sizes in point supported stopes

Support spacing (m)	Block Size (m^3)					
	1	**2**	**3**	**4**	**5**	**6**
1x1	*7.3%*	*1.5%*	*0.57%*	*0.5%*	*0.05%*	*0*
1x1(offset)	*7%*	*1%*	*0.5%*	*0.43%*	*0.2%*	*0*
1.5x1.5	*9%*	*1.2%*	*0.6%*	*0.5%*	*0.4%*	*0*
1.5x1.5(offset)	*9%*	*1.5%*	*0.93%*	*0.57%*	*0.22%*	*0*
2x2	*14%*	*4%*	*2.7%*	*1.67%*	*1%*	*0.3%*
2x2 (offset)	*10.3%*	*3%*	*2.67%*	*1.33%*	*0.3%*	*0*

Table 4.3 Failure probabilities for different block sizes in line supported stopes

Support spacing (m)	Block Size (m^3)					
	1	**2**	**3**	**4**	**5**	**6**
1x1	*7.3%*	*1.1%*	*0.37%*	*0.18%*	*0.07%*	*0*
1x1(offset)	*6%*	*0.6%*	*0.47%*	*0.23%*	*0.1*	*0*
1.5x1.5	*9.7%*	*1.9%*	*1.07%*	*0.7%*	*0.35*	*0*
1.5x1.5(offset)	*8.7%*	*1.17%*	*0.57%*	*0.3%*	*0.03*	*0.01%*
2x2	*11.5%*	*3.5%*	*1.75%*	*1.01%*	*0.5%*	*0.25%*
2x2 (offset)	*10%*	*2.67%*	*1.83%*	*1.02%*	*0.33%*	*0*

4.4 Conclusions

The practical application of mapped joint data has been demonstrated by using two different modelling tools to analyse excavation stability for two gold mines. Results from the JPLOT modelling indicate that the size of most keyblocks encountered in underground stopes is less than a cubic metre. There are at most two possible keyblocks that result from the interaction of joints in each of these stopes. Using the same modelling tool, 95 percentile potential rock fall thicknesses predicted were 1.6m and 2.2m for South Deep and Tau Tona respectively. The former, for South Deep, is comparable with the thickness

determined from empirical methods suggested by Roberts (1999) and Daehnke et al (2001) for use in stope support design. The Tau Tona value is much greater than the 1.1m recommended by Daehnke et al (2001), but it is noted that the latter value is based on only a small number of observations.

From JBLOCK results, it can be concluded that most keyblocks (70-80%) are less than a cubic metre in size and this matches the results obtained from the JPLOT program. Failure probabilities of the blocks are heavily influenced by joint geometry, and these are 10-15% for South Deep and less than 5% for Tau Tona stopes. The shallow dipping joint planes usually act as critical sliding planes for blocks. Common failure modes are single plane sliding and 'drop-outs' for blocks less than a cubic metre, whilst larger blocks are more likely to fail by rotation. Small blocks are mainly stabilized by friction, while blocks greater than a cubic metre in size are stabilized by support elements. Areal support coverage, be it headboards or optimum support alignment, significantly reduces failure probabilities by decreasing unsupported hangingwall spans.

CHAPTER 5

CONCLUSIONS AND RECOMMENDATIONS

There are apparently no published, documented joint data from systematic mapping of natural joints in South African gold mines. The results presented in this dissertation are believed to be the first such data available on jointing in gold mines. The results were obtained from joint surveys carried out in different geotechnical areas in two different mines, and the following conclusions were drawn from these results:

a. There are at least two joint sets in stope hangingwalls and one set of bedding planes in footwall tunnels. At least one of the sets in stope hangingwalls is shallow dipping.
b. Considering the numbers of random joints mapped in the two hangingwalls it can be concluded that, in thin reef gold operations, nearly 60 % of the joints may be described as random. These random joints are usually steep dipping. Random joints in the footwall make up to about 40% of joints and do not dip as steeply as the random hangingwall joints.
c. The footwall joints/bedding planes are usually unfilled, although in South Deep some bedding planes were observed to contain a soapy phyllonite filling material. Those in Tau Tona contain no filling.
d. Statistical characteristics of joint geometric properties demonstrate similar statistical trends to those described in the literature. It can be concluded that joint orientations are normally distributed, while joint lengths and spacings can be described by both negative-exponential and lognormal distributions. Footwall joints in both mines were consistent in their characteristics and gave nearly ideal statistical distributions.
e. Stress induced fractures are sub-parallel to the stope face and have been mapped systematically and the data are well documented in the literature.

The research carried out has demonstrated that measured joint characteristics can form the basis for the prediction of rockfalls in gold mine stopes. Potential hangingwall instabilities have been predicted from the joint data obtained by analysing the interaction between the excavation geometry and the joint planes to form keyblocks. The characterisation of the possible keyblocks with regard to excavation stability reveals the following:

a. Most potentially unstable blocks (about 70%) in stope hangingwalls are less than a cubic metre in size. Results from both modelling tools, JPLOT and JBLOCK, confirm this. In this size category, rock falls are mainly as a result of blocks falling between support elements. Fewer blocks (less than 20%) are greater than a cubic metre in size and their potential instability is more likely to be due to failure of support.
b. Failure probabilities are controlled by joint geometry in the rockmass. This can be demonstrated by different failure probabilities of the two mines. Although both mines have same number of joint sets, South Deep has a higher failure probability (15%) than Tau Tona (5%) due to the occurrence of an extra shallow dipping joint set. Additionally, the extra steep dipping set in Tau Tona results in blocks with a greater (rock fall) thickness than those in South Deep. The geometry of stress induced fractures (parallel to stope faces) limits their influence on failure probabilities, but they have an influence on the size distribution of blocks.
c. Small blocks are more prone to failure by single plane sliding and ‘dropping out’. The common failure mode for larger blocks is rotation.
d. Small blocks are mostly stabilized by friction, while those greater than one cubic metre are stabilized by support elements. Besides avoiding hangingwall punching, improved areal support coverage reduces the likelihood of ‘drop-outs’ by reducing unsupported spans in the hangingwall. Since most unstable blocks are less than a cubic metre in size, more emphasis should be placed on support layouts that reduce unsupported spans such as with offsetting of support elements.

The study has demonstrated the important influence that natural joints have on hangingwall stability, and the importance of joint mapping to produce statistical joint data that can be used in the assessment of stability against rock falls. The conclusions from this work could be enhanced if more data were to be obtained by rock mechanics personnel through new systematic joint mapping and documentation exercises in mines. In a typical South African gold mining operation, strata control officers, assisted by technicians could be trained to obtain representative joint data in stopes as part of their responsibilities when carrying out routine stope support audits. Detailed scan-line surveys could then be carried out at suitable intervals in one or two stopes per geotechnical area. This scanline mapping could be carried out simultaneously with survey or geological reconciliation mapping. If the procedure was well planned, a detailed scan-line survey could be carried out along the same measuring tape used by the reconciliation mapping crew.

Although joint mapping may be a tedious exercise in mines, it has been shown to give similar results to that given from collection of empirical incident and accident record data over a ten-year period. It is considered that this provides good input data for the design of stope support. Besides helping in the understanding of block failure modes in stopes, the methodology described can be used as a check on existing support design processes. Alternatively, the design parameters from the methodology can be used, for instance, for monthly to quarterly support design plans and be calibrated annually with the Daehnke et al (2001) methodology after collecting annual rock fall accident data. Thus the joint data could be used as a short-term design tool and then, together with the Daehnke et al (2001) data, as a long-term design tool to combat rock falls in underground excavations. Such an approach contributes to good engineering practice as the design parameters are obtained from independent sources.

The results of the analyses of block stability that have been reported in this dissertation show disturbingly high probabilities of failure in the stope face area (or working area), particularly for blocks that are smaller than about 1.5 cubic

metres in size. The use of headboards to improve the stability has been shown to be largely unsuccessful – probabilities of failure are reduced slightly. These results point strongly to the importance of using improved areal support to reduce the rock fall hazard in South African gold mines. It is recommended that this issue be pursued strongly.

REFERENCES

Adams, D. J. and Handley, M. F. (2004) Rockburst control and the implications for profitability and sustainability of the South African Gold Mining Industry, Proc. 2nd International Seminar on Deep and High Stress Mining, S. Afr. Inst. Min. Metall., Johannesburg, pp. 55-66.

Adams, D. J. (2005) Personal communication (23/05/2005).

Adams, G. R. and Jager, A. J. (1980) Petroscopic observations of rock fracturing ahead of stope faces in deep-level gold mines, J. S. Afr. Inst. Min. Metall., vol. 80, pp. 204-209.

Baecher, G. B., Lanney, N. A. and Einstein, H. H. (1977) Statistical description of rock properties and sampling, Proc. 18th U.S. Symposium on Rock Mechanics, 5 C 1-8.

Barton, N. and Bandis, S. (1990) Review of predictive capabilities of joint roughness coefficient and joint compressive strength model in engineering practice, Proc. International Symposium on Rock Joints, Barton and Stephansson (eds), Balkema, Norway, pp.603-610.

Barton, N. (1978) Analysis of joint trace length, Proc. 19th U.S. Symposium on Rock Mechanics, Colorado School of Mines, vol. 1, pp. 38-41.

Barton, N. and Choubey, V. (1977) The shear strength of joints in theory and in practice, Rock Mech., vol. 10, pp. 1-65.

Barton, N. R. (1976) The shear strength of rock and rock joints, Int. J. Rock Mech. Min. Sci. and Geomech. Abstr., vol. 13, no 9, pp. 255-279.

Barton, N. (1973) Review of a new shear strength criterion for rock joints, Engng Geol., vol. 8, pp. 287-332.

Beer, G., Oppriessnig, G., Gosler, H., Fasching, A. and Gaich, A. (1999) Geotechnical data acquisition, numerical simulation and visualization on site, Proc. 9th Int. Cong. Int. Soc. Rock Mech., Balkema, pp. 1333-1338.

Beer, A. J., Stead, D. and Coggan, J. S. (2002) Estimation of joint roughness coefficient (JRC) by visual comparison, Rock Mech. Rock Engng, vol. 35, pp. 65-74.

Brady, B. H. G. and Brown, E. T. (1993) Rock Mechanics for underground mining, Allen and Unwin, London, pp. 571.

Bridges, M. C. (1975) Presentation of fracture data for rock mechanics, Proc. 2nd Australian - New Zealand Conference on Geomechanics, Brisbane, pp. 144-148.

Brummer, R. K. (1987) Fracturing and deformation at the edges of tabular gold mining excavations and the development of a numerical model describing such phenomena, Ph.D. thesis, Rand Afrikaans University, Johannesburg.

Call, R. B., Savely, J. and Nicholas, D. E. (1976) Estimation of joint set characteristics from surface mapping data. Proc. 17th U.S. Symposium on Rock Mechanics, pp. 2B2-1-9.

Cruden, D. M. (1977) Describing the size of discontinuities, Int. J. Rock. Mech. Min. Sci. and Geomech. Abstr., vol. 14, pp. 133-137.

Cundall, P. A. and Strack, O. D. L. (1979) A discrete numerical model for granular assemblies, Geotechnique, vol. 29, pp. 47-65.

Davis, H. and Reynolds, S. J., (1996) Structural Geology of Rocks and Regions, Wiley and Sons, U.S.A.

Daehnke, A., Van Zyl, M. and Roberts, M. K. C. (2001) Review and application of stope support design criteria, J. S. Afr. Inst. Min. Metall., vol.101, pp. 135-164.

Dershowitz, W. S. and Einstein, H. H. (1988) Characterising rock joint geometry with joint system models, Rock Mech. Rock Engng, vol. 21, pp. 21-51.

Dershowitz, W. S. (1979) A probabilistic model for the deformability of jointed rock masses, MSc. Thesis, Massachusetts Institute of Technology.

DME16/3/2/1-A3 (2002) Tau Tona Internal report: Mandatory code of practice to combat rockfall and rockburst accidents.

Du, S. J., Esaki, T. Mitani, Y. and Zhou, G. Y. (2001) A numerical simulation and visualisation of shear process of rock masses by using Geographic Information Systems, Rock Mechanics in National Interest, vol.1, Proc. 38th U.S. Rock Mechanics Symposium, Balkema, pp. 895-900.

Einstein, H. H., Baecher, G. B. and O'Reilly, K. J. (1983) The effect of discontinuity persistence on rock slope stability, Int. J. Rock Mech. Min. Sci., vol. 20, pp. 227-236.

Einstein, H. H. and Hirschfeld, R. C. (1973) Model studies on mechanisms of jointed rock, Journal of the Soil Mechanics and Foundations Division, ASCE, vol. 99, pp. 833-848.

Esterhuizen, G. S. and Streuders, S. B. (1998) Rockfall Hazard evaluation using probabilistic keyblock analysis, J. S. Afr. Inst. Min. Metall., vol. 98, pp. 59-63.

Esterhuizen, G. S. (2003) J Block user manual, Pretoria.

Feng, Q., Stephansson, O. and Boberg, A. (2001) Fracture mapping at exposed rock faces by using close range digital photogrammetry and geodetic total station, Rock Mechanics in National Interest, vol. 1, Proc. 38th U.S. Rock Mechanics Symposium, Balkema, pp. 829- 836.

Feng, Q., Fardin, N., Jing, L. and Stephansson, O. (2003) A new method for in-situ non contact roughness measurement of large rock fracture surfaces, Rock Mech. Rock Engng, vol. 36, pp. 3-25.

Franklin, J. A., Maerz, N. H. and Bennett, C. P. (1988) Rock mass characterisation using photoanalysis, Engng. Geol., vol. 6, pp. 97-112

Goodman, R. E. (1974) The mechanical properties of joints, Proc. 3rd Int. Cong. Int. Soc. Rock Mech., vol. 1, pp. 127 – 140.

Goodman, R. E., Shi, G. H. and Boyle, W. (1982) Calculation of support for hard, jointed rock using the keyblock principle, Key issues in rock mechanics, Proc. 23rd U S Symposium on Rock Mechanics, SME, pp. 883-898.

Goodman, R. E. and Shi, G. (1985) Block theory and its application to rock engineering, Prentice-Hall, USA.

Grenon, M. and Hadjigeorgiou, J. (2000) Stope design based on realistic joint networks, MassMin 2000, Brisbane.

Grenon, M. and Hadjigeorgiou, J. (2003) Drift reinforcement design based on discontinuity network modelling, Int. J. Rock Mech. Min. Sci, vol. 40, pp. 833-845.

Grenon, M. and Hadjigeorgiou, J. (2003) Open stope stability using 3D joint networks, Rock Mech. Rock Engng, vol. 36, pp. 183 –206.

Grossman, N. F. (1985) The bivariate normal distribution on the tangent plane at the mean attitude, Proc. Int. Symposium on Fundamentals of Rock Joints, Centek, Bjorkliden, pp. 3-11.

Haberfield, C. M. and Johnston, I. W. (1994) Mechanically based model for rough rock joints, Int. J. Rock Mech. Min. Sci. Geomech. Abstr., vol. 31, pp. 279-292.

Hadjigeorgiou, J., Lenny, F., Cote, P. and Maldague, X. (2003) Evaluation of image analysis algorithms for constructing discontinuity trace maps, Rock Mech. Rock Engng, vol. 36, pp. 163-179.

Hagan, T. O. (1980) A photogrametric study of mining induced fracture phenomena and instability on a deep level longwall stope face with variable lag-lengths, MSc thesis, Rand Afrikaans University, Johannesburg.

Haines, A. The application of generated rock mass discontinuity patterns, Proc. 8th Regional Conference for Africa on Soil Mechanics and Foundation Engineering, Harare, Zimbabwe, pp. 13-21.

Hammah, R.E and Curran J. H (1998) Optimal delineation of joint sets using a fuzzy clustering algorithm, Int. J. Rock Mech. Min. Sci., vol. 35, pp. 889-905.

Harrison, J. P. (1993) Improved analysis of rock mass geometry using mathematical and photogrammic methods, Ph.D. thesis, Imperial College, London.

Hobbs, B. E., Means, W. D. and Williams, P. F. (1976) An outline of Structural Geology, Wiley, New York.

Hoek, E., Kaiser, P. K. and Bawden, W. F. (1998) Support of underground excavations in hard rock, Balkema, Rotterdam.

Hoek, E. and Bray, J. W. (1977) Rock Slope Engineering, Institution of Mining and Metallurgy, London.

Hoek, E. and Brown, E. T. (1982) Underground excavations in rock, Institution of Mining and Metallurgy, London.

Hsiung, S. M. and Shi, G. H. (2001) Simulation of earthquake effects on underground excavations using the DDA, Rock Mechanics in National Interest, vol. 2, Proc. 38th U.S. Rock Mechanics Symposium, Elsworth, Tinucci and Heasley (eds), pp. 1413-1420.

Huang, T. H. and Doong, Y. S. (1990) Anisotropic shear strength of rock joints, Proc. International Symposium on Rock Joints, Barton and Stephansson (eds), Balkema, Norway, pp. 211-218.

Hudson, J. A. and Priest, S. D, (1979) Discontinuities and rock mass geometry, Int. J. Rock Mech. Min. Sci, vol. 16, pp. 339-362.

Jakubowski, J. and Stypulkowski, J. B. (2002) The effect of natural geologic discontinuities on behaviour of rock in tunnels, revisited, Proc. 5th North American rock mechanics symposium and the 17th Tunnelling Association of Canada conference, Hammer, Bawden, Curran and Telesnicki (eds), University of Toronto Press, vol. II, pp. 1755-1761.

Joughin, W. and Petho, S. Z. (2004) Massive mining at South Deep, Proc. 2nd International Seminar on Deep and High Stress Mining, Johannesburg, S. Afr. Inst. Min. Metall., pp. 233-252.

Kersten, R. W. O. (1969) Structural analysis of fractures around underground excavations on a Witwatersrand Gold Mine, MSc thesis, Pretoria University, Pretoria.

Kulatilake, P. H. S. W., Chen J., Teng, J. Pan, G. and Shufang, X. (1995) Discontinuity network modelling of the rockmass around a tunnel close to the proposed permanent shiplock area of the three gorges dam site in China, Proc. 35th U.S. Rock Mechanics Symposium, Daemen and Schultz (eds), Balkema, pp. 807-812.

Kulatilake, P. H. S. W, Wathugala, D. N. and Stephansson O. (1993) Joint network modelling with validation exercise in Stripa Mine, Int. J. Rock Mech. Min. Sci and Geomech. Abstr., vol. 30, pp. 503-1526.

Kulatilake, P. H. S. W. (1988) State of the art in stochastic joint geometry modelling, Key Questions in Rock Mechanics, Proc. 29th U.S. Rock Mechanics Symposium, Cundall, Sterling and Starfield (eds), Balkema, pp. 215- 229.

Kulatilake, P. H. S. W. and Wu, T. U. (1984) Estimation of mean trace length of discontinuities, Rock Mech. Rock Engng, vol. 17, pp. 215-232.

Kuszmaul, J. S. and Goodman, R. E. (1992) An analytical model for estimating keyblock sizes in excavations in jointed rock masses, International Conference on Fractured and Jointed Rock Masses, Lake Tahoe, pp.26-33.

Kuszmaul, J. S. (2000) The effect of varied joint set orientations on keyblock size, Pacific Rocks 2000, Proc. 4th North American Rock Mechanics Symposium, Girard, Liebman, Breeds and Doe (eds), Balkema, pp. 953-958.

Landanyi, B. and Archambault, G. (1970) Simulation of the shear behaviour of a jointed rock mass, 11th Symposium on Rock Mechanics, American Inst. Min. Met. Petr. Engineers, New York, pp 105-125.

Landmark, G. L. and Villaescusa, E (1992) Geotechnical mapping of Mount Isa Mines, Proc. Western Australia Conference on Mining and Geomechanics, Szwedzicki, Baird and Little (eds), Western Australian School of Mines, pp. 329-333.

Leith C. K. (1923) Structural Geology, Holt, New York, pp. 29 – 99.

MacMahon, B. K. (1974) Design of rock slope against sliding on pre-existing fractures, Proc. 3rd Int. Cong. Int. Soc. Rock Mech., Denver, vol. 13, pp. 803- 808.

Maerz, N. H. and Zhou, W. (2001) Multivariate clustering analysis of discontinuity data: implementation and applications, Rock Mechanics in the National Interest, vol. 1, Proc. 38th U.S. Rock Mechanics Symposium, Balkema, pp. 861-868.

Malina, H. (1970) The numerical determination of stresses and deformations, Rock Mech. vol. 2, pp. 1- 16.

Mathis, J. I. (1987) Discontinuity mapping – A comparison between line and area mapping, Proc. 6th Int. Cong. Int. Soc. Rock Mech., vol. 2, Balkema, pp. 1111-1114.

Morris, J. P. and Blair, S. C. (2000) An efficient displacement discontinuity method using fast multipole techniques, Pacific Rocks 2000, Proc. 4th North American Rock Mechanics Symposium, Girard, Liebman, Breeds and Doe (eds), Balkema, Washington, pp. 959-966.

Nagel, M., Petho, S. Z. and Joughin, W. C. (2004) Low angle stress fracturing in de-stress stopes at South Deep mine, Proc. 2nd International Seminar on Deep and High Stress Mining, S. Afr. Inst. Min. Metall., Johannesburg, pp. 253-264.

Newland, P. L. and Alley, B. H. (1957) Volume changes in drained triaxial tests on granular materials, Geotechnique, vol. 7, pp. 17-34.

Nicholas, D. E and Sims, D. B. (2000) Collecting and using geological data for slope design, International conference on slope stability in surface mining, Hustrulid, McCarter and Van Zyl (eds), SME, USA, pp. 11-21.

Ohnishi, Y. Tanaka, M. and Sasaki, T (1995) Modification of the DDA for elasto-plastic analysis with illustrative generic, Rock Mechanics, Proc. 35th US Symposium on rock mechanics, Balkema, pp. 45-50.

Patton, F. D. (1966) Multiple modes of shear failure in rock, Proc. 1st Int. Cong. Int. Soc. Rock Mech., Colouste Gulbenkian Foundation, Lisbon, vol. 1, pp. 509-513.

Patton, F. D. (1971) Determination of shear strength of rock masses, Course notes on the analysis and design of rock slopes.

Piteau, D. R. (1973) Characterising and extrapolating rock joint properties in engineering practice, Rock Mech. Rock Engng, pp. 5-31.

Piteau, D. R. (1970) Engineering geology contribution to the study of stability of slopes in rock with particular reference to De Beers Mine, Ph.D. Thesis, University of Witwatersrand, Johannesburg.

Piteau, D. R. and Jennings, J. E. (1970) The effects of plan geometry on the stability of natural slopes in rock in the Kimberley area of South Africa, Proc. 2nd Int. Cong. Int. Soc. Rock Mech, Institute for Development of Water Resources, Yugoslavia, vol. 1, pp. 289-295.

Price, N. J. (1966) Fault and joint development in brittle and semi-brittle rock, Pergamon, London.

Priest, S.D. (1985) Hemispherical projection methods in Rock mechanics, Allen and Unwin, London.

Priest, S. D. and Hudson, J. A. (1981) Estimation of discontinuity spacing and trace length using scan line surveys, Int. J. Rock Mech. Min. Sci and Geomech. Abstr., vol.18, pp. 183-197.

Priest, S.D. and Hudson, J. A. (1976) Discontinuity spacings in rocks, Int. J. Rock Mech. Min. Sci., vol.13, pp. 135-148.

Reid, T. R. and Harrison, J. P. (2000) A semi-automated methodology for discontinuity trace detection in digital images of rockmass exposures, Int. J. Rock Mech. Min. Sci., vol. 37, pp. 1073-1089.

Roberts, M. K. C. (1999) The design of stope support systems in South African gold and platinum mines, Ph.D. Thesis, University of Witwatersrand, Johannesburg.

Robertson, A. M. (1977) The determination of the stability of slopes in jointed rock with particular reference to the determination of strength parameters and mechanics of failure, Ph.D. Thesis, University of Witwatersrand, Johannesburg.

Rorke, A. J. and Brummer, R. K. (1985) A stereographic mapping technique, SANGORM Symposium on rockmass characterisation, Mintek, Johannesburg, pp. 117-119.

Saayman, A. F. (1991) A study on the geotechnical input required for the determination of the stability of rock slopes, employing the probabilistic approach, MSc Thesis, University of Witwatersrand, Johannesburg.

Safety in Mines Research Advisory Committee (SIMRAC) 2004-2005, Annual report (in print).

Safety in Mines Research Advisory Committee (SIMRAC) 2003-2004, Annual report.

Safety in Mines Research Advisory Committee (SIMRAC) 2002-2003, Annual report.

South Deep Mine Code of Practice 2003.

Sen, Z. and Kazi, A. (1984) Discontinuity spacing and RQD estimates from finite length scan lines, Rock Mech. Rock Engng, vol. 16, pp. 39-72.

Shi, G. (2001) Three dimensional Discontinuous Deformation Analyses, Rock mechanics in the National Interest, Proc. 38th US Symposium on rock mechanics Tinucci and Heasley (eds), Balkema, Washington, pp. 1421-1435.

Song, W. K., Kim, K. E. and Park, H. D (2000) Development of 3D visualisation program for the analysis of geotechnical information, Pacific Rocks 2000, Proc. 4th North American rock mechanics symposium, Girard, Liebman, Breeds and Doe (eds) Balkema, Washington, pp. 1335-1337.

Stacey, T. R. and Haines, A. (1984) Design of large underground openings in jointed rock- An integrated approach, SANCOT Seminar.

Stacey, T. R. (1989) Potential rock falls in conventionally supported stopes- a simple probabilistic approach, J. S. Afr. Inst. Min. Metall., vol. 89, pp. 111-115.

Steffen, O. K. H. (1978) Some aspects of three dimensional and two dimensional rock slope stability analyses with two case histories, Ph.D. Thesis, University of Witwatersrand, Johannesburg.

Steffen, O. K. H., Kerrich, J. E. and Jennings, J. E. (1975) Recent developments in interpretation of data from joint surveys in rock masses, Proc. 6th Regional Conference on Soil Mechanics and Foundation engineering, Durban, vol. 2, pp. 17-26.

Sun, Y. and Lin, M. (2002) Effects of rock joint patterns on stability of repository emplacement drifts, Proc. 5th North American Rock Mechanics Symposium and the 17th Tunnelling Association of Canada Conference, Hammer, Bawden, Curran and Telesnicki (eds), University of Toronto Press, vol. 2, pp. 1215 –1222.

Suppe, J. (1985) Principles of structural geology, Prentice-Hall, USA.

Te-Chih, K. (1995) Application of the DDA to block in matrix materials, Rock Mechanics, Proc. 35th US Symposium on Rock Mechanics, Balkema, pp. 33-38.

Terzaghi, R. D. (1965) Sources of error in joint surveys, Geotechnique, vol. 15, no. 3, pp. 287-304.

Trueman, R. and Tyler D. B. (1992) Hardrock excavation support design using probabilistic keyblock and associated risk analysis, Proc. Western Australia Conference on Mining and Geomechanics, Szwedzicki, Baird and Little (eds), Western Australian School of Mines, pp. 143-148.

Van Proctor, R. J. (1978) An investigation of the nature and mechanism of rock fracture around longwall faces in a deep gold mine, MSc thesis, Witwatersrand University, Johannesburg.

Villaescusa, E. and Brown, E. T. (1990) Characterising joint spatial correlation using geostatistical methods, Proc. International Symposium on Rock Joints, Barton and Stephansson (eds), Balkema, Norway, pp. 115-122.

Wallis, P. F. and King, M. S. (1981) Discontinuity spacings in a crystalline rock, Int. J. Rock Mech. and Min. Sci. vol. 17, pp. 63-66.

Walpole, R. E. and Mayers, R. H. (1993) Probability and Statistics for Engineers and Scientists, Prentice Hall, U.S.A.

Wang, B. and Garga, V. K. (1993) A numerical method for modelling large displacements of jointed rocks, Canadian Geotechnical Journal, vol. 30, no. 1, pp. 96-108.

Wang, B., Yu. Y.S. and Vongpaisal, S. (1995) A case study of sublevel retreat mining at Detour Lake Mine using BSM models, 2nd International conference on Rock Mechanics of Jointed and Faulted Rocks, Vienna, pp. 927-932.

Wang, B., Kwon, S., Miller, H. D. S., Lee, D. H. and Lee, H. K. (1997) Physical model and numerical model analysis of jointed rocks, Environmental and safety concerns in underground construction, Proc. 1st Asian Rock Mechanics Symposium, Lee, Yang and Chung (eds), Balkema, pp. 649-654.

Windsor, C. R. and Robertson W. V. (1992) Rock structure mapping using an electronic compass and an electronic logging system, Proc. Western Australia Conference on Mining and Geomechanics, Szwedzicki, Baird and Little (eds), Western Australian School of Mines, pp. 355-366.

Wittke, W. (1990) Rock Mechanics: Theory and applications with Case histories, Springer, Berlin.

Yeung, M. R. and Leong, L. L. (1997) Effects of joint attributes on tunnel stability, Int. J. Rock Mech. Min. Sci. 34: 3-4, paper no. 348.

Yeung, M. R. and Blair, S.C. (2000) DDA back analysis of large block test data, Pacific Rocks 2000, Proc. 4th North American Rock Mechanics Symposium, Girard, Liebman, Breeds and Doe (eds), Balkema, pp. 937-943.

Zhu, W., Chen, W. and Wang, B. (1997) Numerical simulation and experimental study of excavation and anchoring support of underground chambers in jointed rock mass, Environmental and Safety Concerns in Underground Construction, Proc. 1st Asian Rock Mechanics Symposium, Lee, Yang and Chung (eds), Balkema, Seoul, pp. 565-570.

Zienkiewicz, O. C. and Cheung, Y. K. (1966) Application of the finite element method to problems of rock mechanics, Proc.1st Int. Cong. Int. Soc. Rock Mech., Laboratorio Nacional De Engenharia Civil, Lisbon, vol. 1, pp. 298-299.